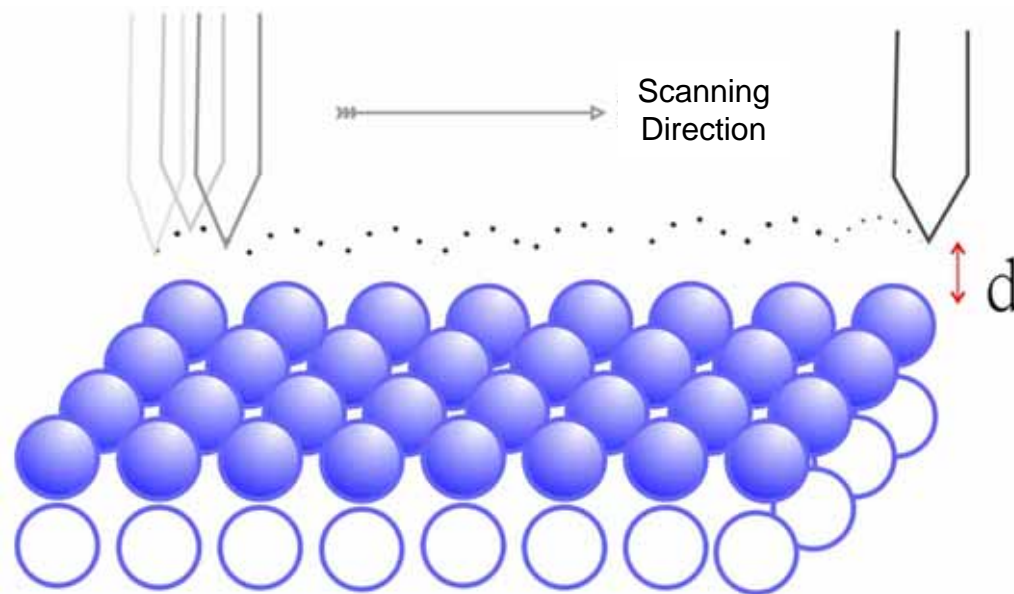


Scanning Tunneling Microscopy

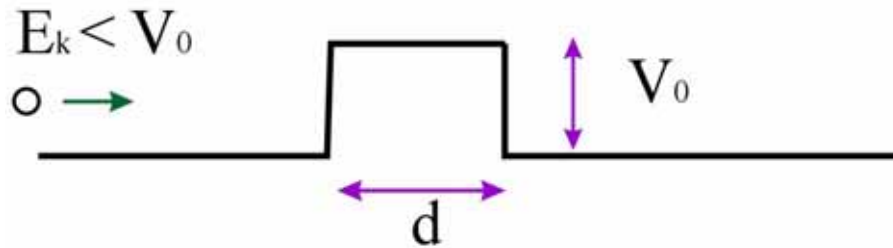


References:

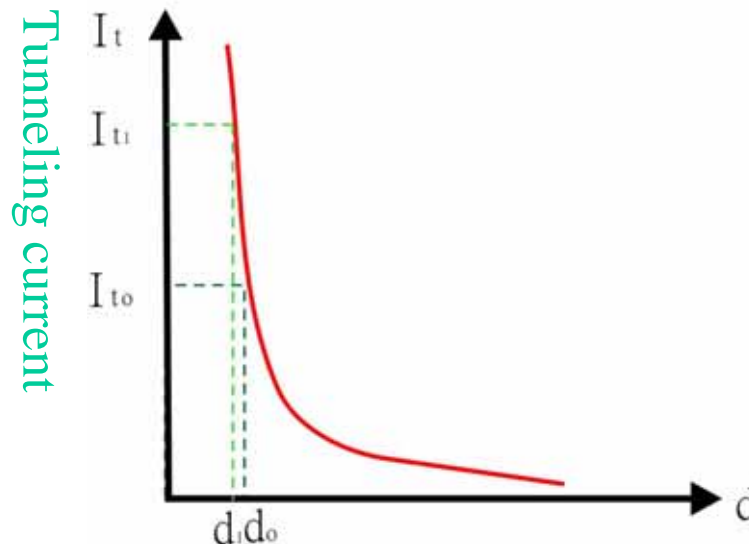
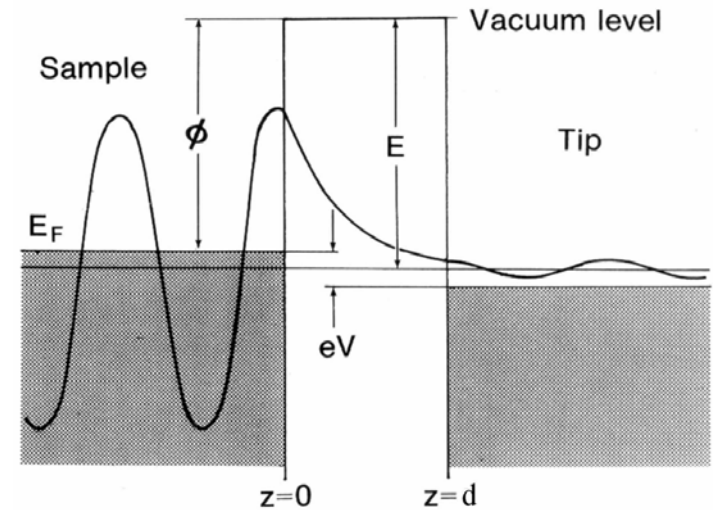
1. G. Binnig, H. Rohrer, C. Gerber and Weibel, Phys. Rev. Lett. **49**, 57(1982); and ibid **50**,120(1983).
2. J. Chen, *Introduction to Scanning Tunneling Microscopy*, New York, Oxford Univ. Press(1993).

Tunneling

Classical



Quantum Mechanics



Tunneling current I_t

$$I_t \propto (V/d) \exp(-A\phi^{1/2}d)$$

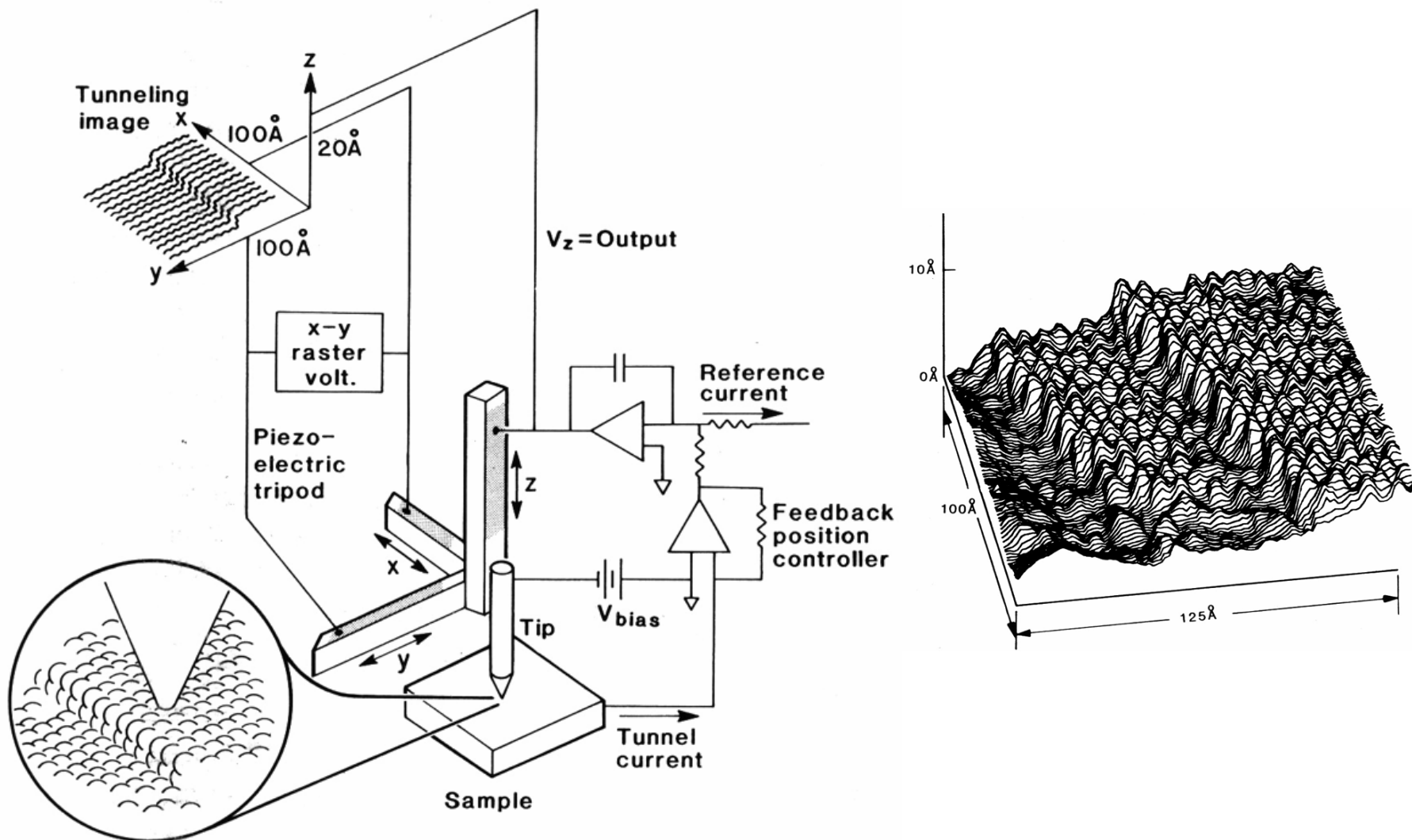
$$A = 1.025 \text{ (eV)}^{-1/2} \text{ \AA}^{-1}$$

$$I_t = 10 \text{ pA} \sim 10 \text{ nA}$$

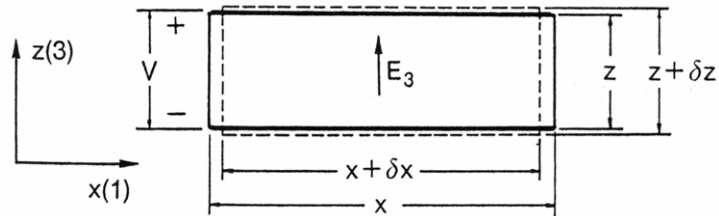
$$V = 1 \text{ mV} \sim 3 \text{ V}$$

d decreases by 1 \AA ,
 I_t will be reduced by 10 times.

Schematics of STM



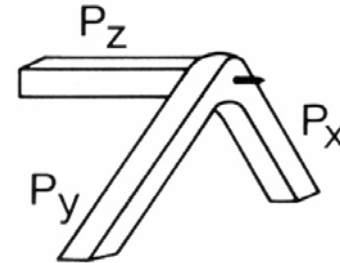
Piezoelectric Scanner



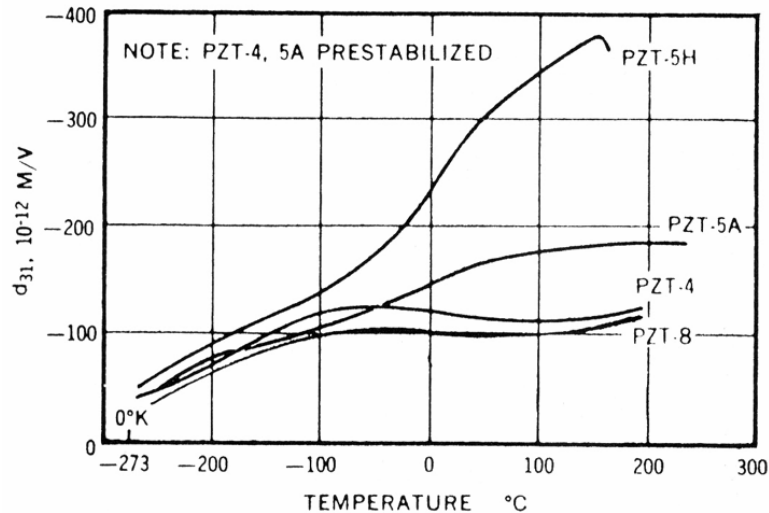
$$d_{31} = S_1/E_3, S_1 = \delta x/x, E_3 = V/z$$

$$d_{33} = S_3/E_3, S_3 = \delta z/z$$

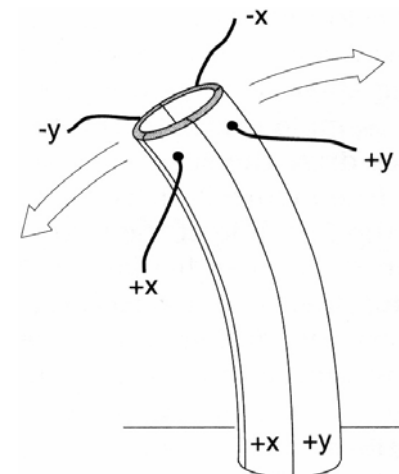
Tripod scanner



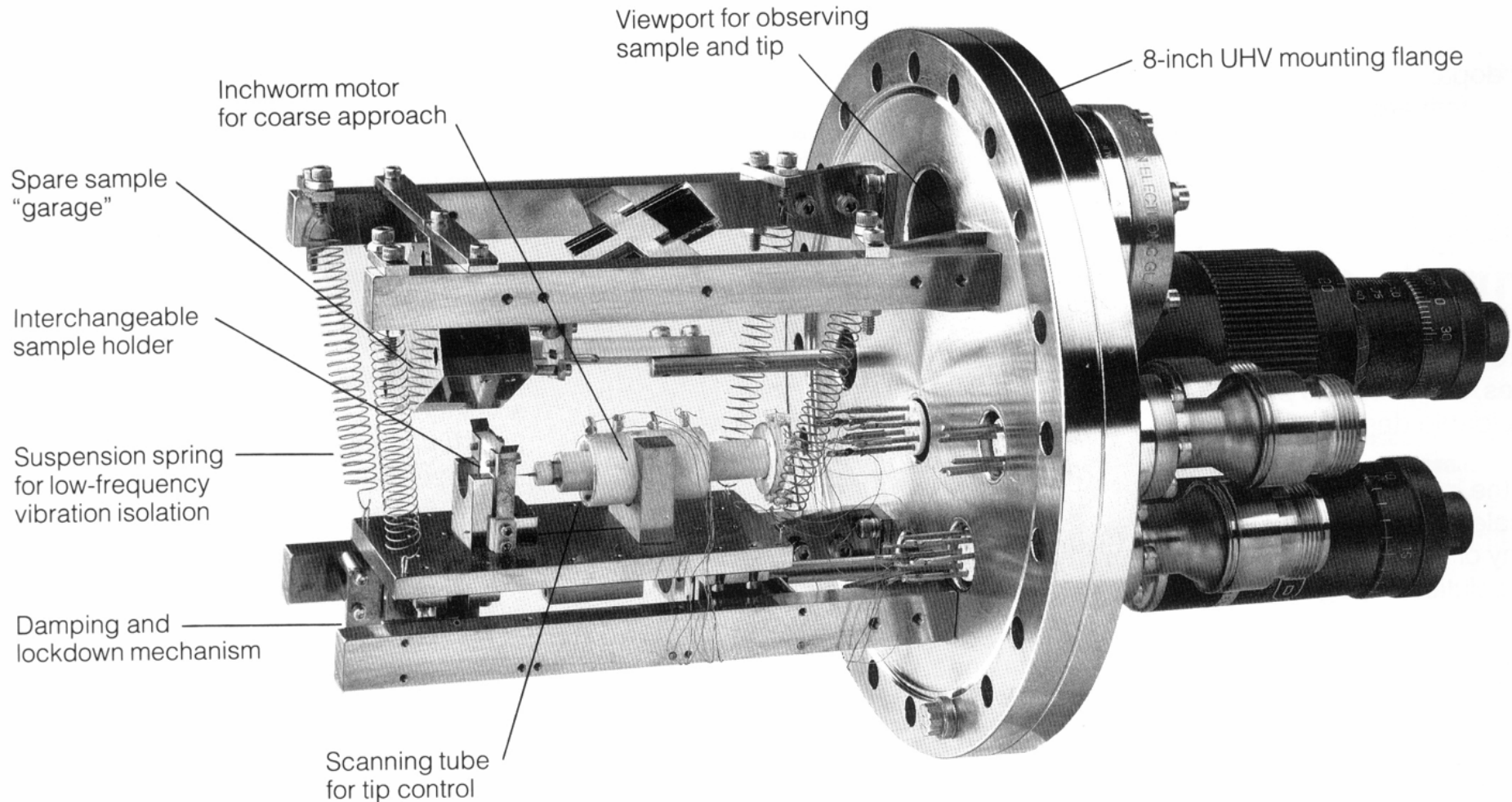
Variation of piezoelectric coefficient with temperature.



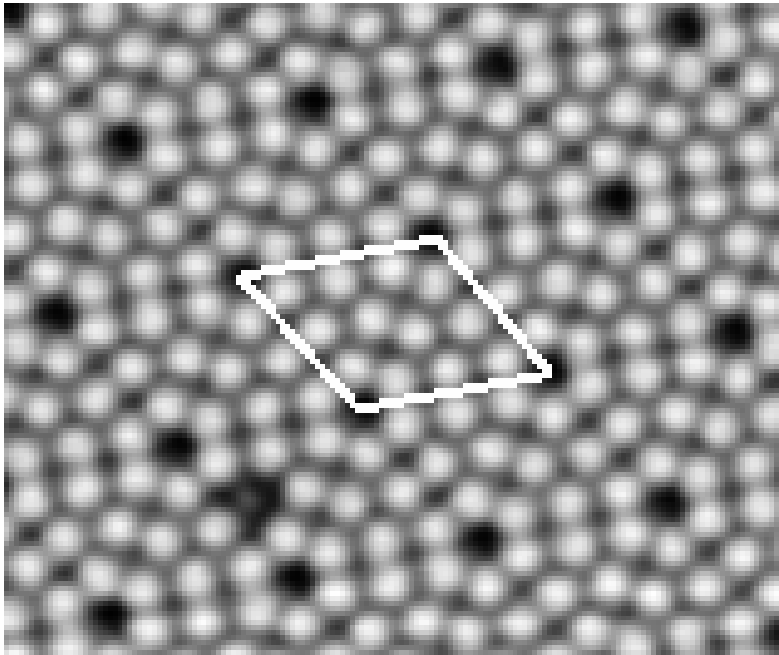
Tube scanner



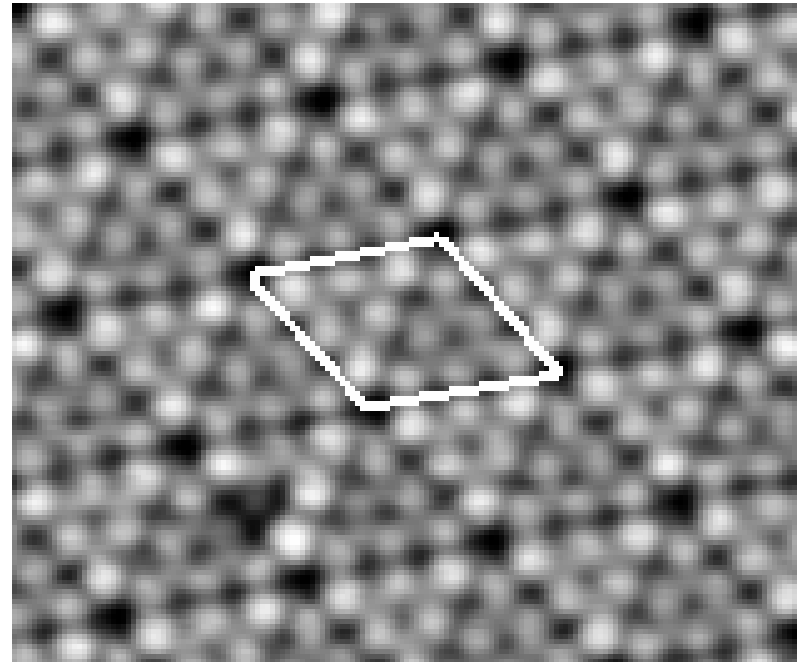
Ultra-High Vacuum Scanning Tunneling Microscope



STM Images of Si(111)-(7×7)



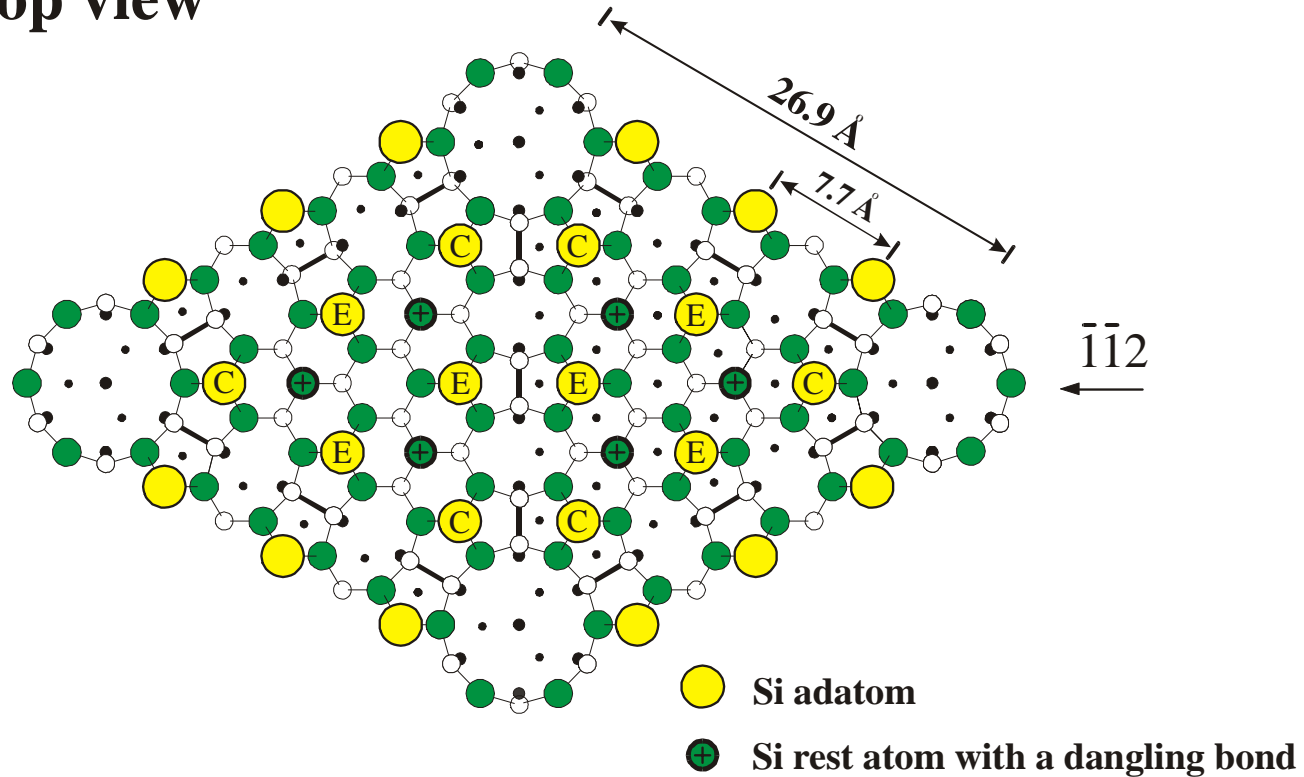
Empty-state image



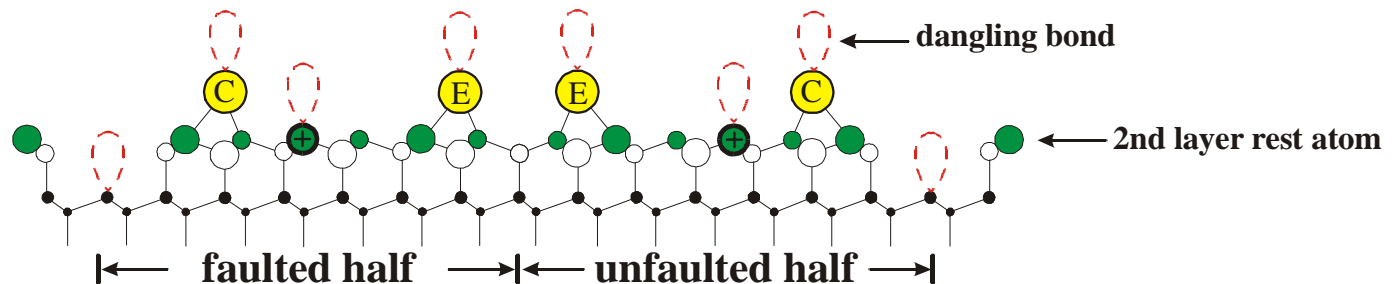
Filled-state image

Atomic Model of Si(111)-(7×7)

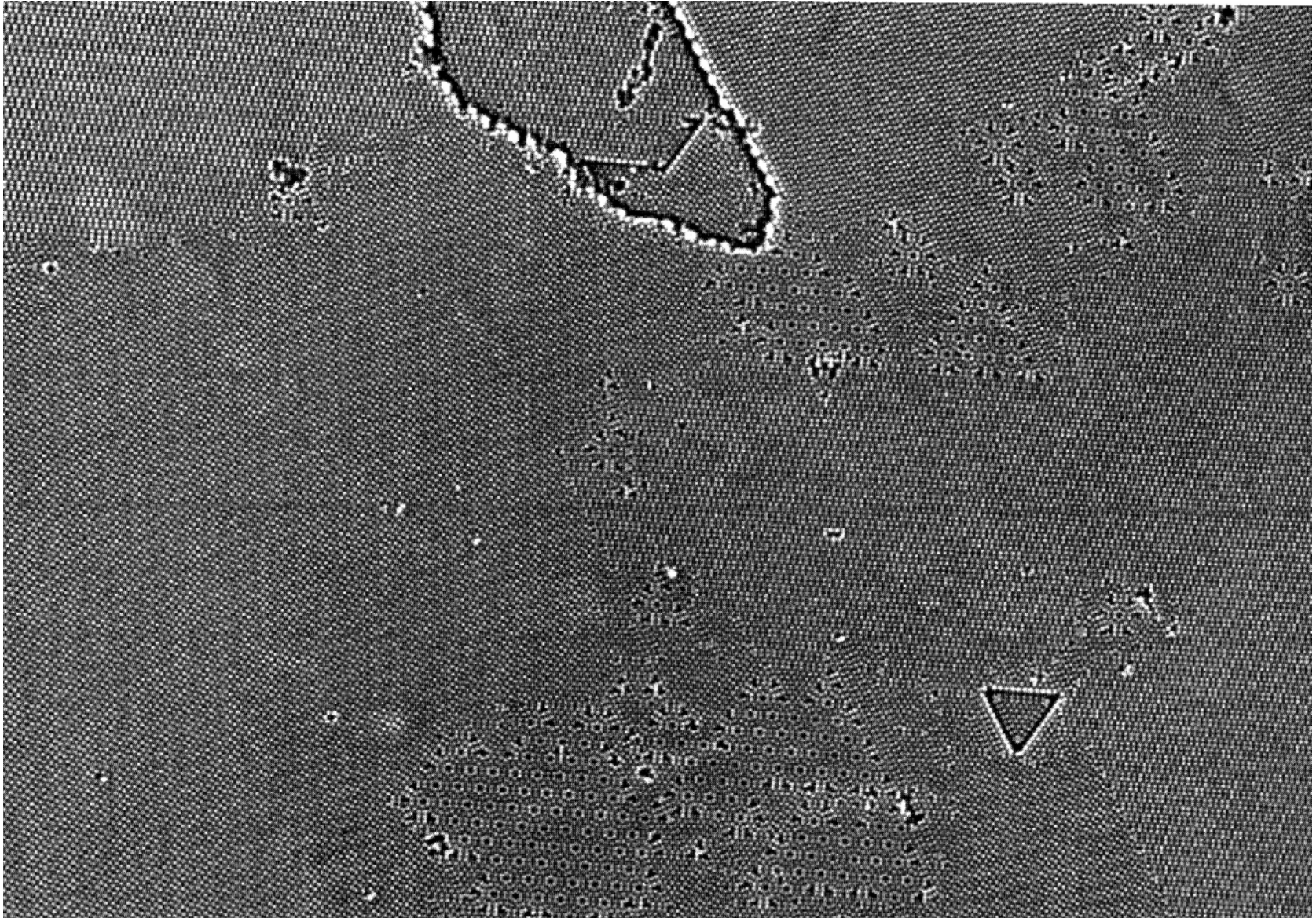
Top view



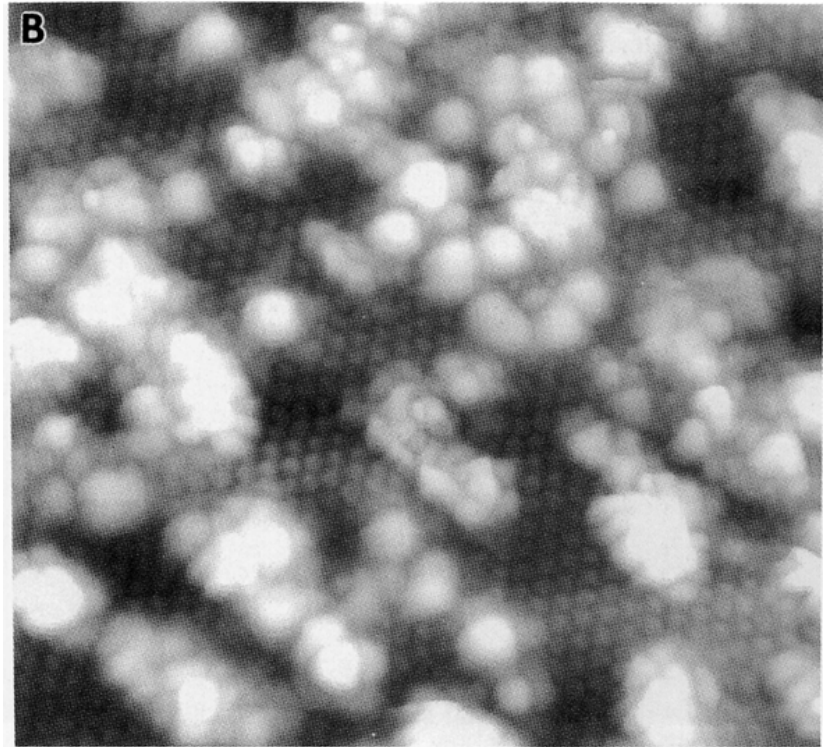
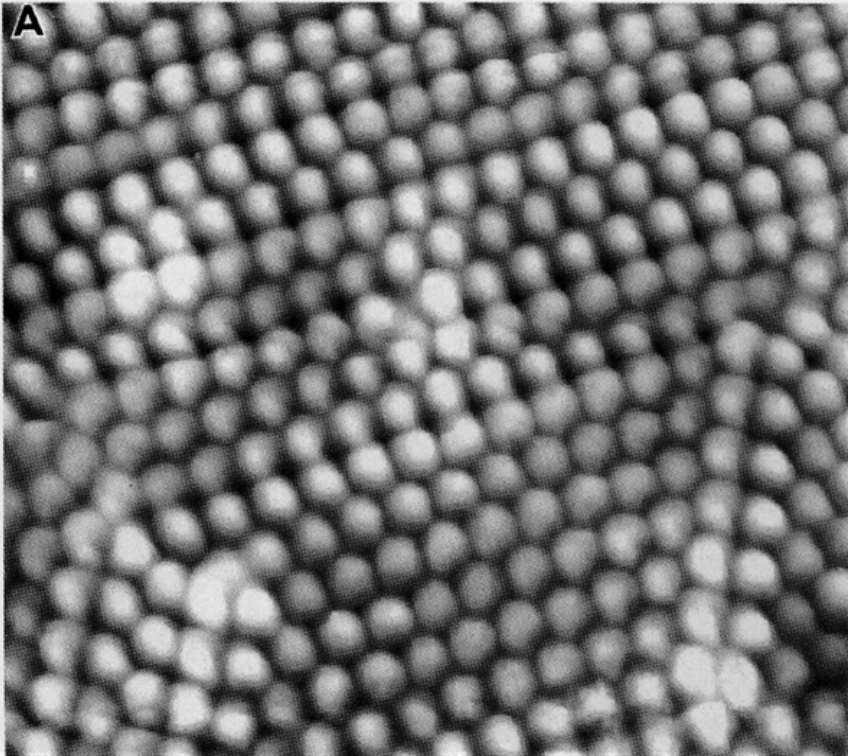
Side view



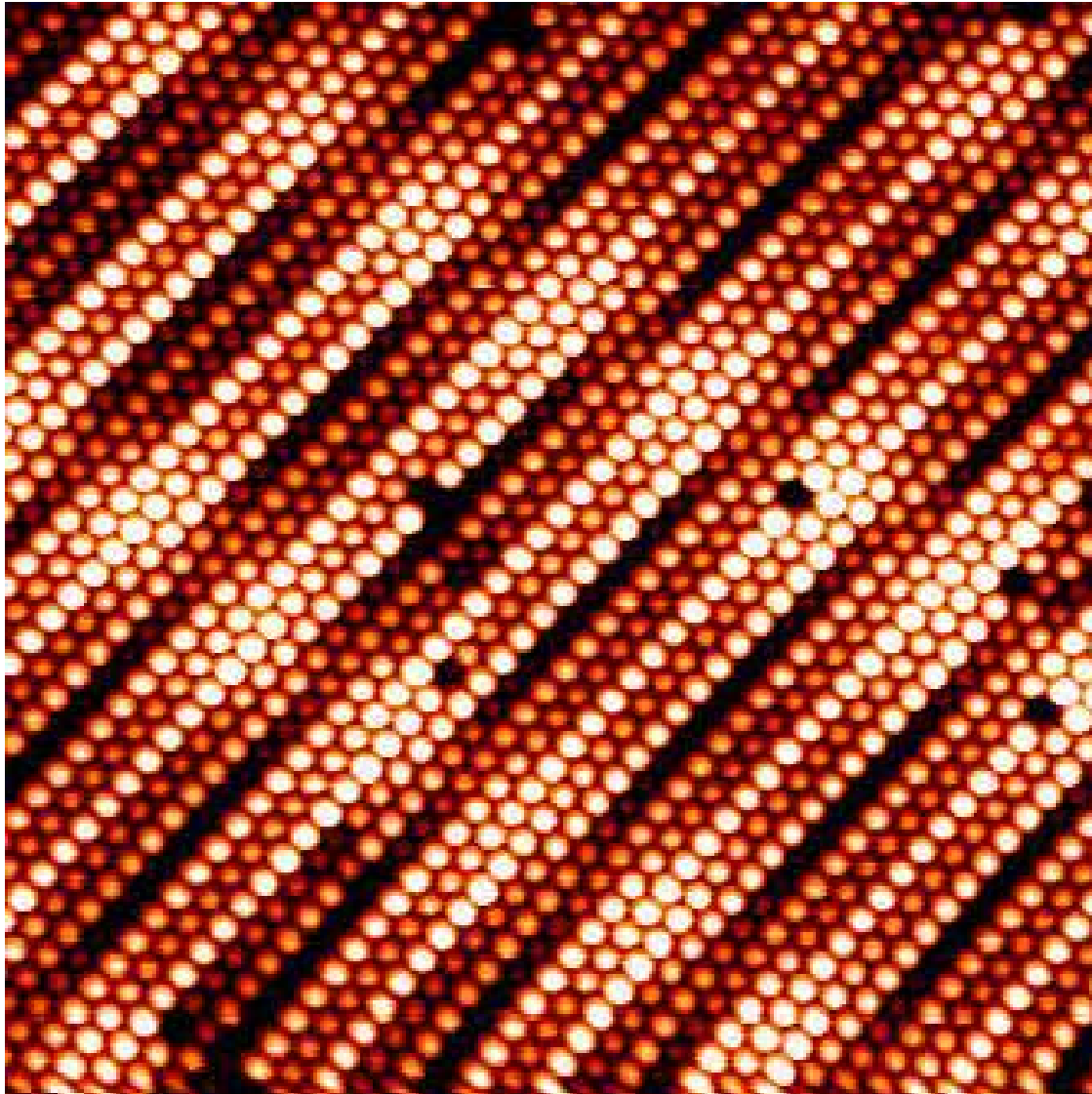
Atomic Structure of the Ge(111) Surface



Ge(111)



Atomic Structure of the Pt(001) Surface



Surface Science **306**, 10 (1994).

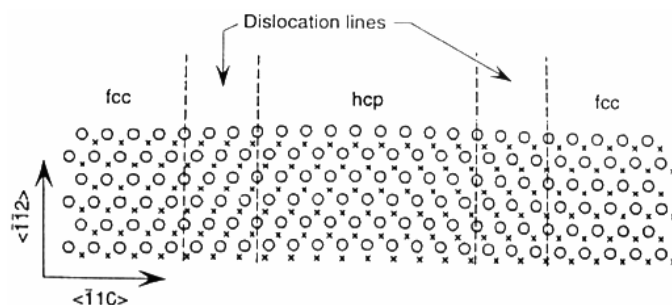
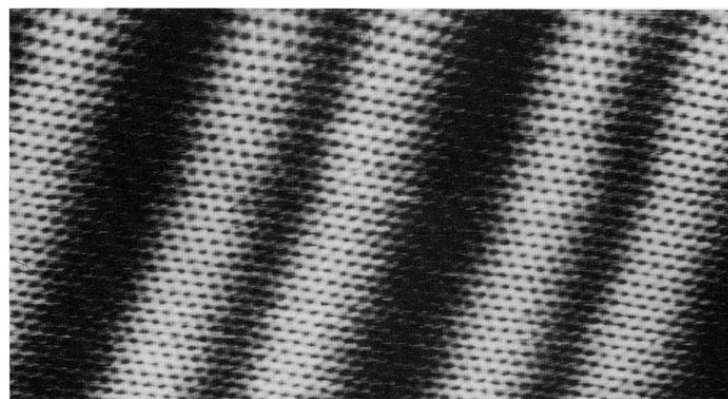
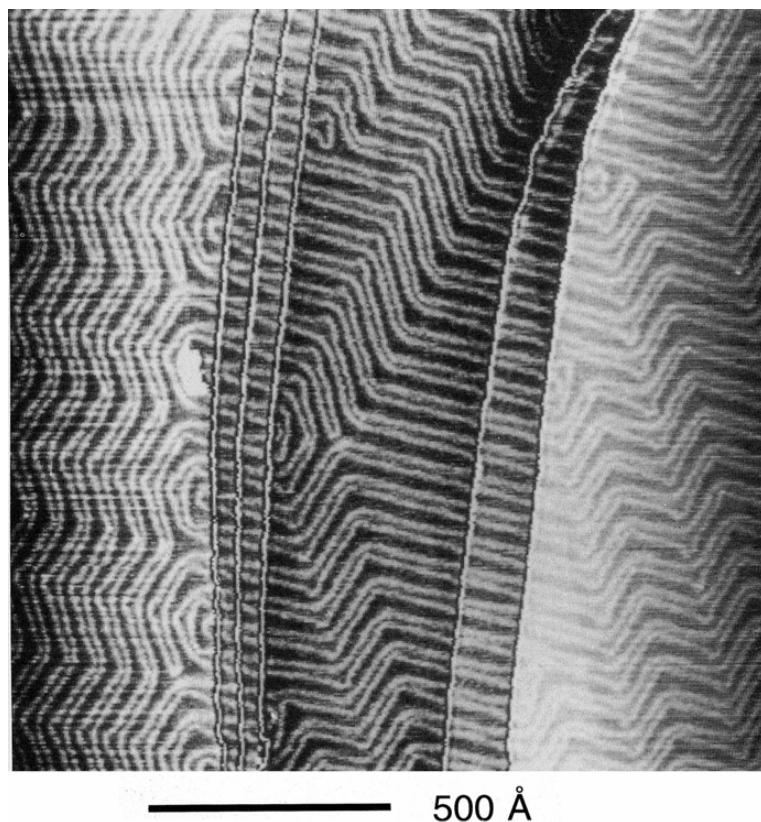
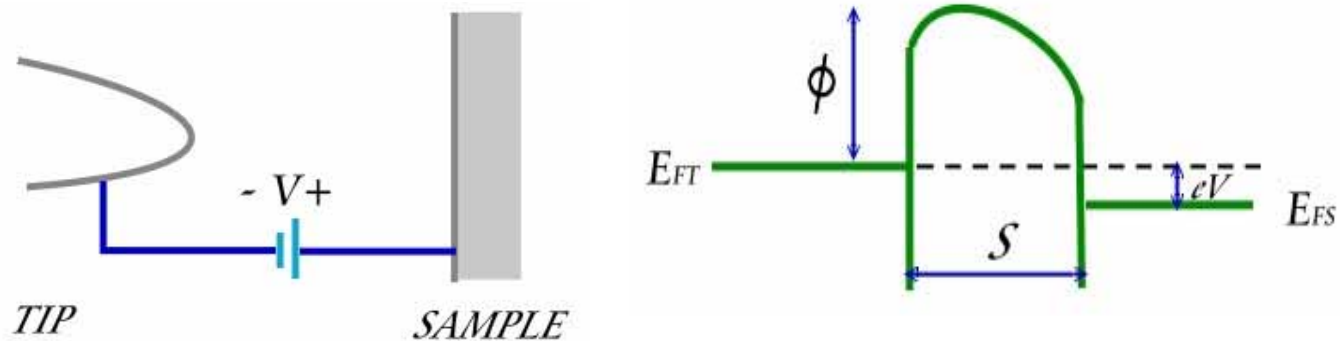


Fig. 1. In-plane structure of the Au(111) surface with a $22 \times \sqrt{3}$ reconstruction. The circles and crosses correspond to atoms in the first and second surface layers, respectively. Surface atoms in both sides of the figure lie on fcc sites, whereas atoms in the center of the figure lie on hcp sites. The domain walls (dislocation lines) involve atoms in bridge sites.

Large-scale image of the Au(111)- $22 \times \sqrt{3}$ reconstruction. The Au(111) surface reconstructs at room temperature to form a $22 \times \sqrt{3}$ structure, which has a two-fold symmetry. On a large scale, three equivalent orientations for this reconstruction coexist on the surface. Furthermore, on an intermediate scale, a herring-bone pattern is formed.

Science 258, 1763 (1992).

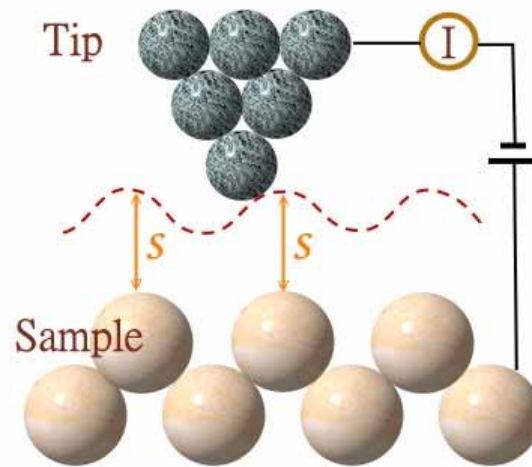
Theory of STM



From one-dimensional tunneling problem
tunneling current ($eV \ll \phi$)

$$I \propto \frac{V}{S} \exp\left(-A\phi^{\frac{1}{2}}S\right)$$

$$A = 1.025(eV)^{-\frac{1}{2}} \text{ } ^0 \text{ } ^{-1} \text{ } \mathbf{A}$$



Constant Current Mode

Tunneling current

$$I_{T \rightarrow S} = \frac{2\pi e}{\hbar} \sum_{\mu\nu} f(E_\mu) [1 - f(E_\nu + eV)] |M_{\mu\nu}|^2 \delta(E_\mu - E_\nu - eV)$$

where $f(E)$ is Fermi function

E_μ is the energy of state μ , where μ and ν run over all the states of the tip and surface, respectively.

$M_{\mu\nu}$ is tunneling matrix element

$$M_{\mu\nu} \equiv \frac{\hbar^2}{2m} \int d\vec{s} (\psi_\mu^* \nabla \psi_\nu - \psi_\nu \nabla \psi_\mu^*)$$

where ψ_μ is the wave function, and the integral is over any plane in the barrier region.

$$\begin{aligned} I &= I_{T \rightarrow S} - I_{S \rightarrow T} \\ &= A' \int_{-\infty}^{\infty} \rho_T(E) \rho_S(E + eV) |M(E)|^2 [f(E) - f(E + eV)] dE \end{aligned}$$

where ρ_S and ρ_T are the densities of states in the sample and the tip, respectively.

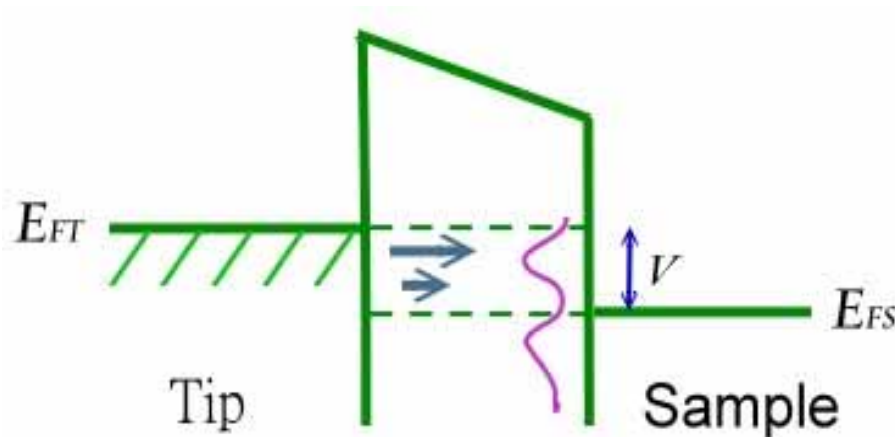
Tunneling current

$$I \equiv A' \int_{-\infty}^{\infty} \rho_T(E) \rho_S(E + eV) |M(E)|^2 [f(E) - f(E + eV)] dE$$

Transmission probability of the electron

$$M(E) = \exp \left[-A \phi^{\frac{1}{2}} S \right]$$

Usually, we assume ρ_T is featureless (ie. $\rho_T \approx \text{const.}$), and the sample electronics states dominate the tunnel spectra.



However, the tips might have effect on the tunnel spectra, if

1. we have atomically sharp tips ,or
2. the tip has picked up a foreign atom.

Case I -----metals

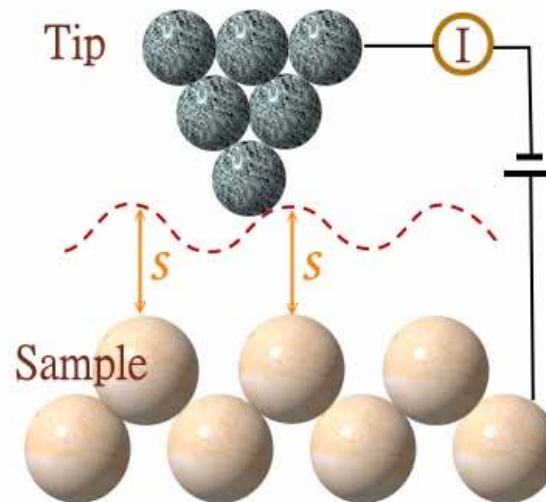
In the low-voltage limit

$$I \propto V \rho_S(\tilde{r}_t; E_F) \rho_t(E_F)$$

where $\rho_S(\tilde{r}_t; E_F)$ is the surface density of states of the sample at the center of the tip(\tilde{r}_t),

$$\rho_S(\tilde{r}; E) \equiv \sum_v |\psi_v(\tilde{r})|^2 \delta(E_v - E)$$

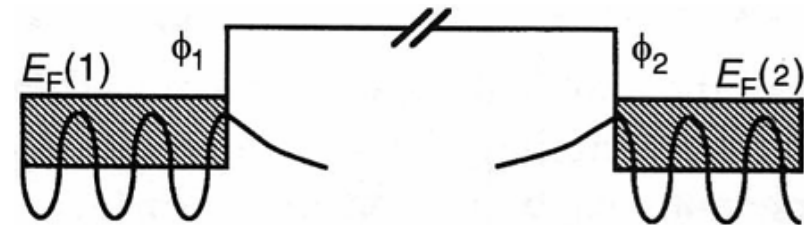
$\rho_t(E_F)$ is the density of states of the tip at the Fermi level and is often regarded as a constant.



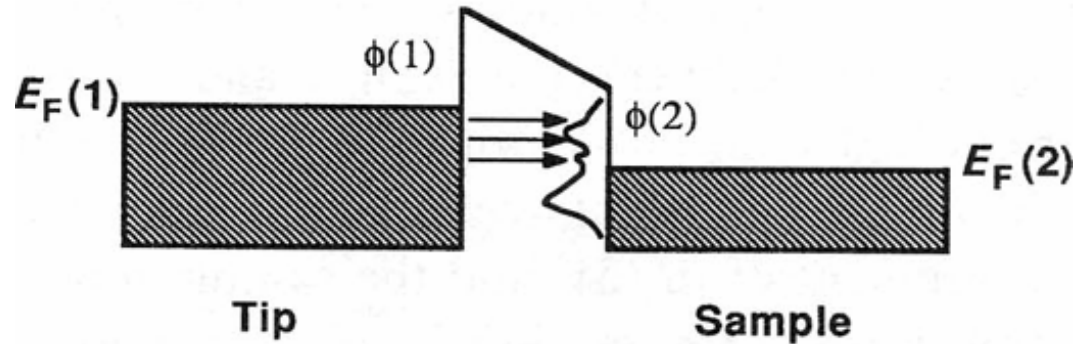
Constant Current Mode

Electronic Structures at Surfaces

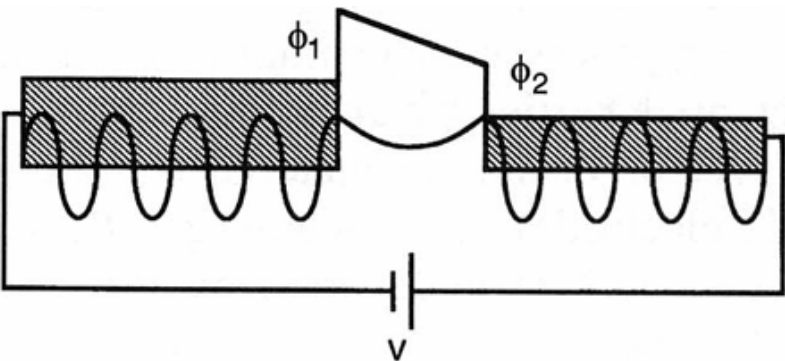
Not Tunneling



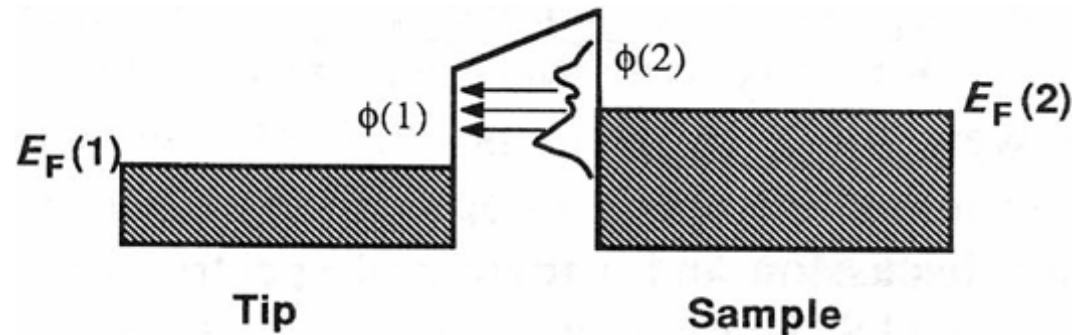
Empty-State Imaging



Tunneling

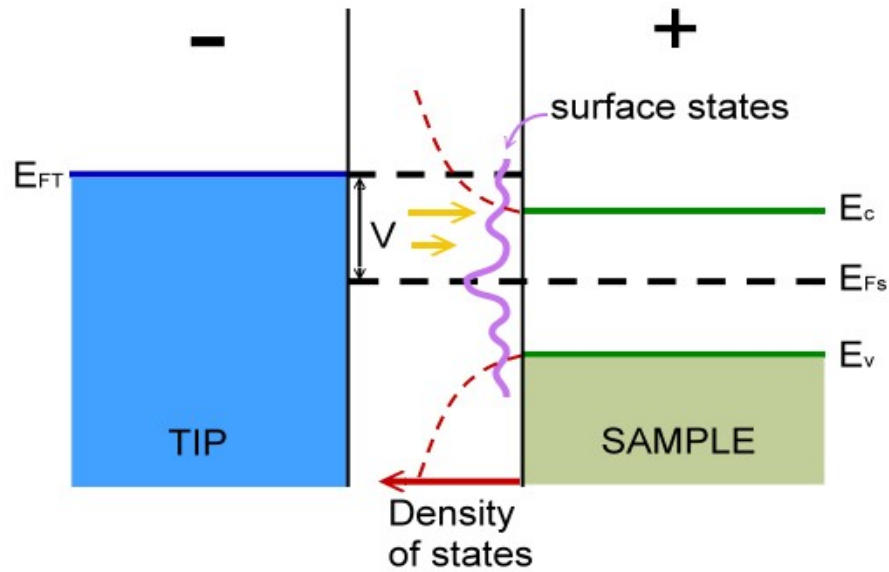


Filled-State Imaging

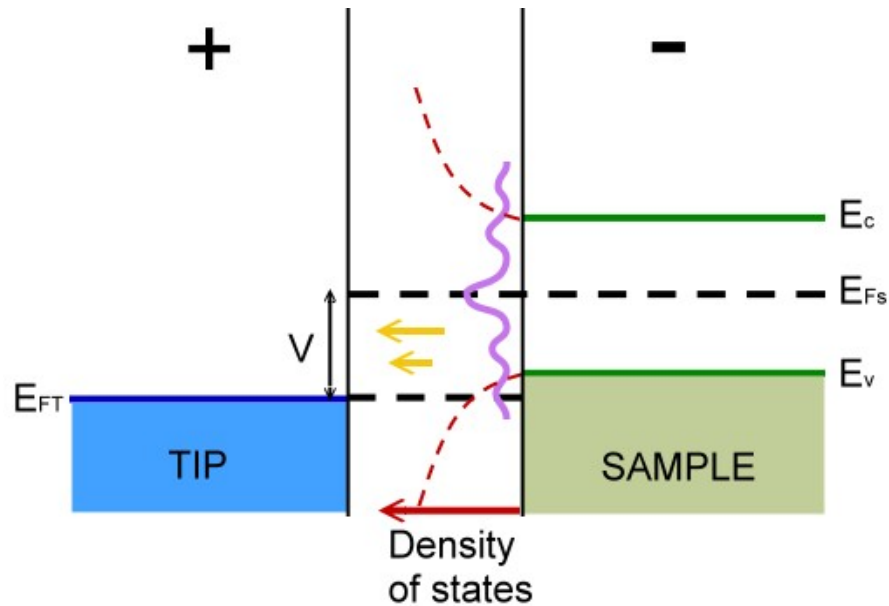


Example -----Semiconductor

1. Tip-negative



2. Tip -positive



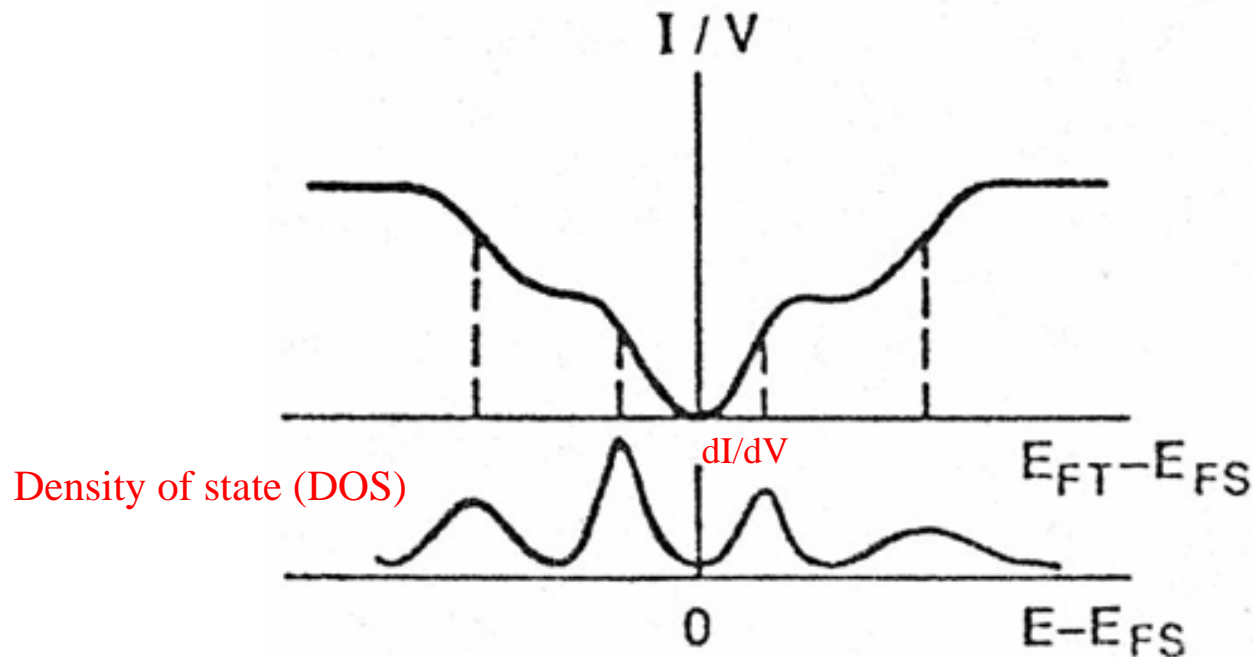
Science **234**, 304 (1986).

Scanning Tunneling Spectroscopy

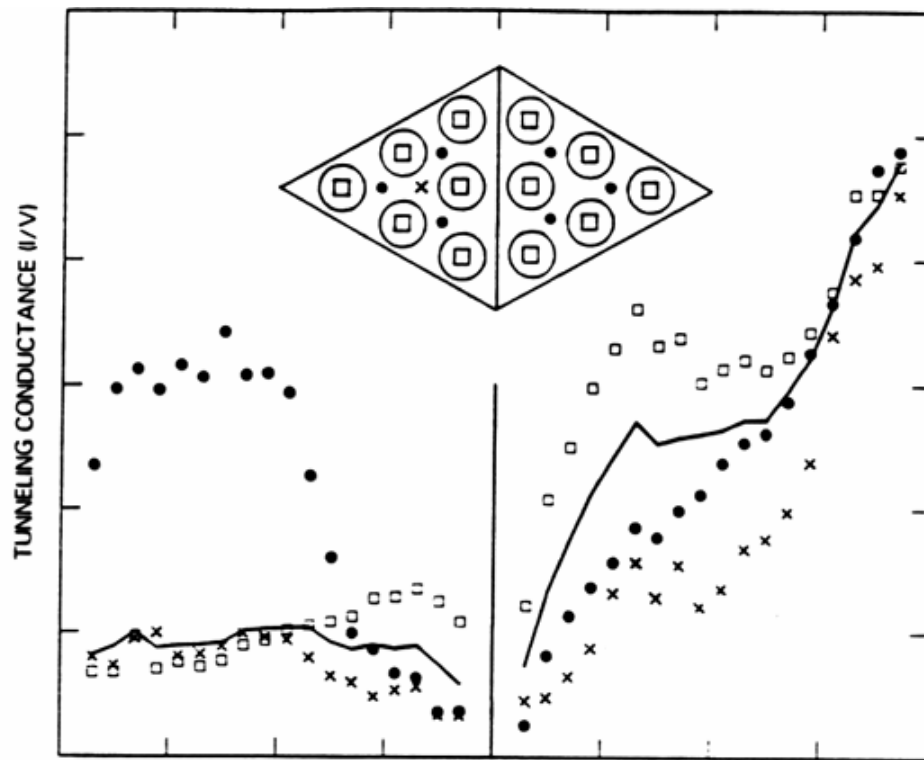
STM provides atomic-scale topographic information, and atomic-scale electronic information. However, the mixture of geometric and electronic structure information often complicates interpretation of observed feature.

Several spectroscopic modes:

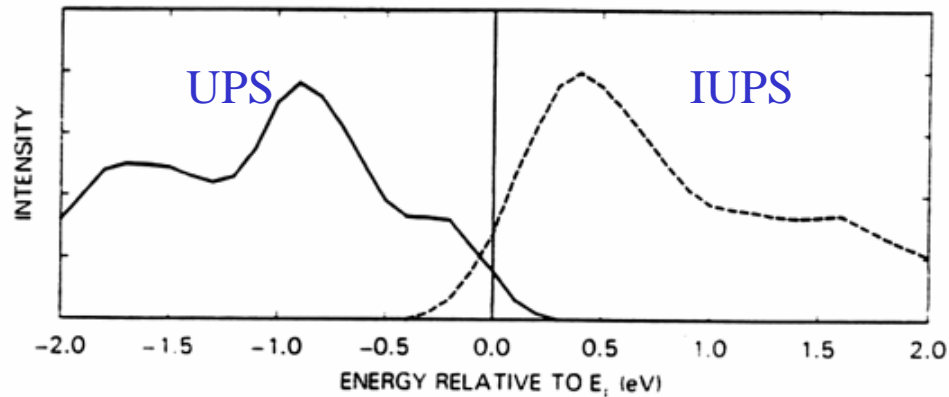
1. Voltage-dependent STM imaging.
2. Tunneling I-V curves, current-imaging-tunneling spectroscopy (CITS).
3. Scanning tunneling spectroscopy (STS): dI/dV and topograph.



STS of Si(111)-(7x7)



(a)



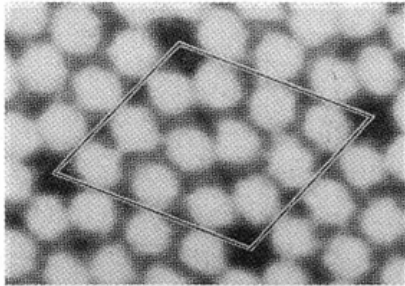
(b)

Science **234**, 304 (1986).

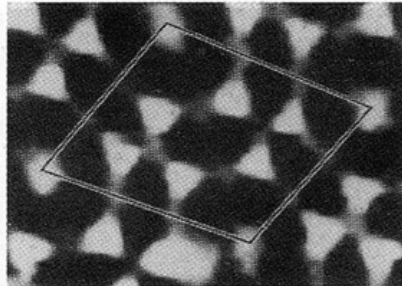
STS of Si(111)-(7x7)

topograph

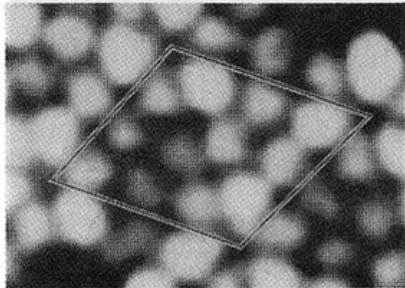
+2V



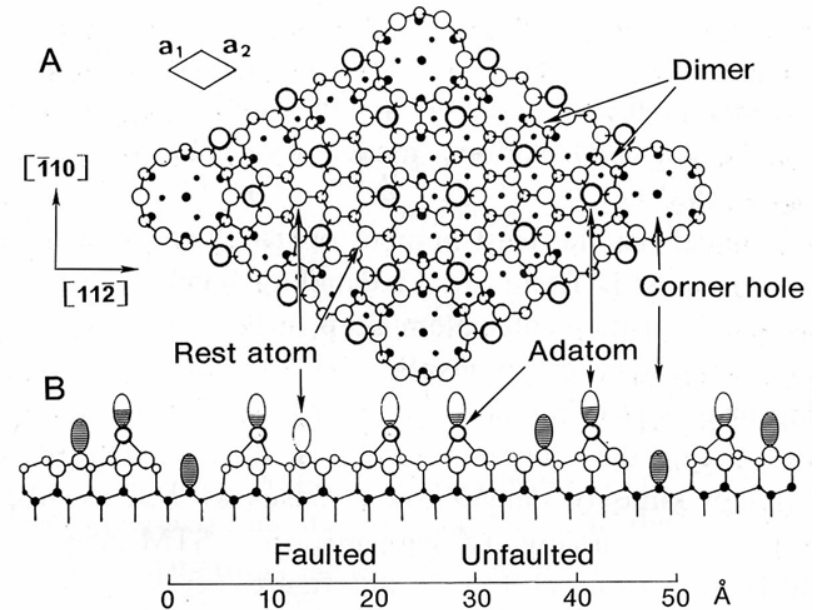
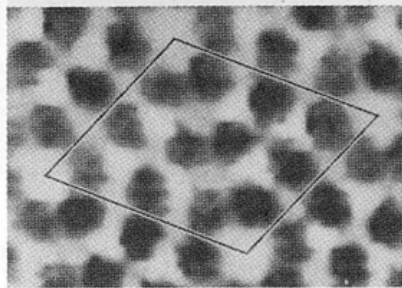
-0.8V



-0.35V

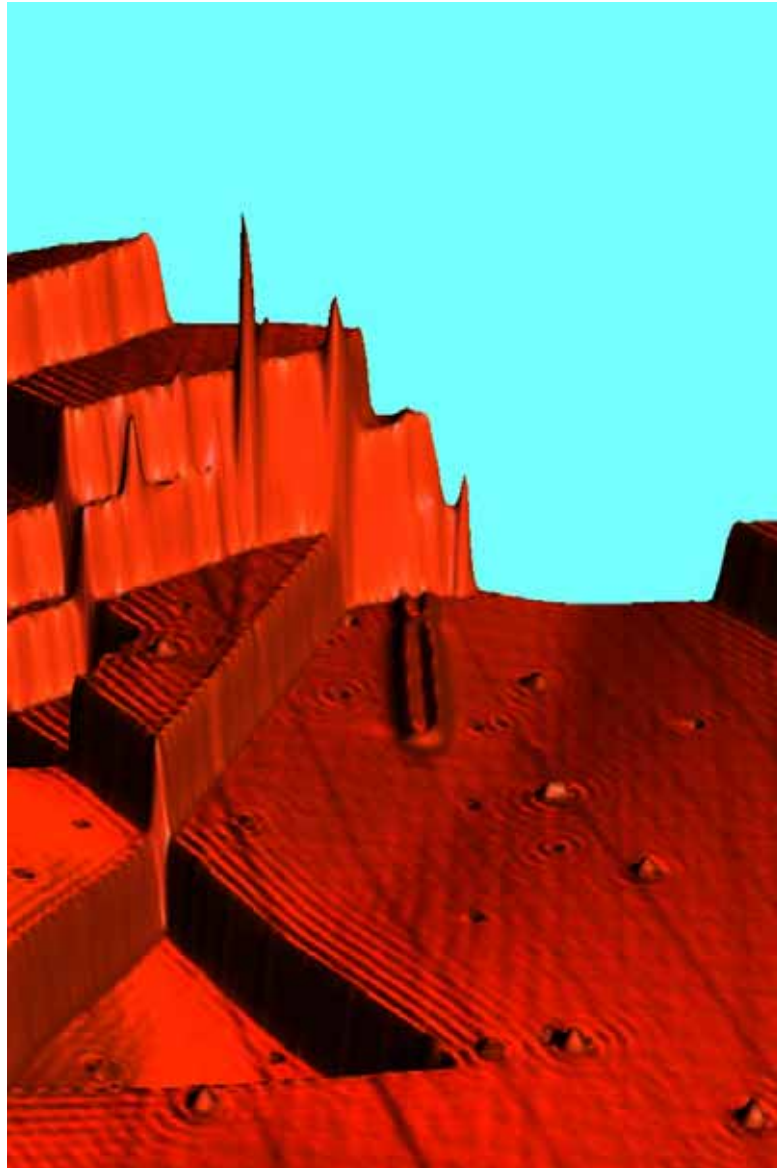


-1.8V



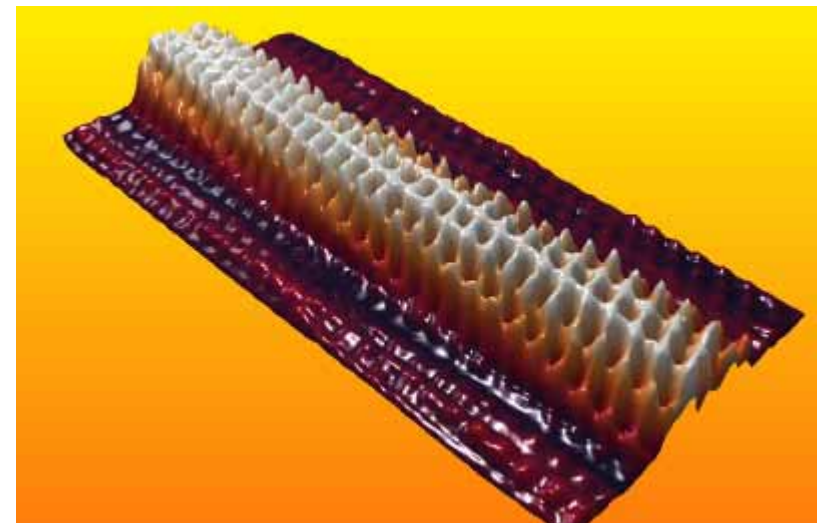
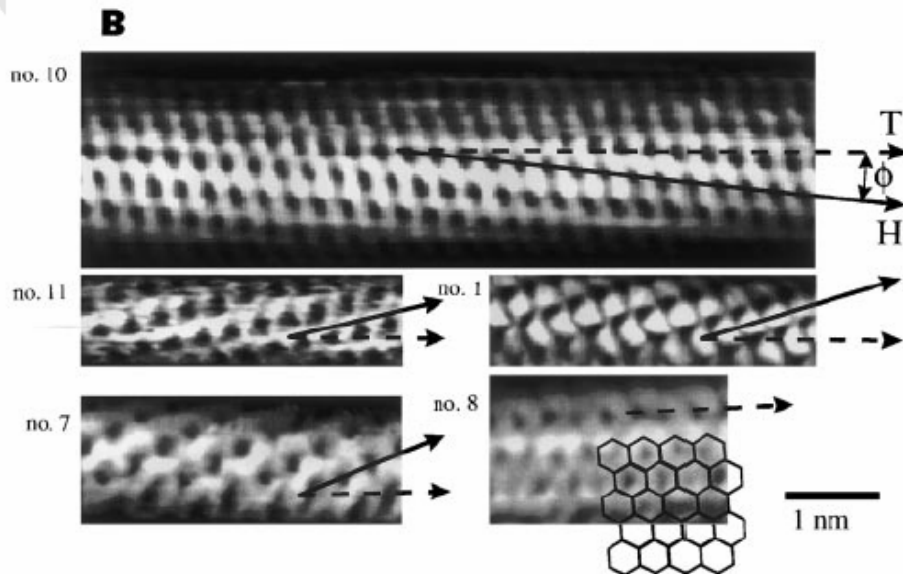
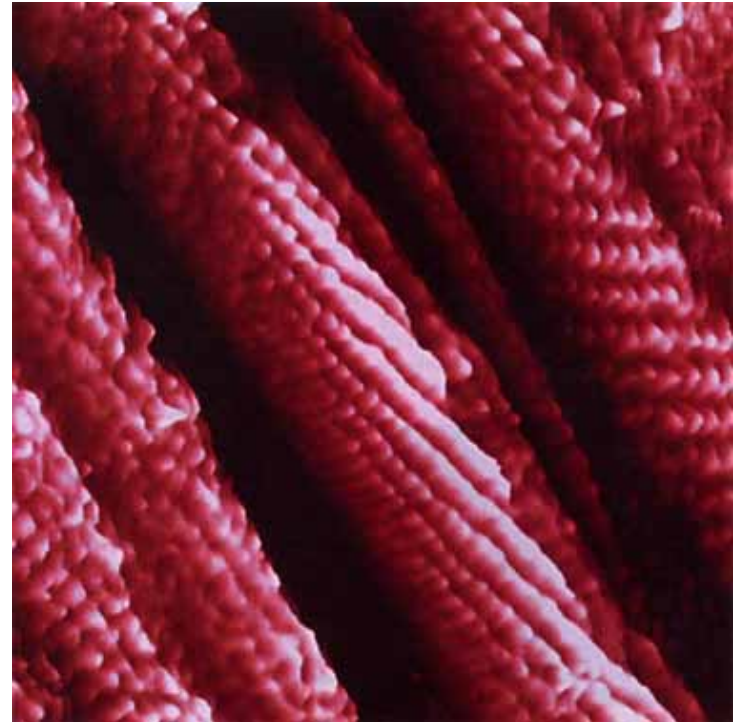
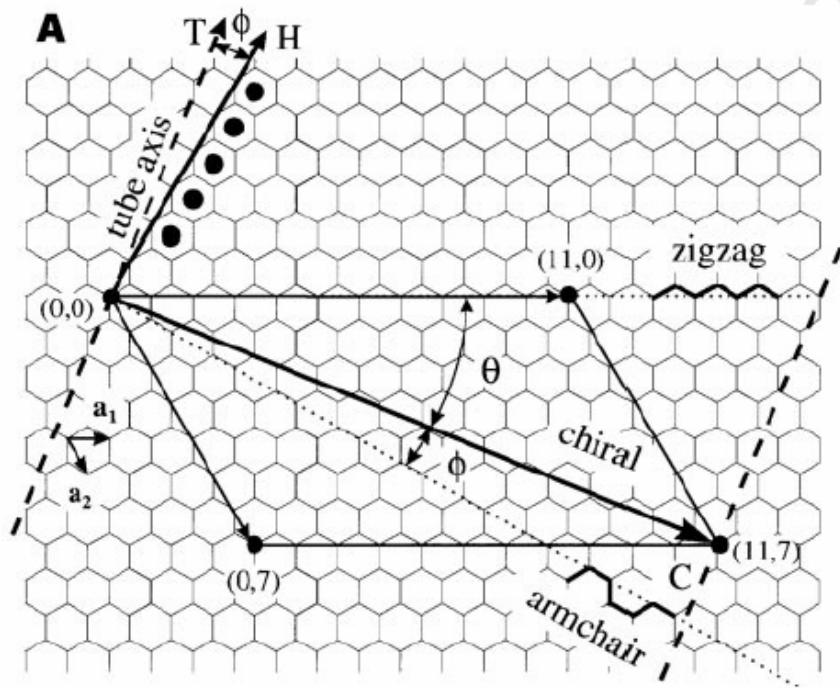
1. Science **234**, 304-309 (1986).
2. Phys. Rev. Lett. **56**, 1972-1975 (1986).

Surface States at Cu(111)



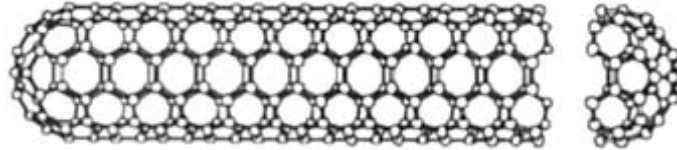
Nature **363**, 524 (1993).

Single-Wall Carbon Nanotubes

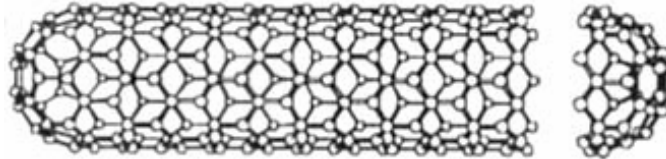


Electronic Structure of Single-Wall Nanotubes

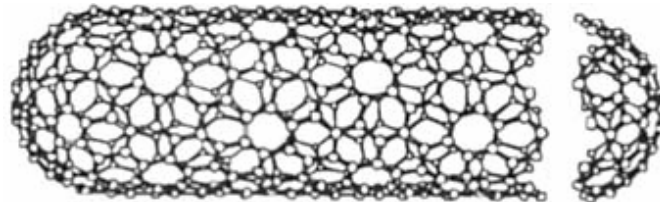
1. Armchair nanotubes $(n,n) \rightarrow$ metallic



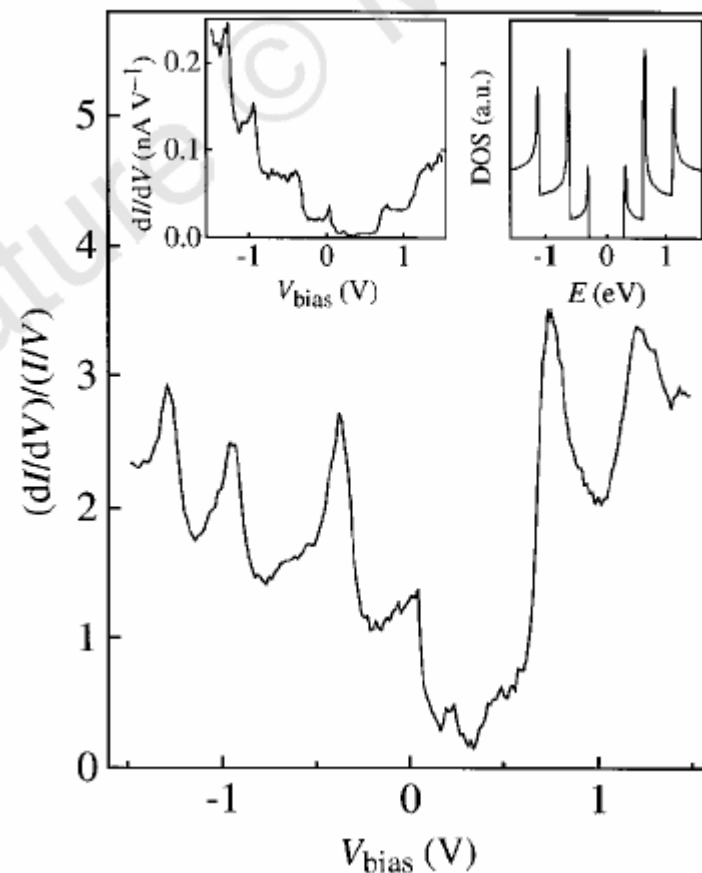
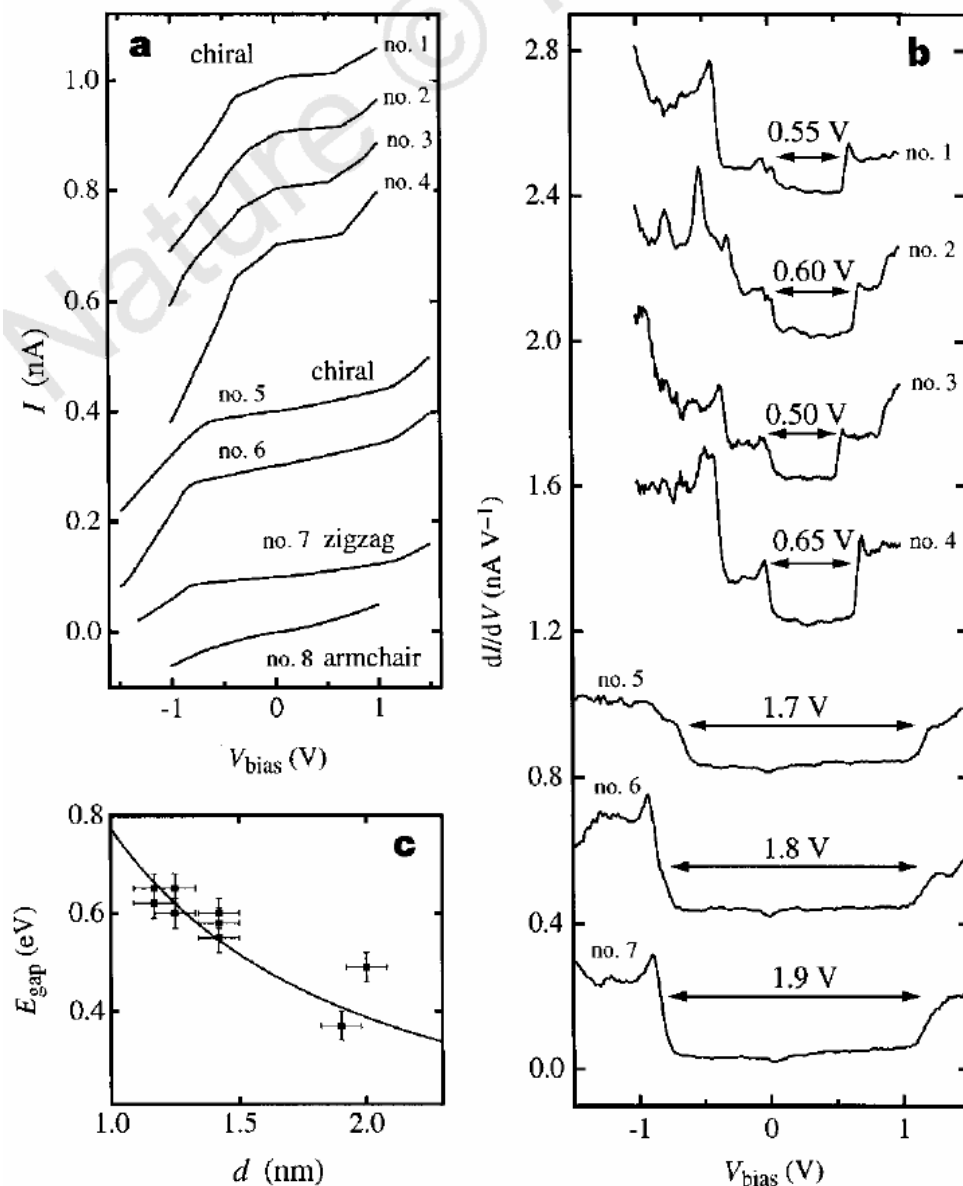
2. Zigzag nanotubes $(n,0) \rightarrow$ metallic, when $n=3q$
 \rightarrow semiconducting, otherwise



3. Chiral nanotubes $(n,m) \rightarrow$ metallic, when $m=n+3q$

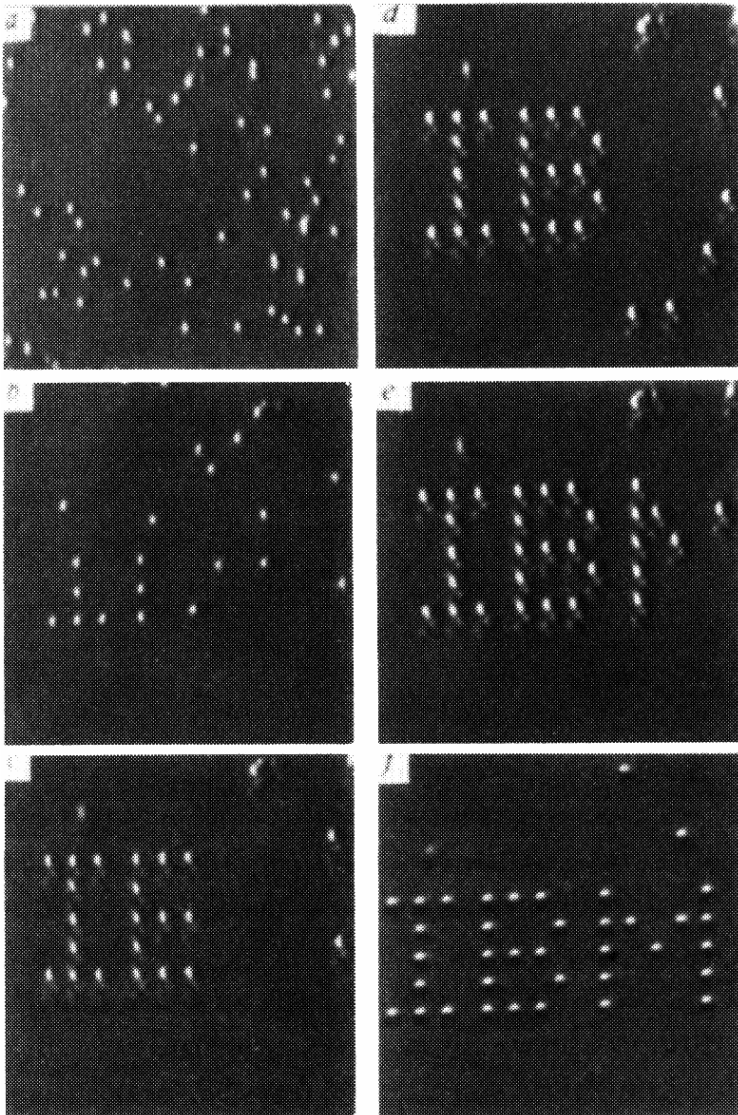


Electronic Structure of Single-wall Nanotubes

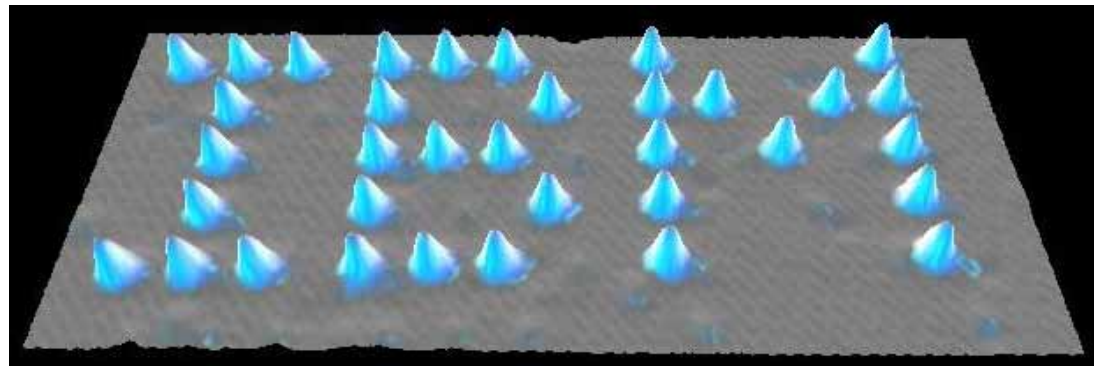


Nature **391**, 59 (1998).

Atomic Manipulation with STM

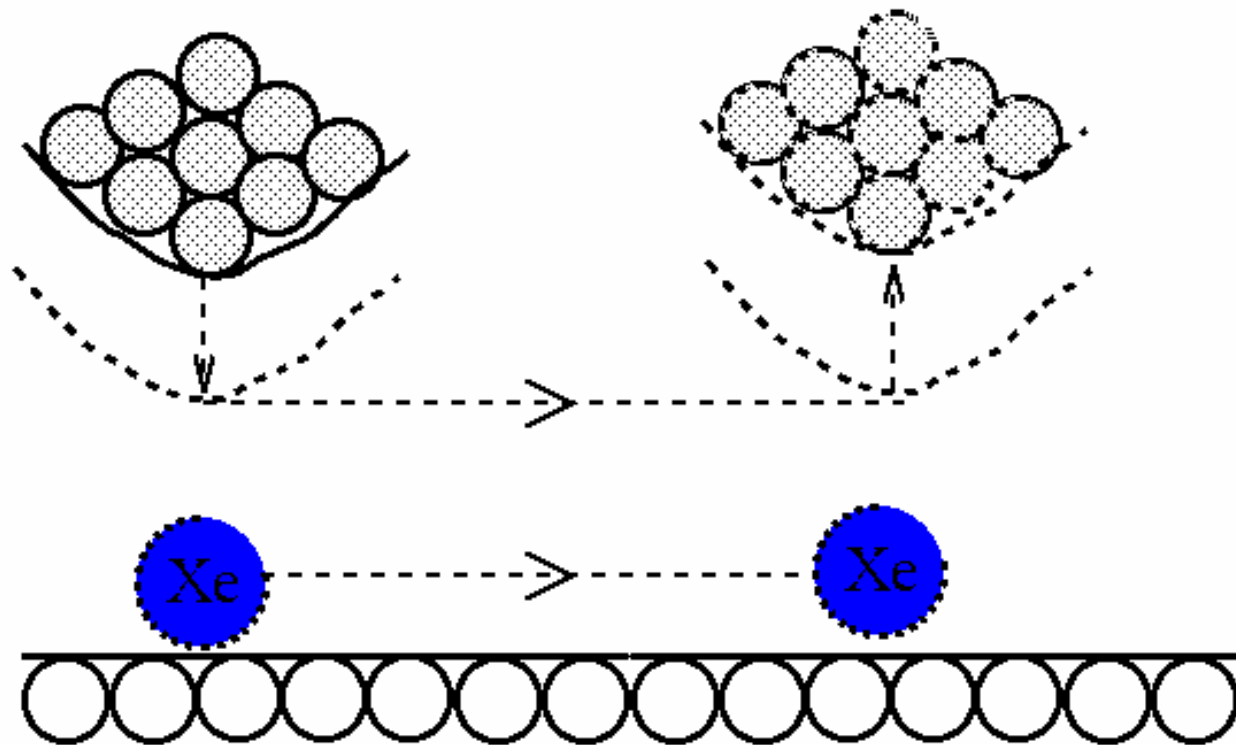


Nature **344**, 524 (1990)



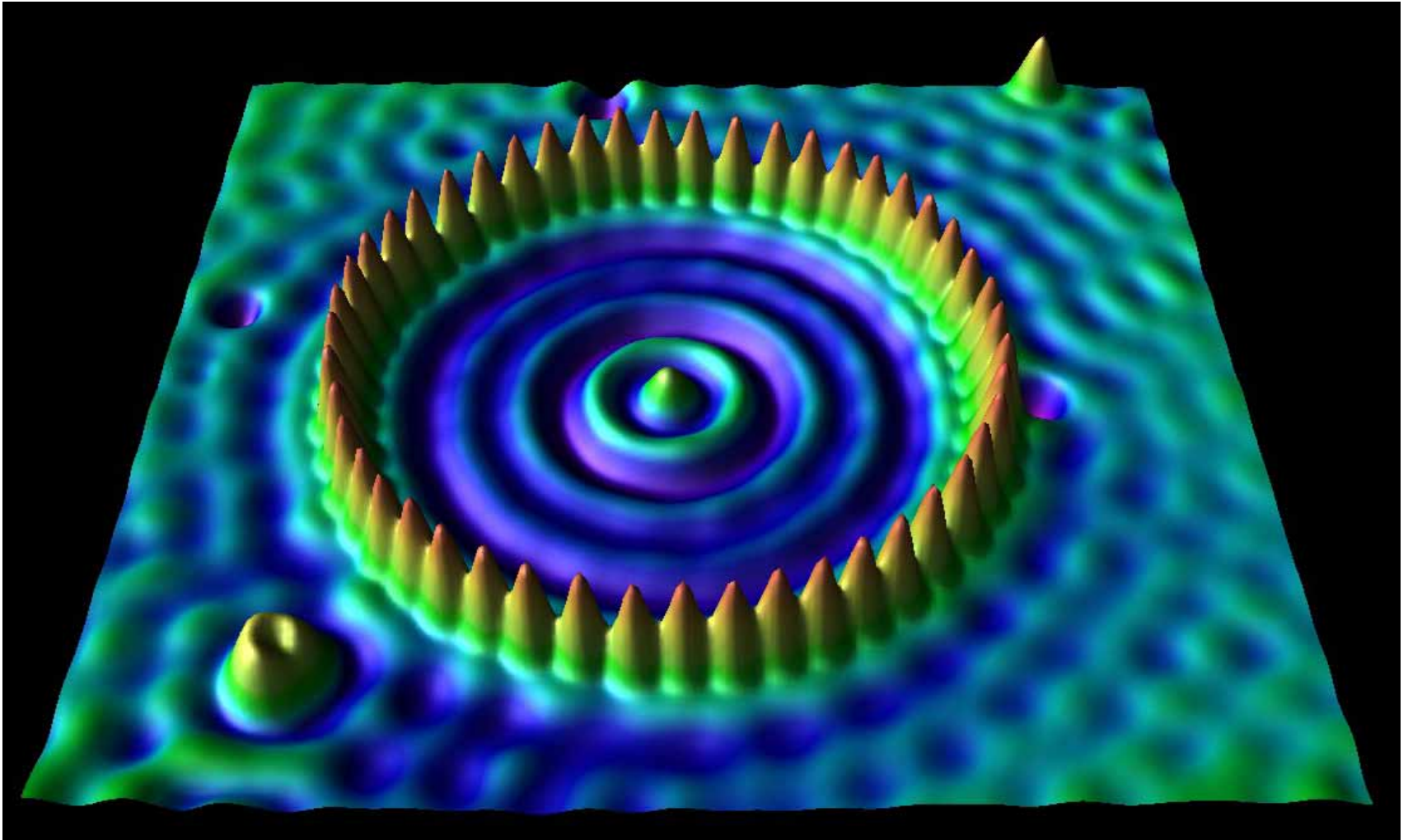
Positioning Atoms with an STM

D.M. Eigler & E.K. Schweizer Nature **344** 524 (1990)

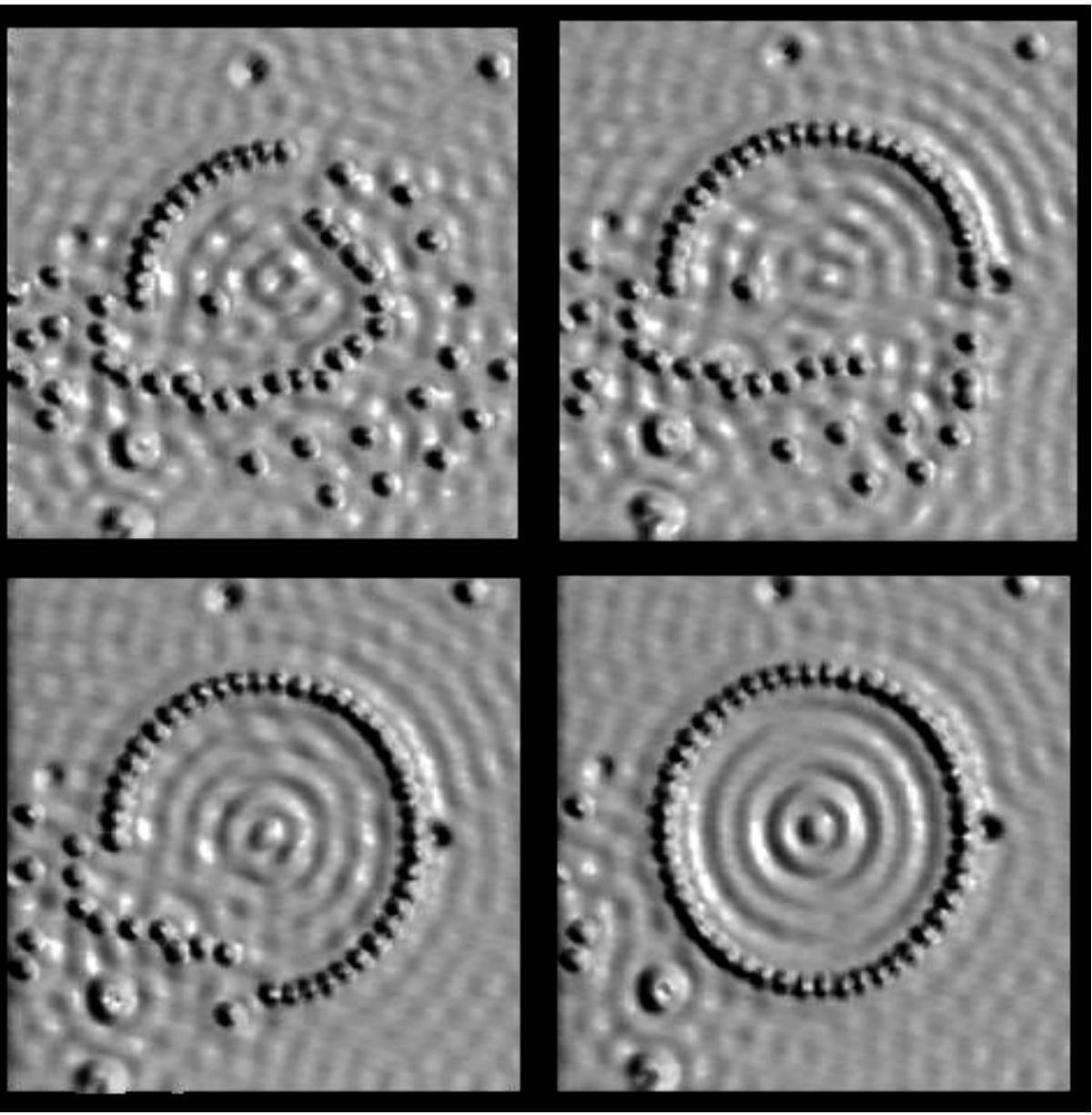


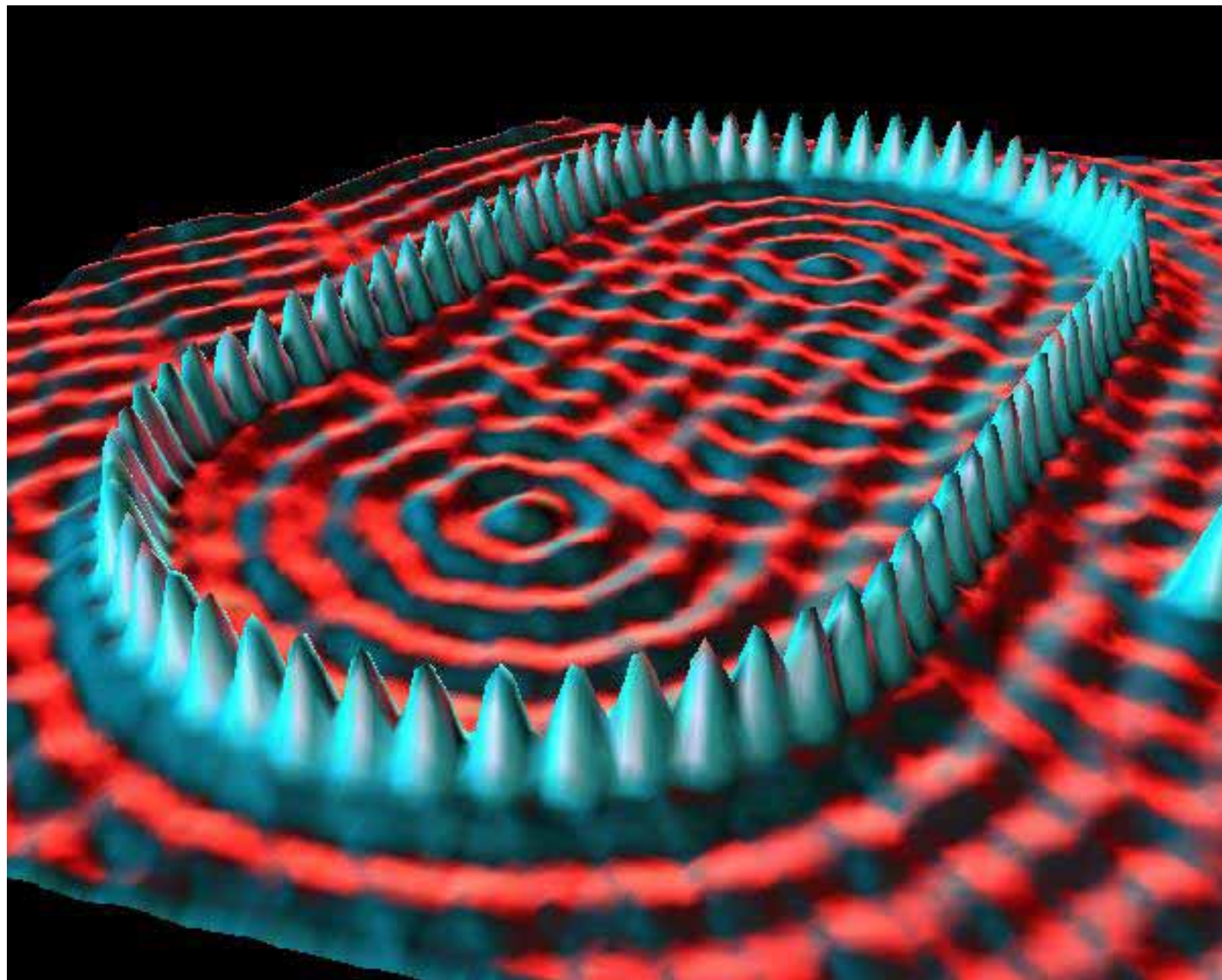
The STM tip is brought down near the atom, until the attraction is enough to hold it as the atom is dragged across the surface to a new position.

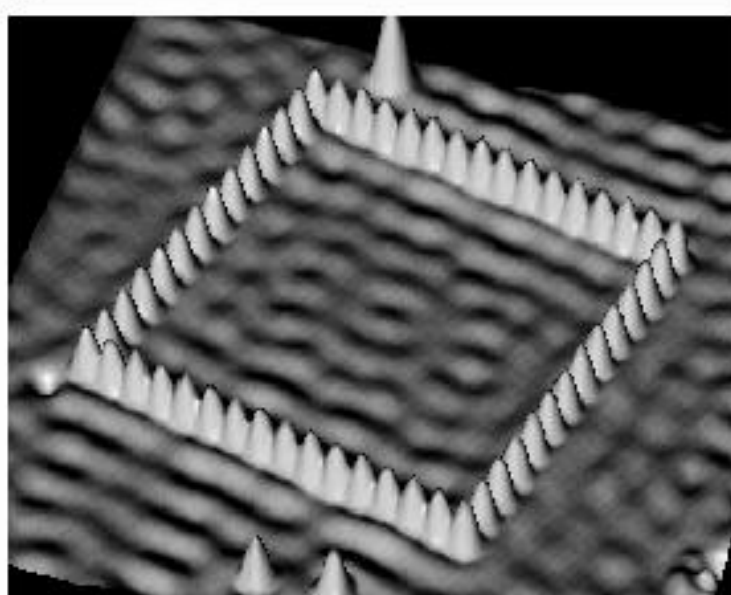
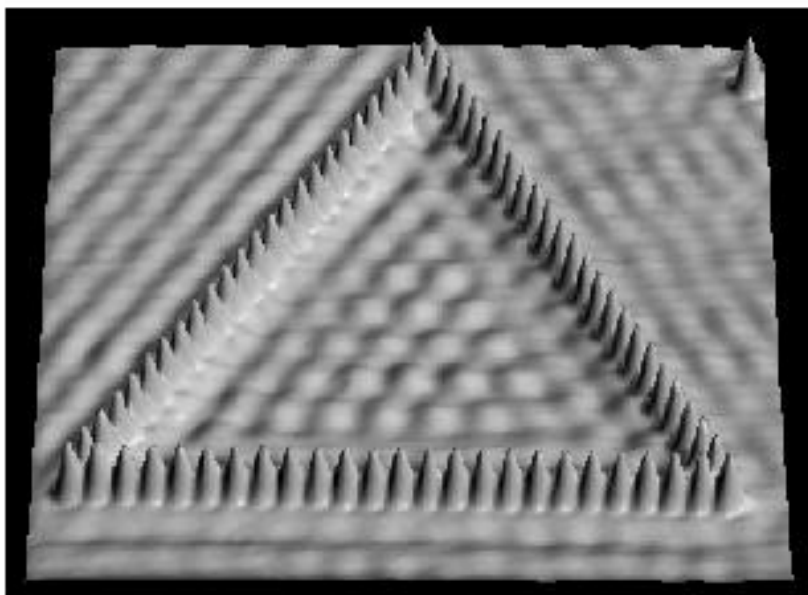
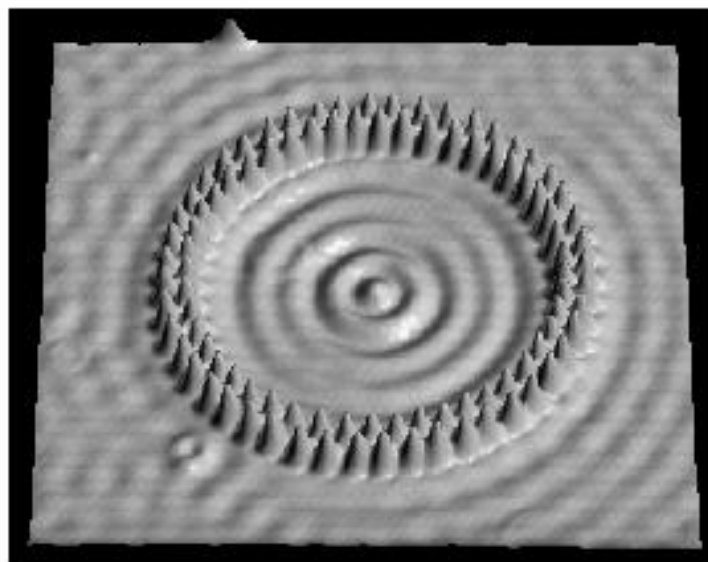
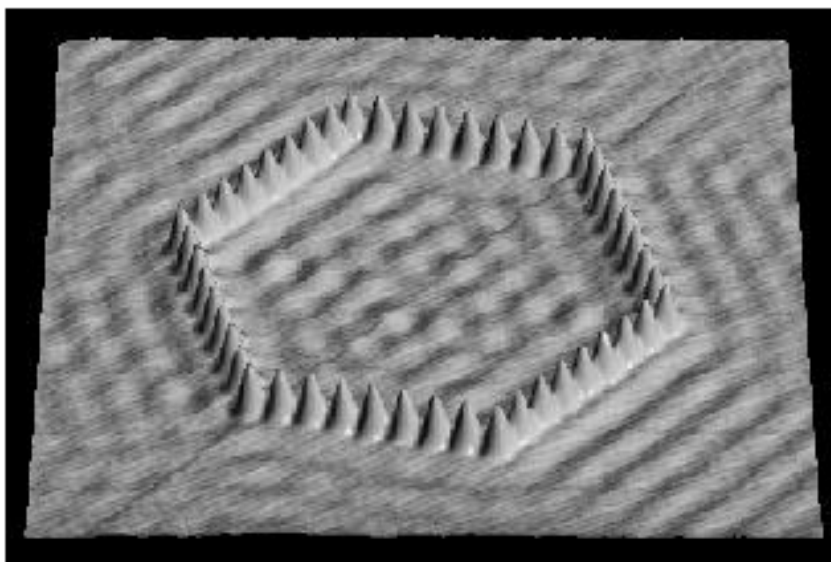
Quantum Corral



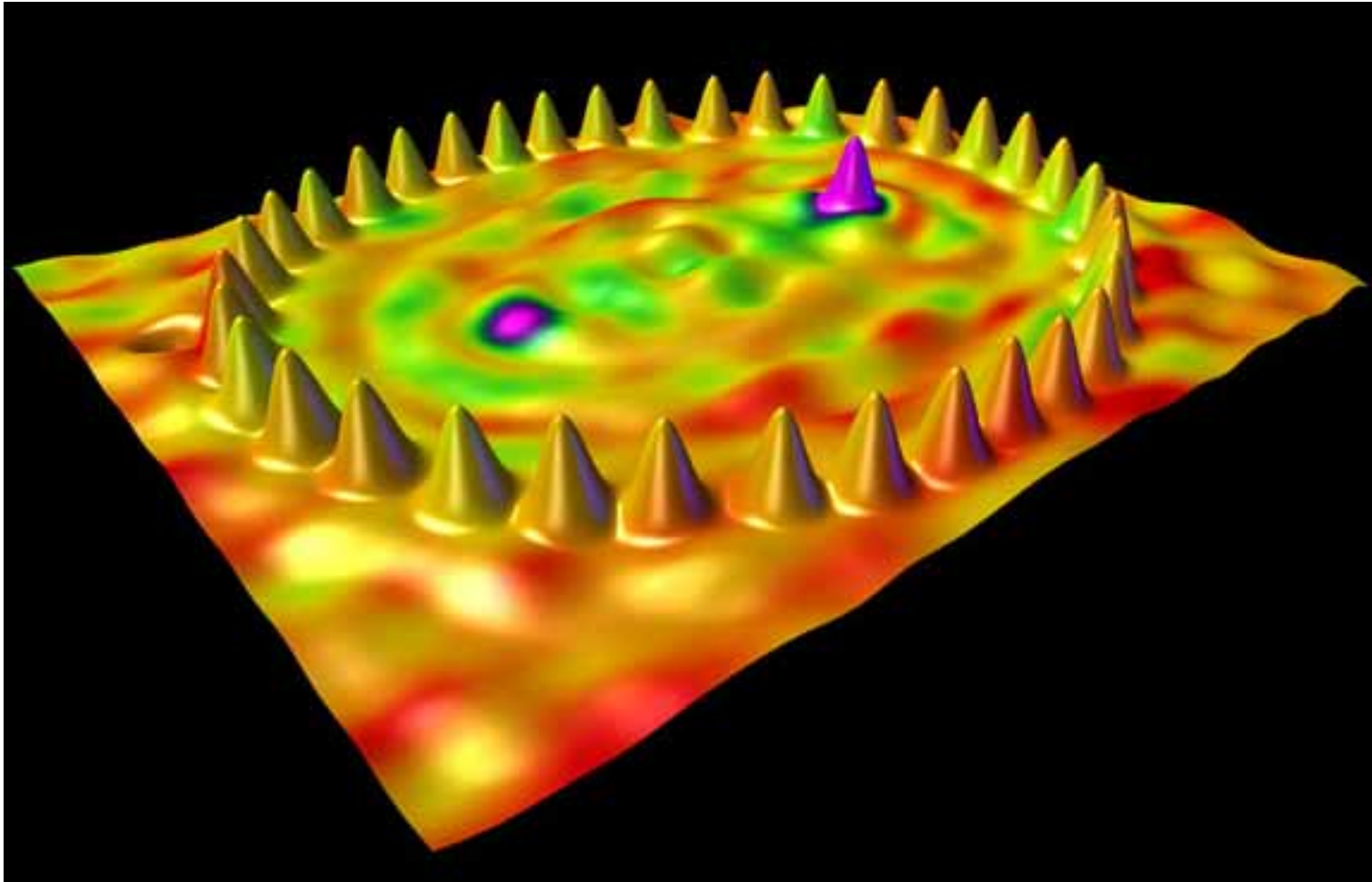
M.F. Crommie *et al.*, *Science* 262, 218 (1993).







Quantum Mirage



H. C. Manoharan *et al.*, *Nature* 403, 512 (2000).

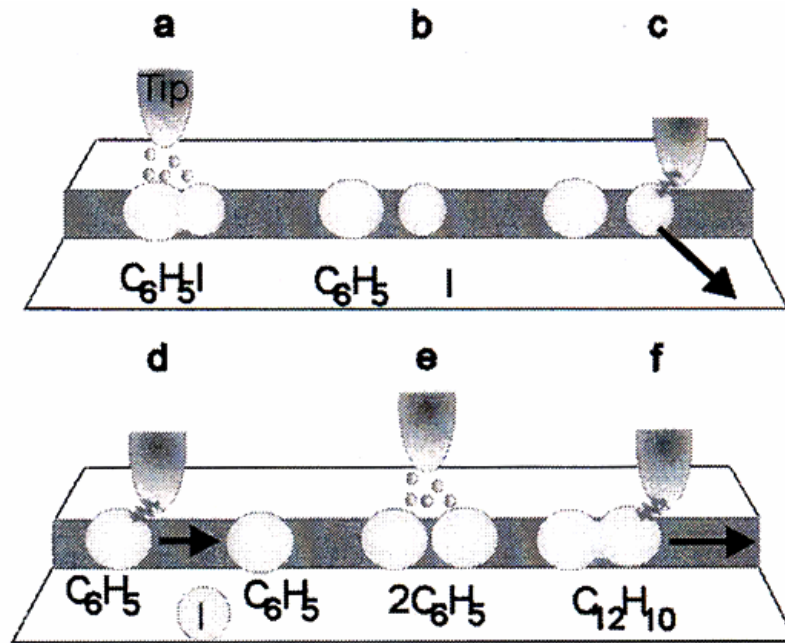
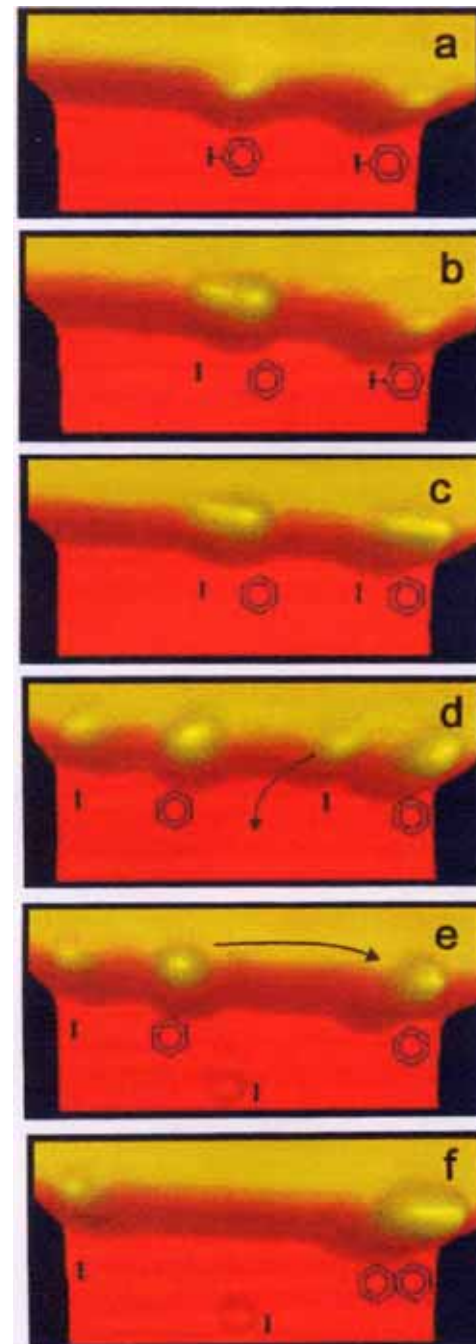
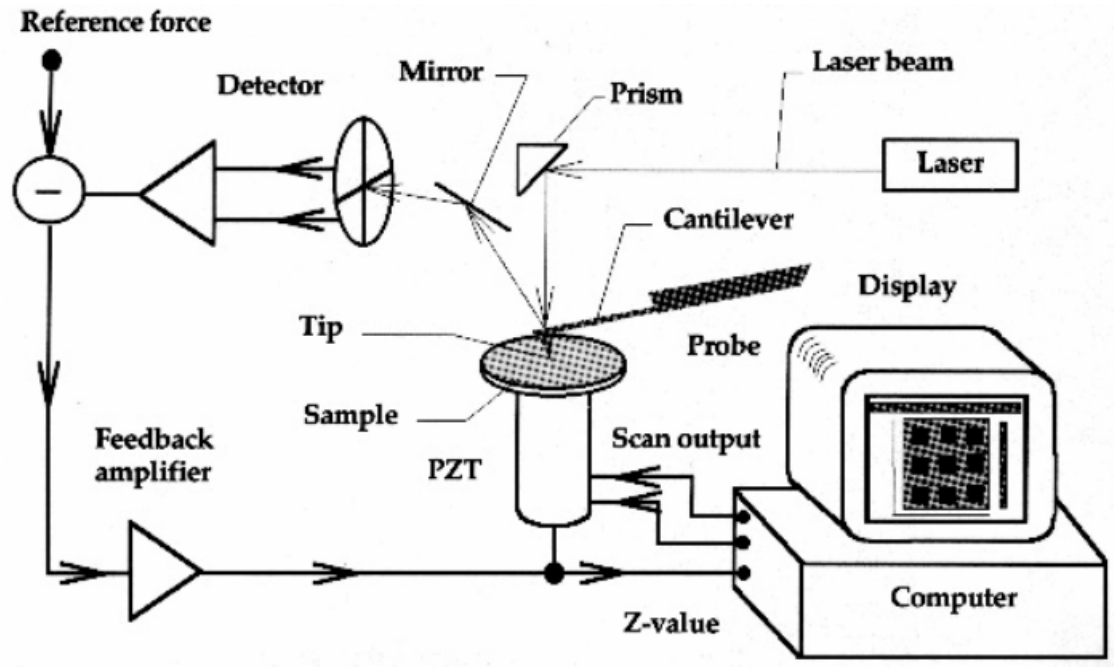


FIG. 1. Schematic illustration of the STM tip-induced synthesis steps of a biphenyl molecule. (a),(b) Electron-induced selective abstraction of iodine from iodobenzene. (c) Removal of the iodine atom to a terrace site by lateral manipulation. (d) Bringing together two phenyls by lateral manipulation. (e) Electron-induced chemical association of the phenyl couple to biphenyl. (f) Pulling the synthesized molecule by its front end with the STM tip to confirm the association.



Phys. Rev. Lett. 85, 2777 (2000)

Atomic Force Microscopy (AFM)



$$F = k\Delta z$$

$$F = 10^{-9} - 10^{-6} \text{ N}$$

$$k = 0.1 - 1 \text{ N/m}$$

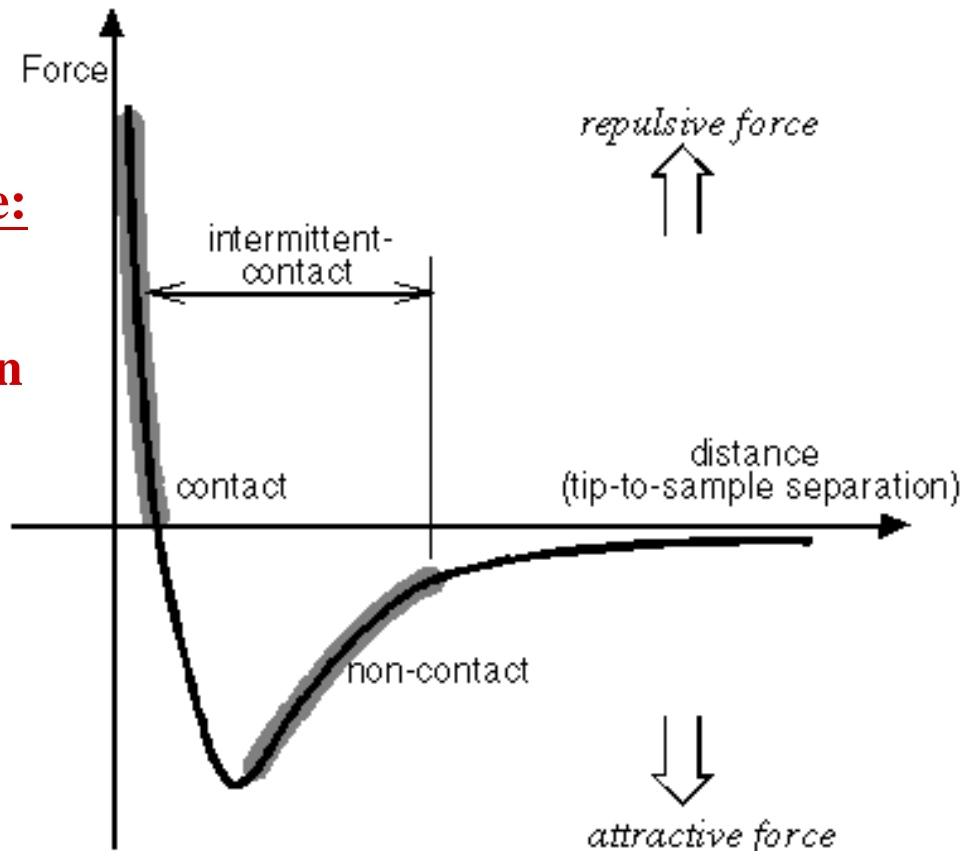
References:

- G. Binnig, C. F. Quate, and C. Gerber, Phys. Rev. Lett. 56, 930 (1986).
- C. Bustamante and D. Keller, Physics Today, 32, December (1995).
- R. Wiesendanger and H.J. Güntherodt, *Scanning Tunneling Microscopy II*, Springer-Verlag, (1992).

Interaction between the probe and sample

Short-range:

- 1) Bonding
- 2) Repulsion



Long-range:

- 1) Van der Waal
- 2) Capillary
- 3) Magnetic
- 4) Electrostatic

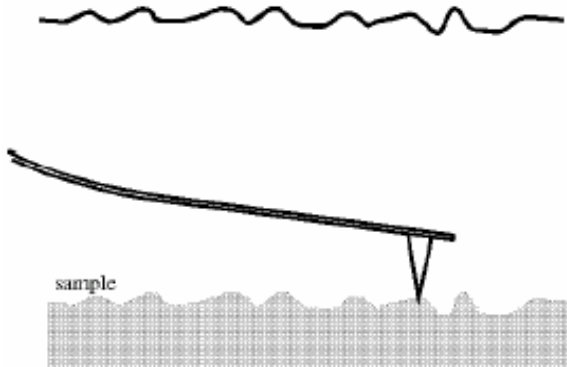
Lennard-Jones potential $\phi(r) = - A/r^6 + B/r^{12}$

Three scanning modes of AFM

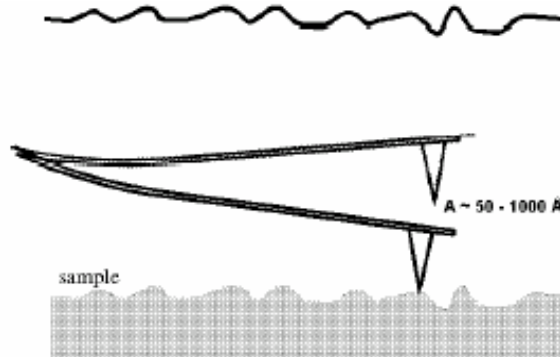
接觸式

暫接觸式

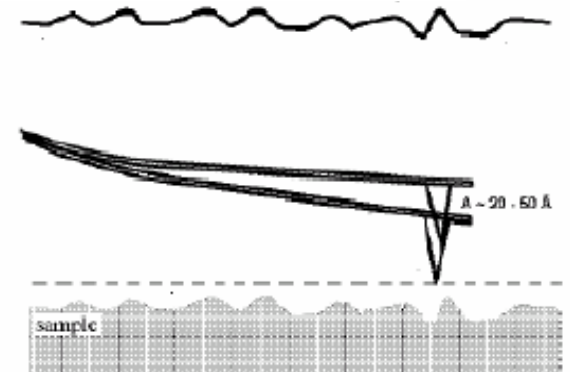
非接觸式



**Contact
Mode AFM**



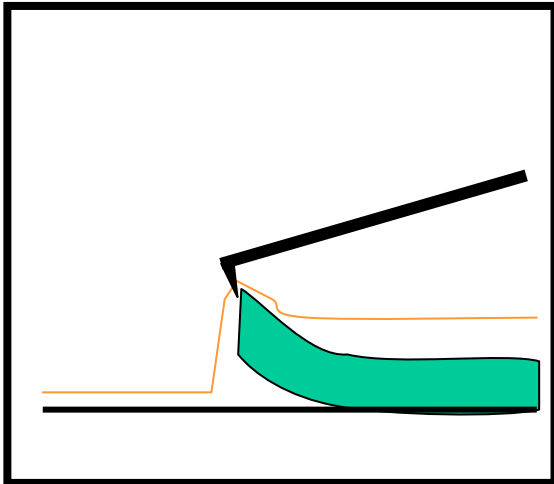
**Semicontact
Mode AFM**



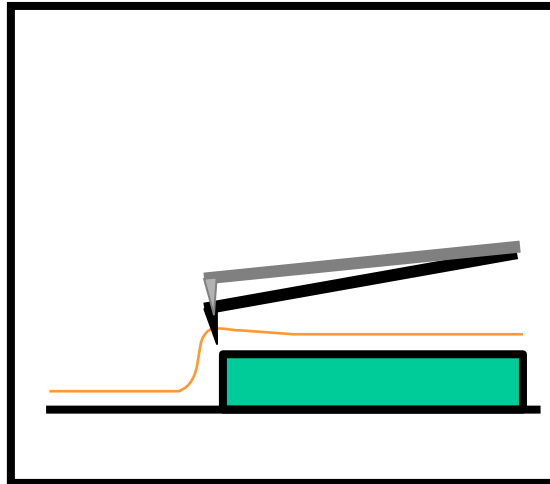
**Non-contact
Mode AFM**

三種 AFM 掃描模式之比較

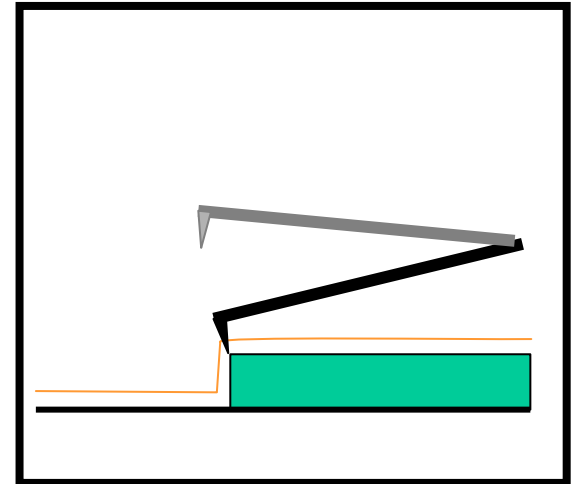
Contact



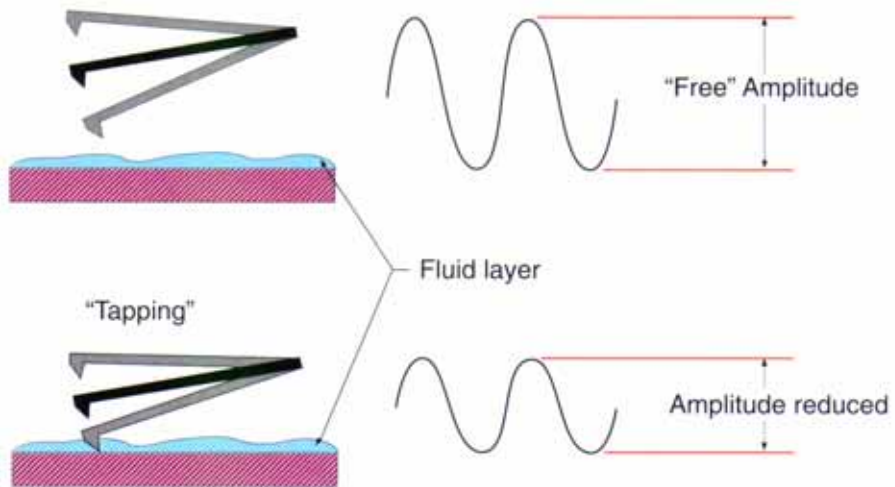
Non-contact



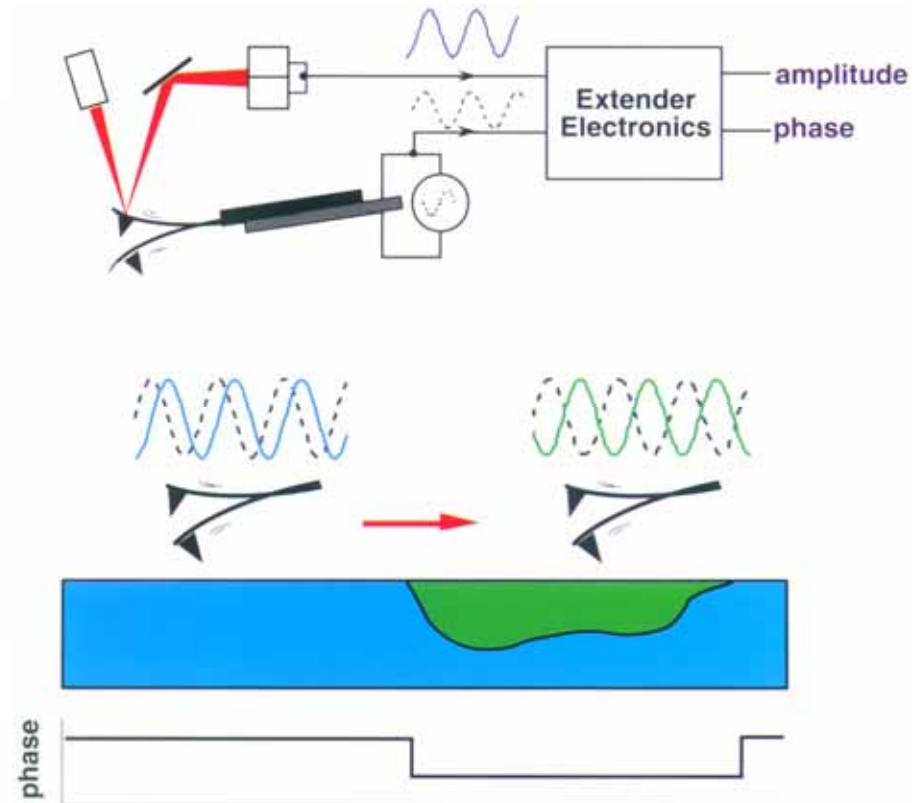
Semi-contact

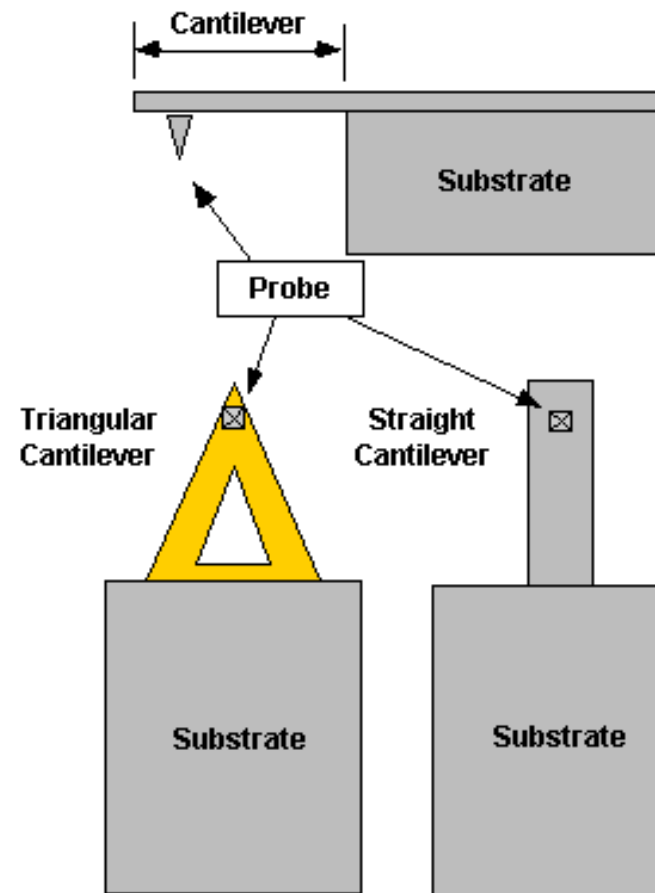
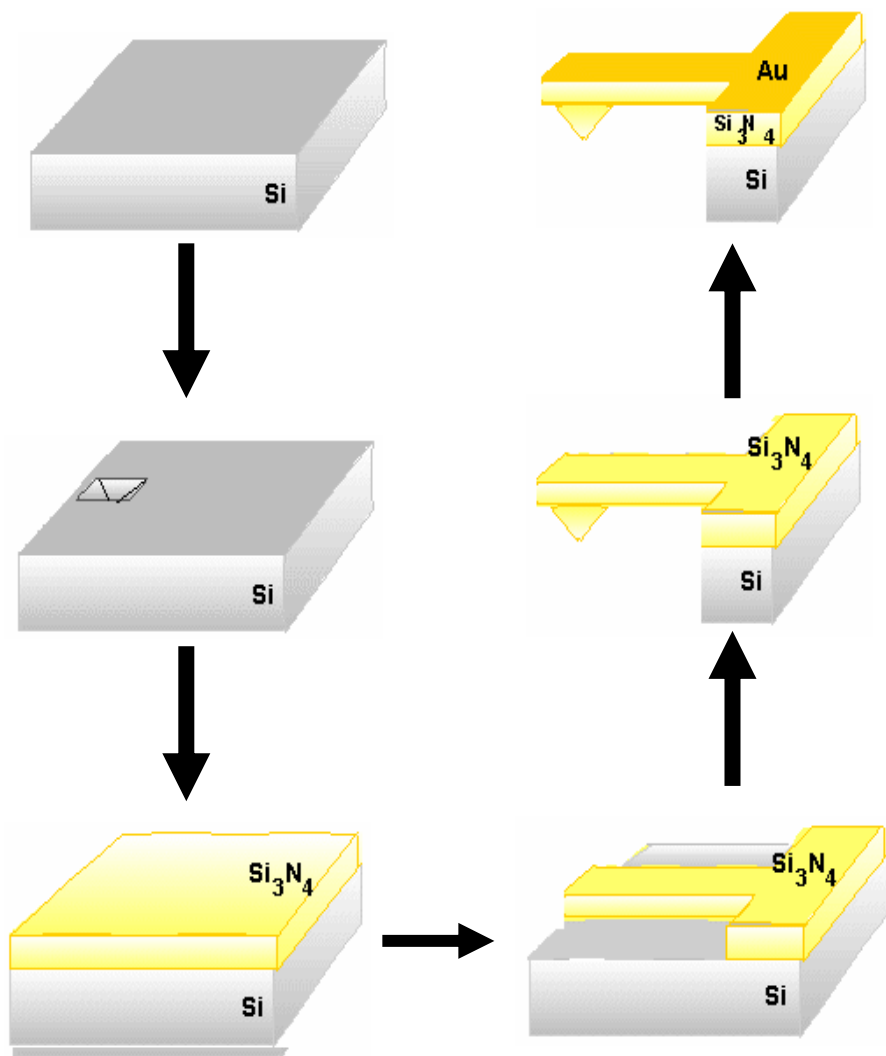


Tapping Mode (10-300 kHz)



Phase image

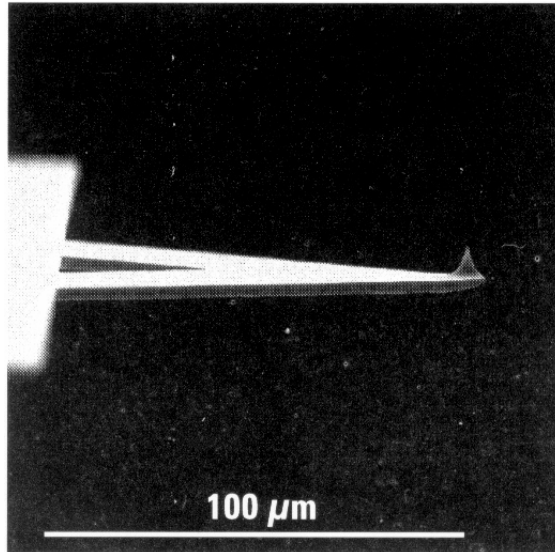




Typical Tip Dimension:
 $150\mu\text{m} \times 30\mu\text{m} \times 0.5\mu\text{m}$
 $k \sim 0.1 \text{ N/m}$
 Materials: Si_3N_4

Typical Tip Dimension:
 $150\mu\text{m} \times 30\mu\text{m} \times 3\mu\text{m}$
 $f_r \sim 100 \text{ kHz}$
 Materials: Si

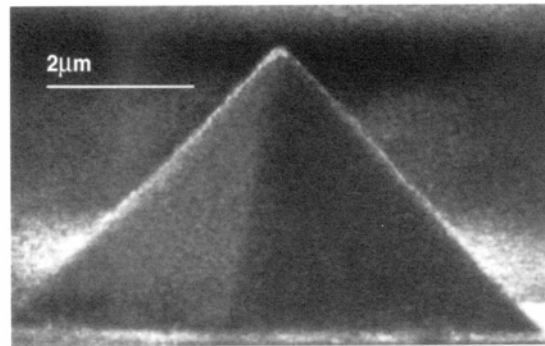
V-shaped



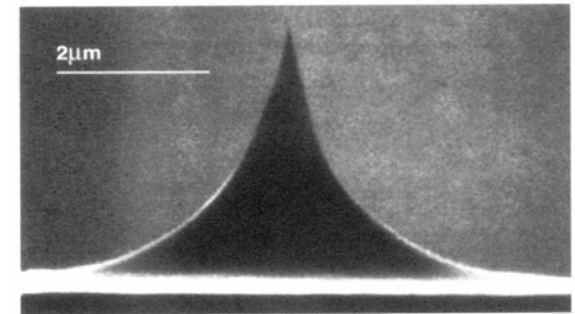
Materials: Si, SiO₂, Si₃N₄

Ideal Tips: hard, small radius of curvature, high aspect ratio

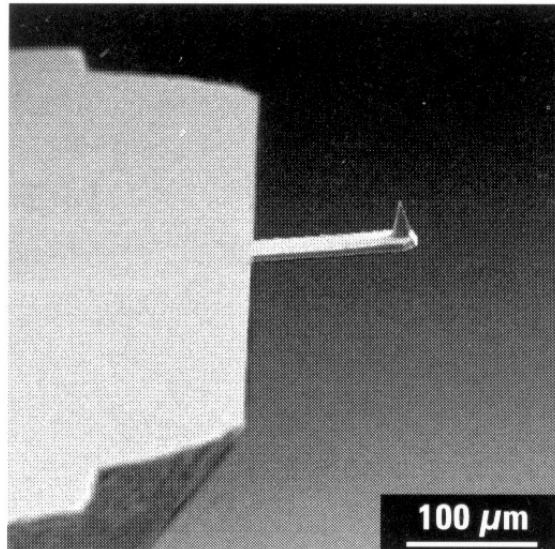
Pyramid Tip



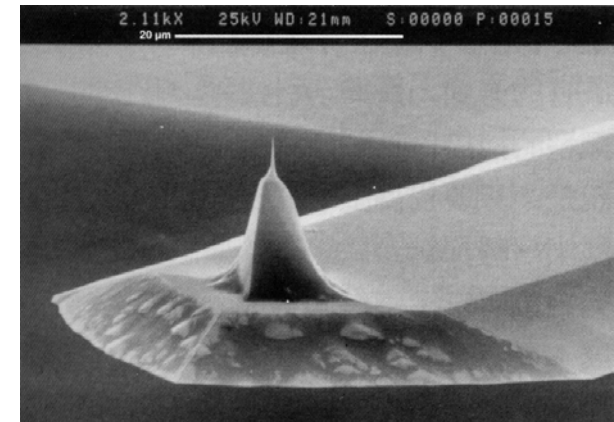
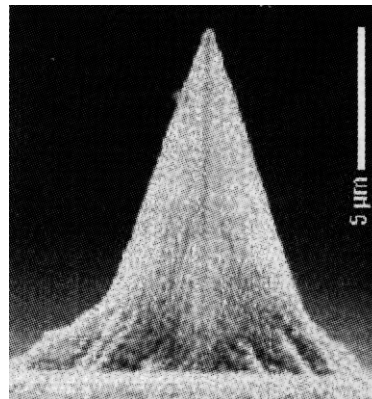
Ultrasharp Tip



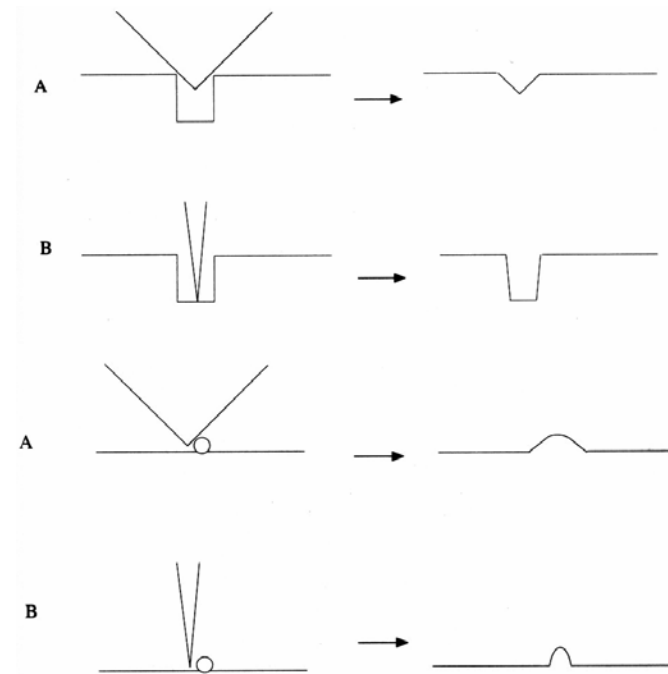
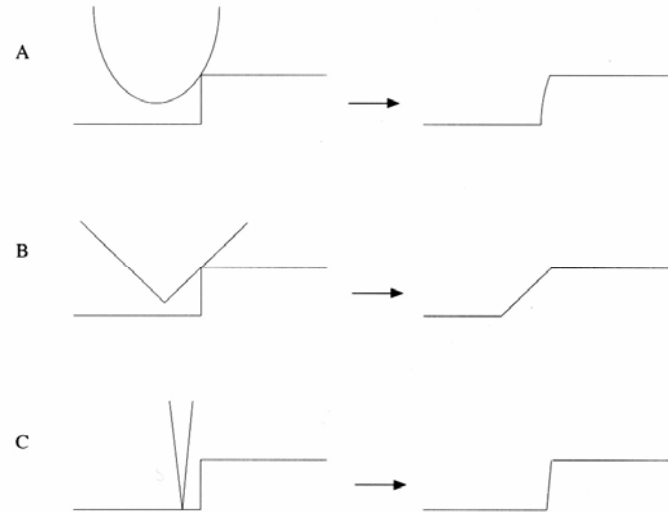
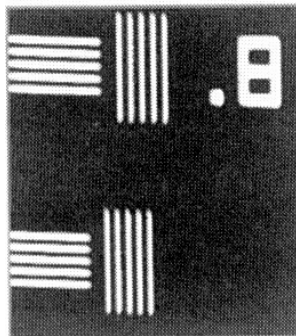
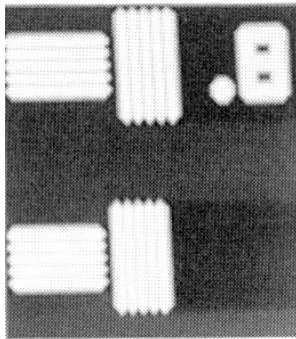
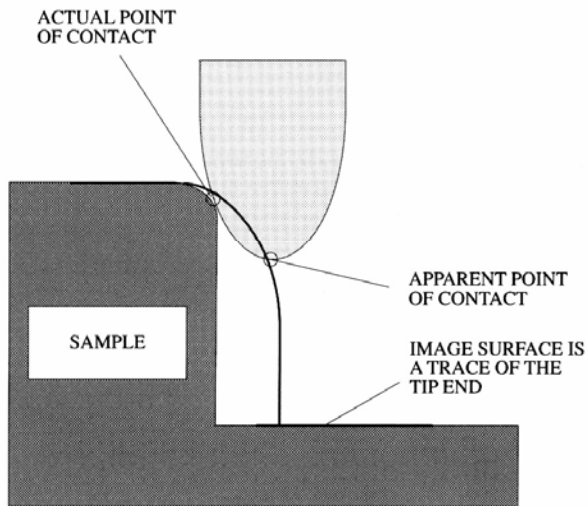
Rectangular-shaped

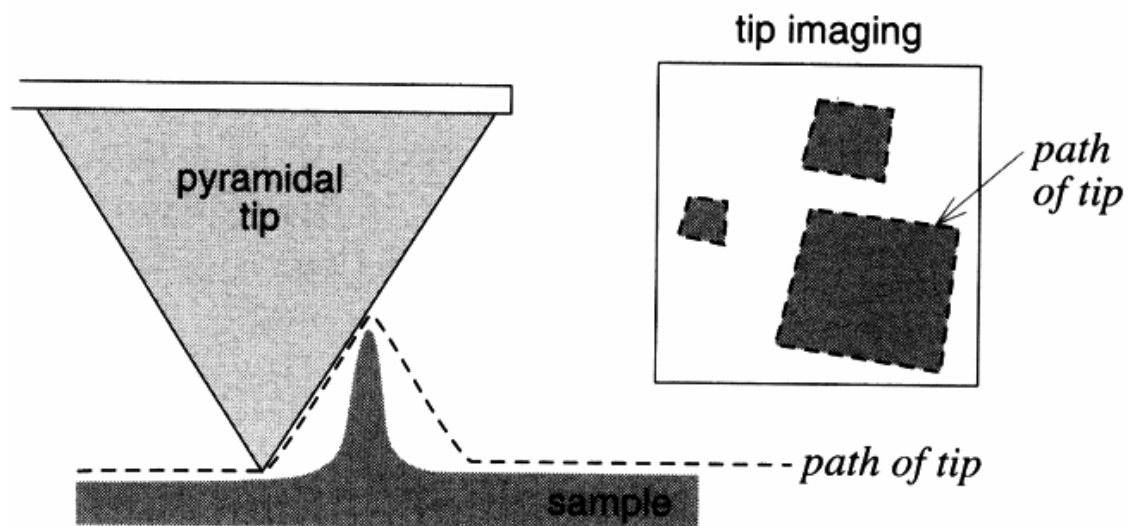
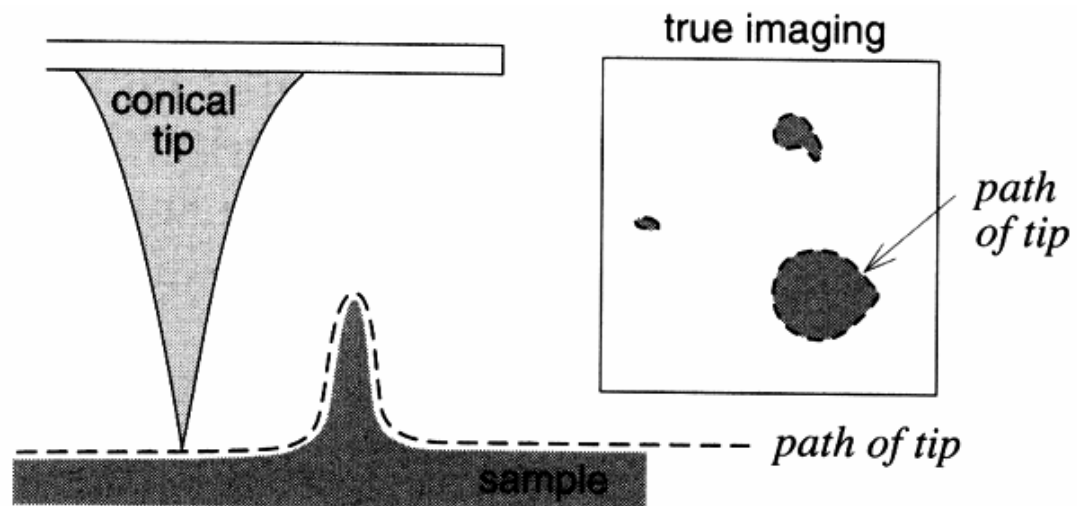


Diamond-coated Tip



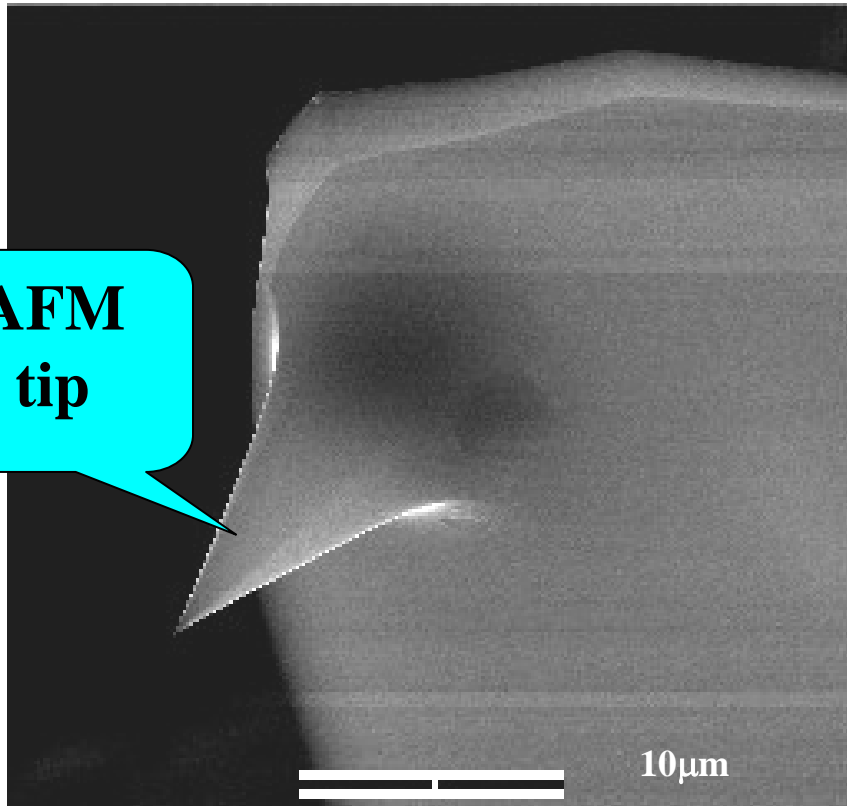
Effects of the Tip Shape



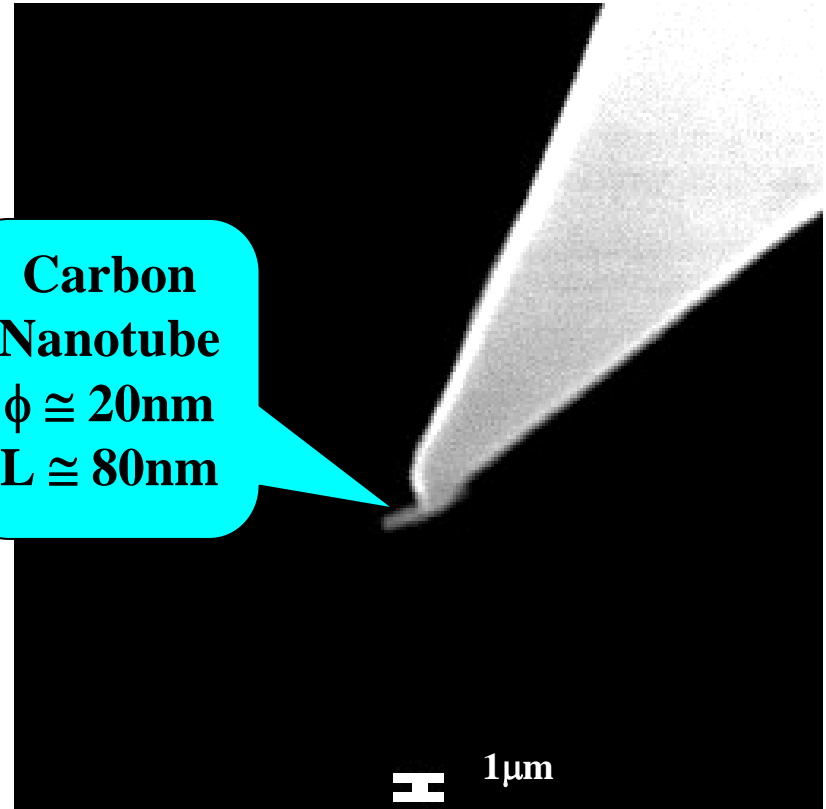


AFM Tip + Carbon Nanotube

**AFM
tip**

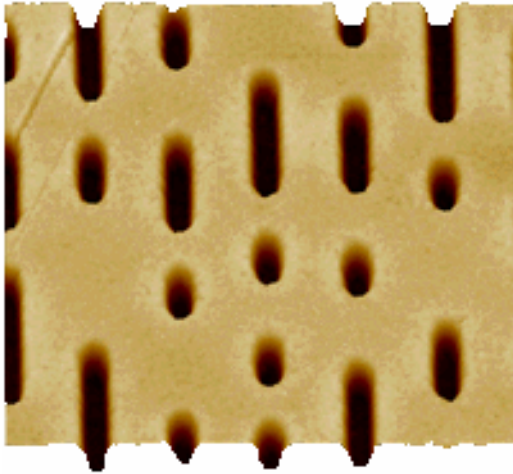


**Carbon
Nanotube**
 $\phi \cong 20\text{nm}$
 $L \cong 80\text{nm}$

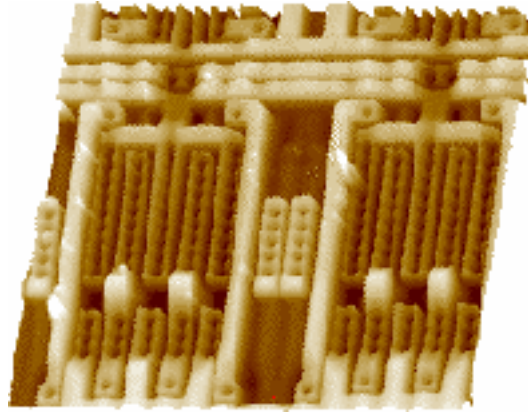


AFM images

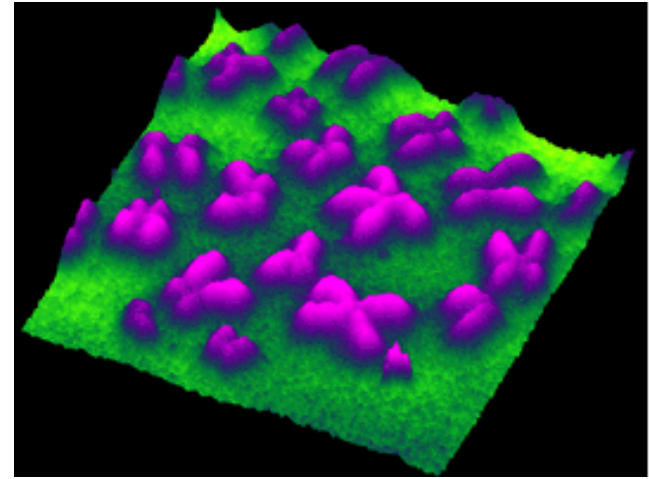
CD pits



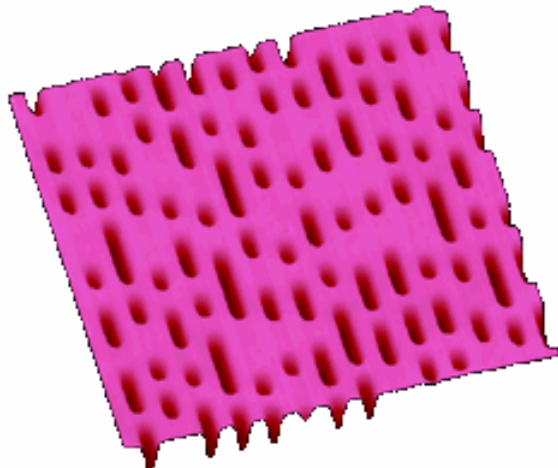
Integrated circuit



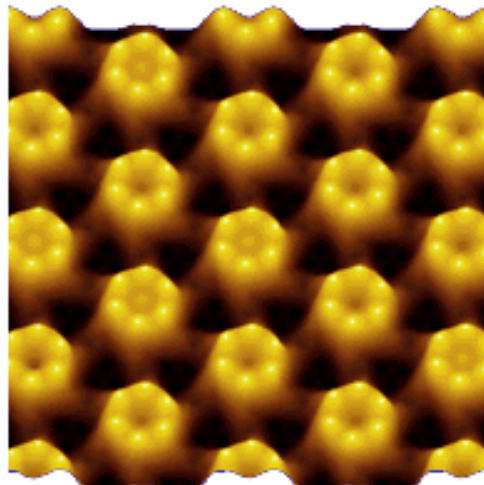
Chromosomes



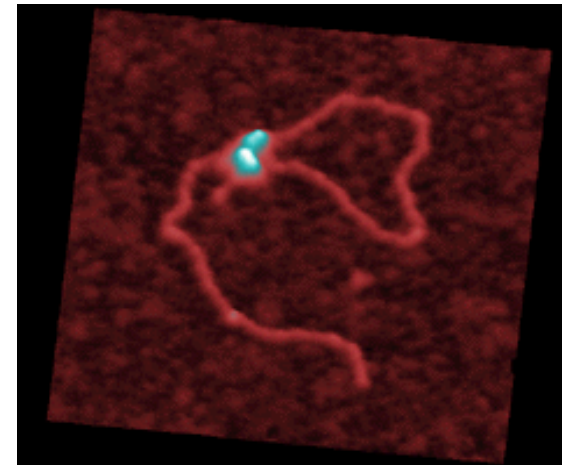
DVD pits



Bacteria

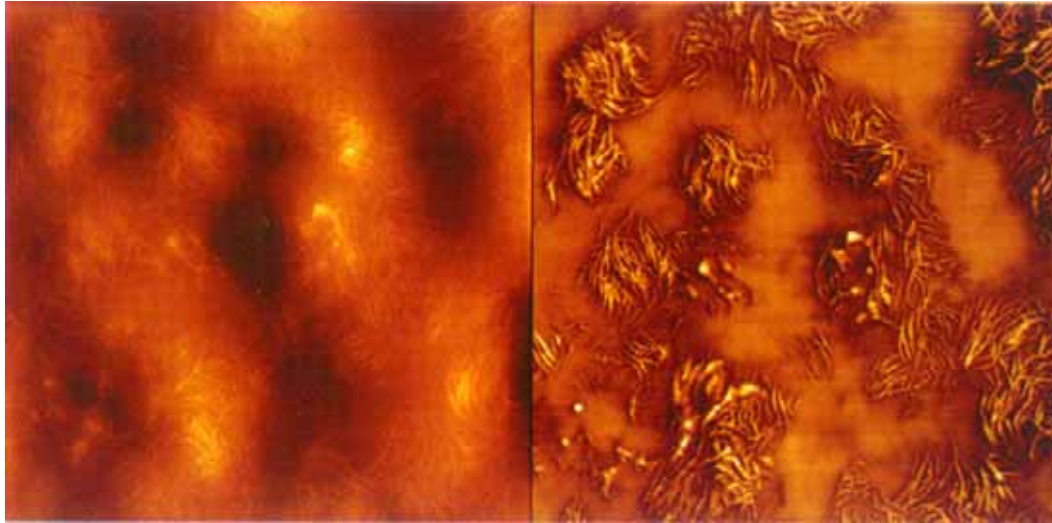


DNA



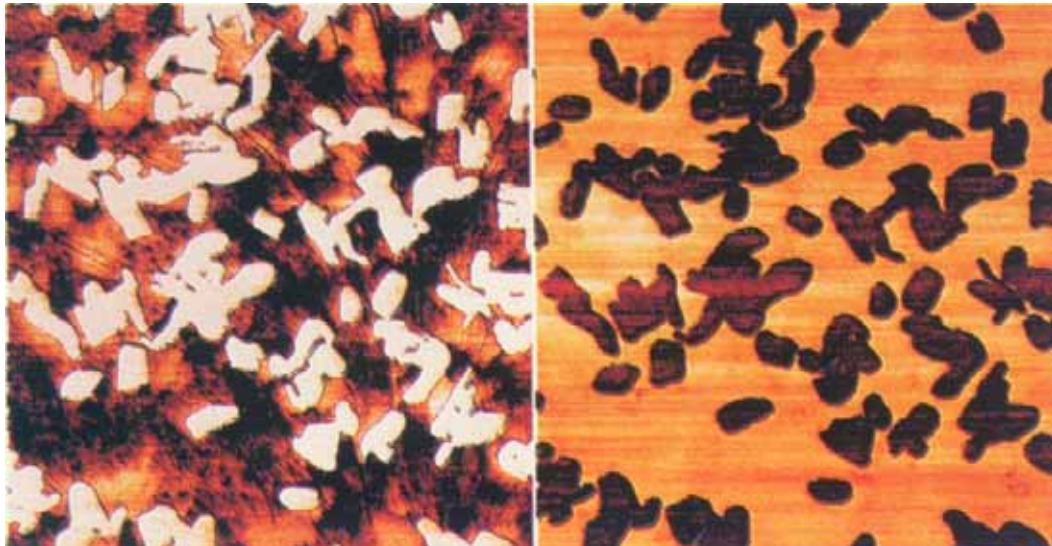
Height image

Phase Image



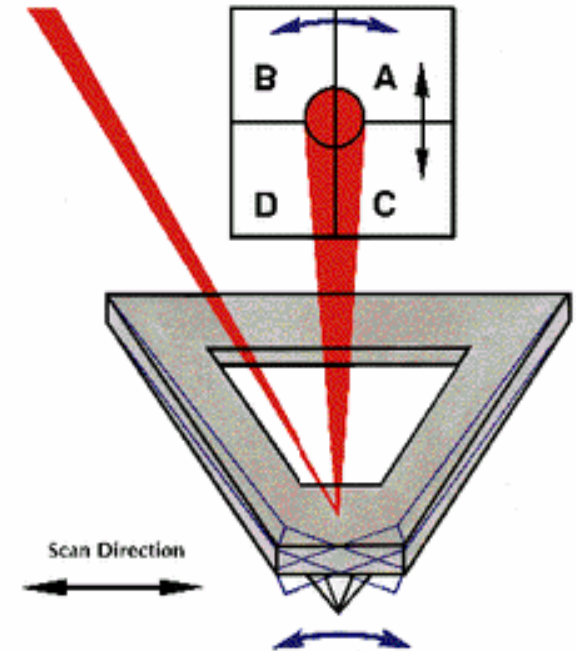
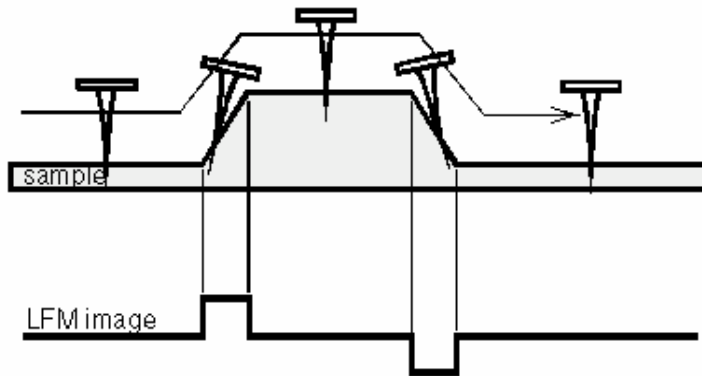
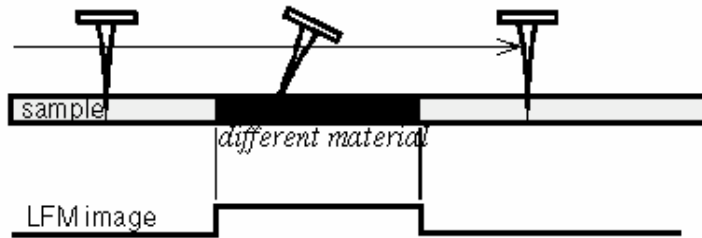
Phase image

Lateral force Image



MoO₃ on
MoS₂

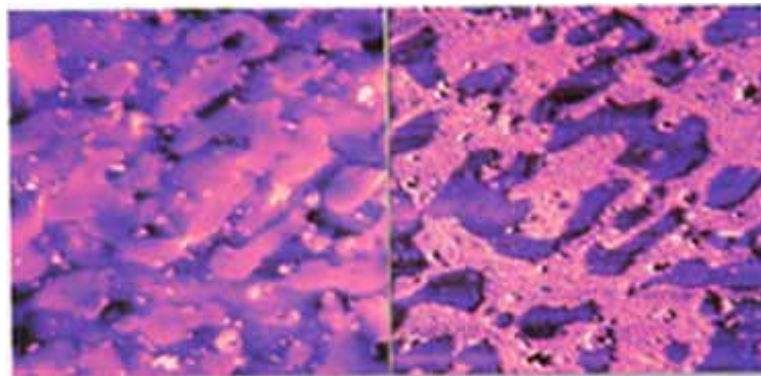
Lateral Force Microscopy



$$(A+C) - (B+D)$$

Topography

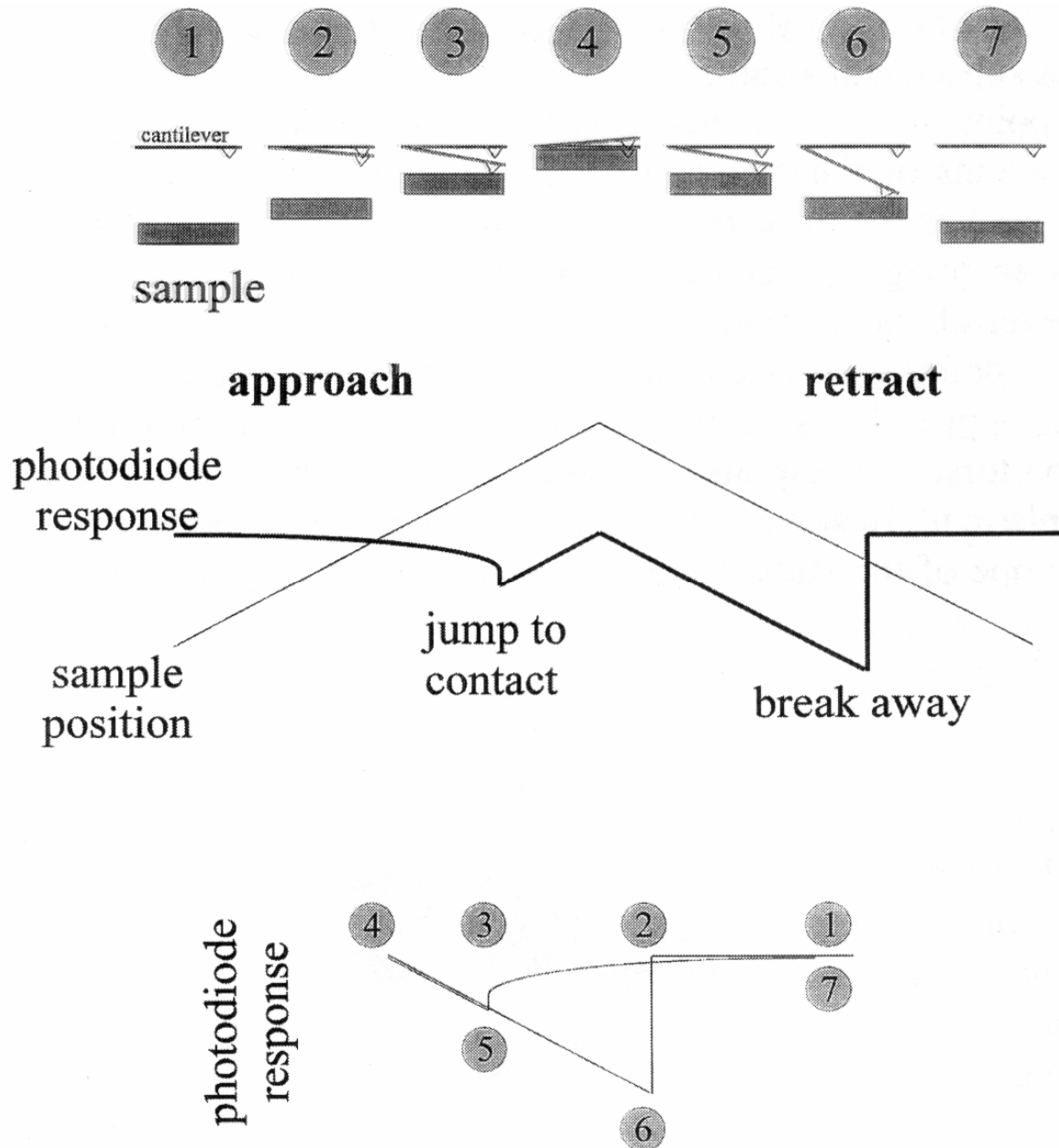
12 μm

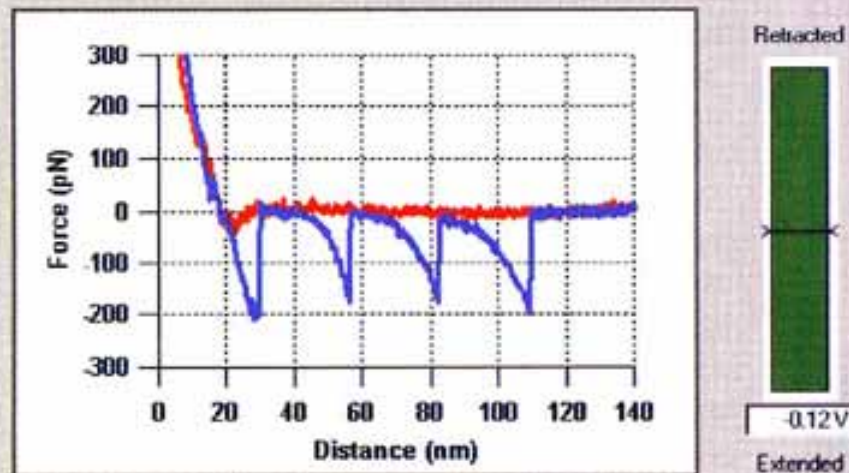
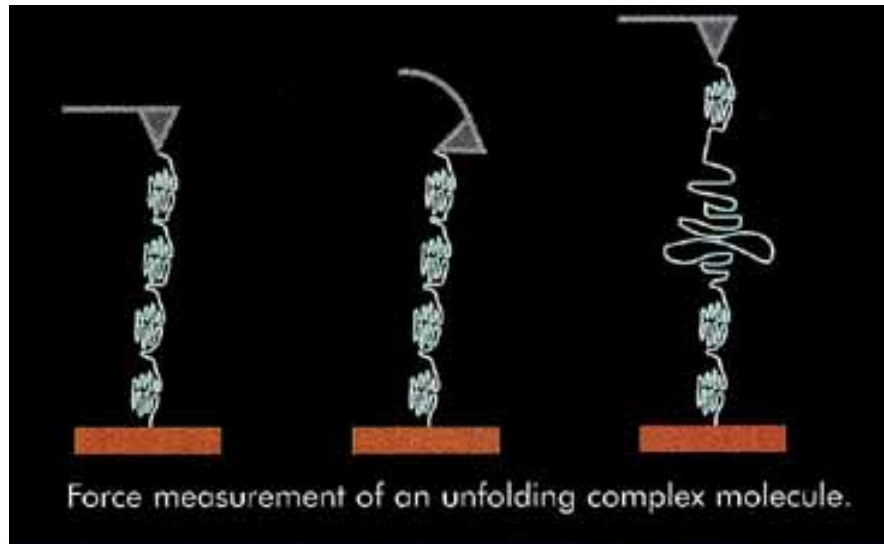


LFM image

Nature rubber/EDPM
blend

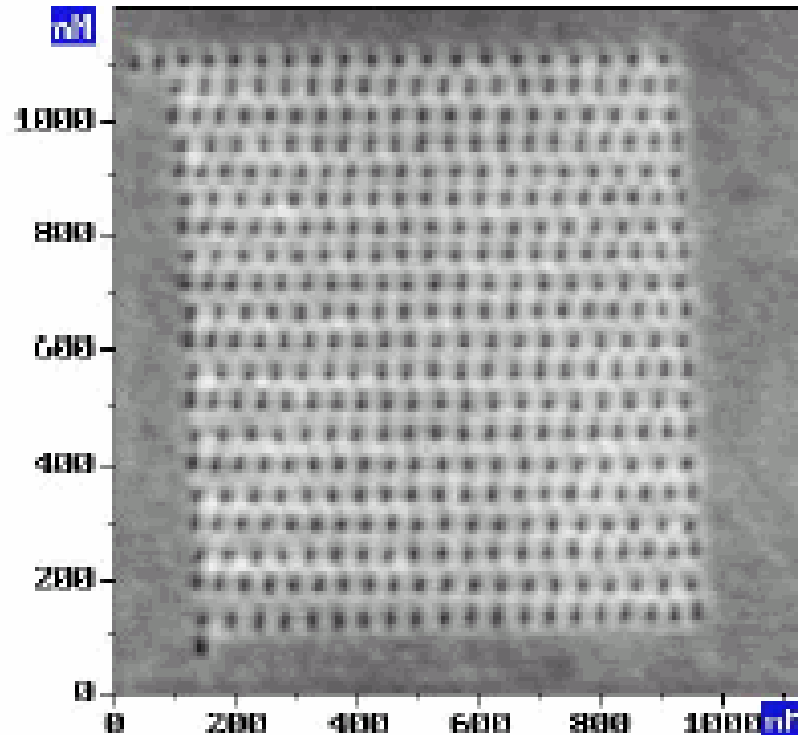
Force-Distance Curve



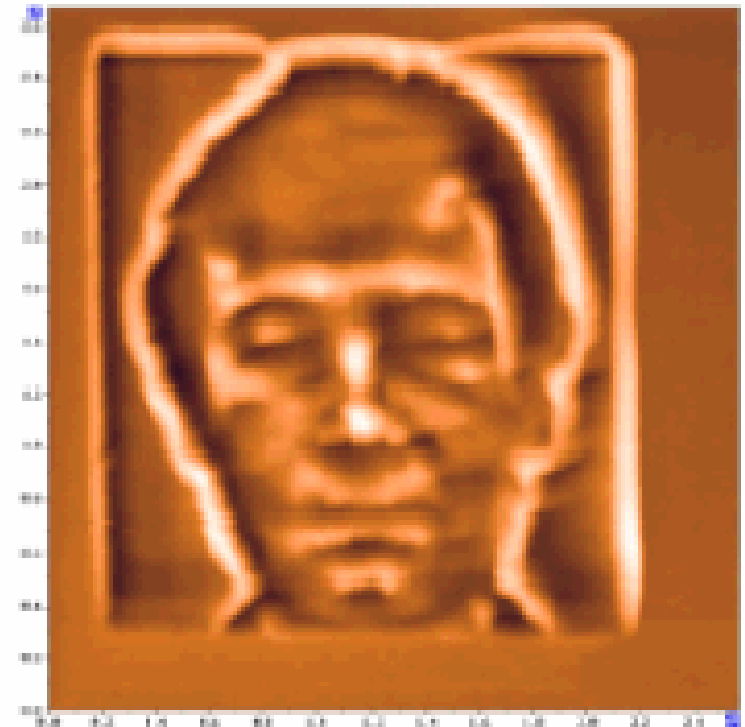


Advanced graphical user interface shows titin muscle molecule force curve.

Nanolithography of Tapping-Mode AFM



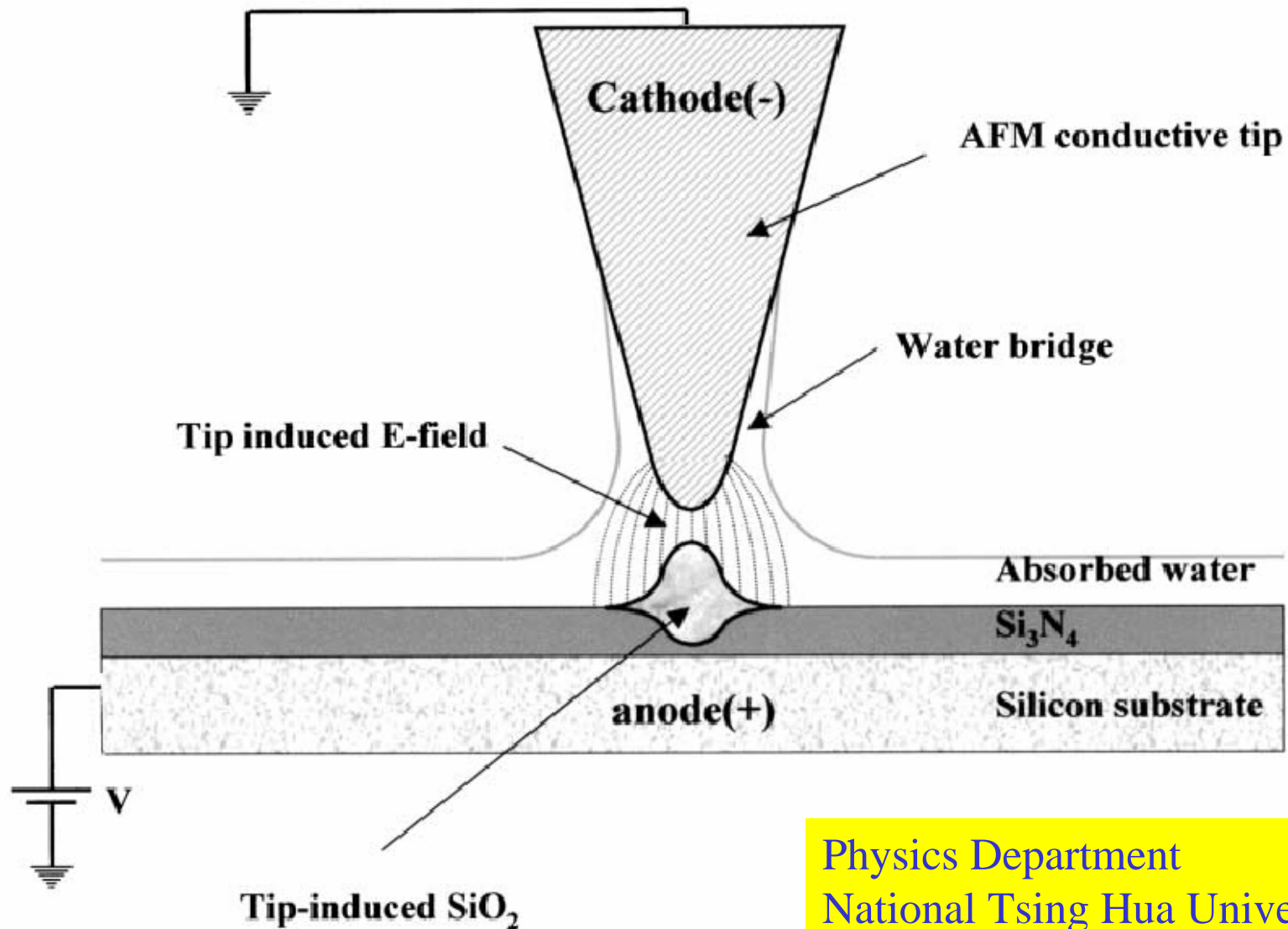
(1.2 μm \times 1.2 μm)



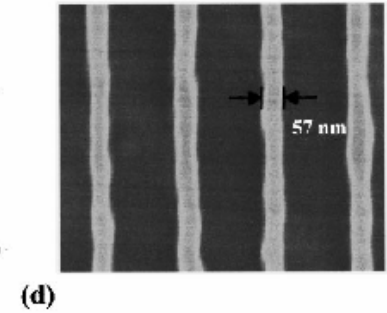
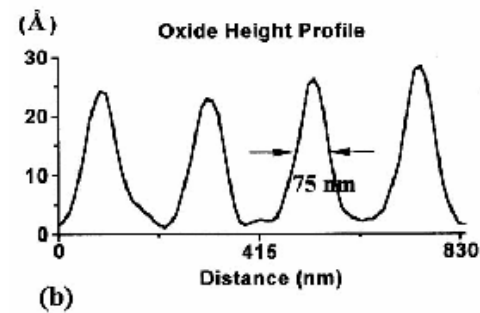
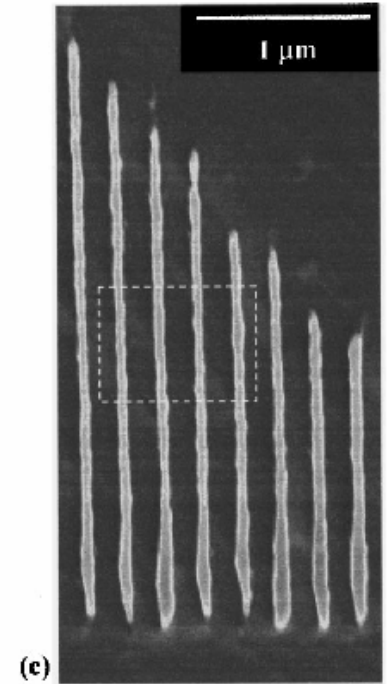
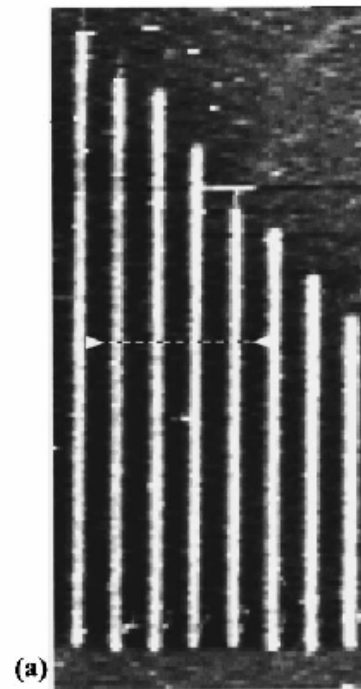
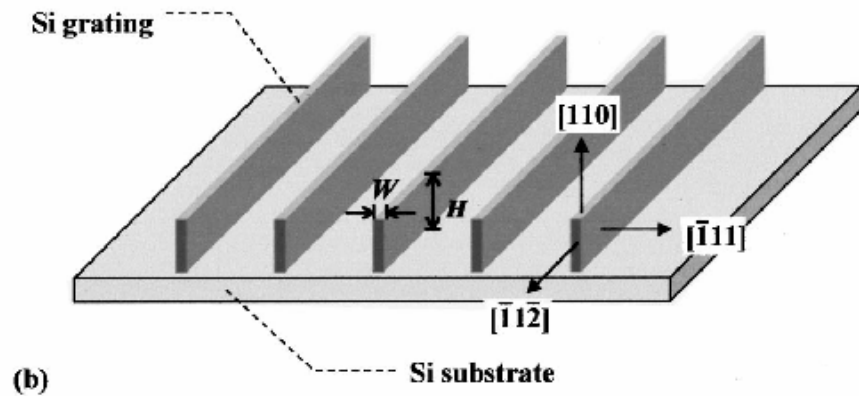
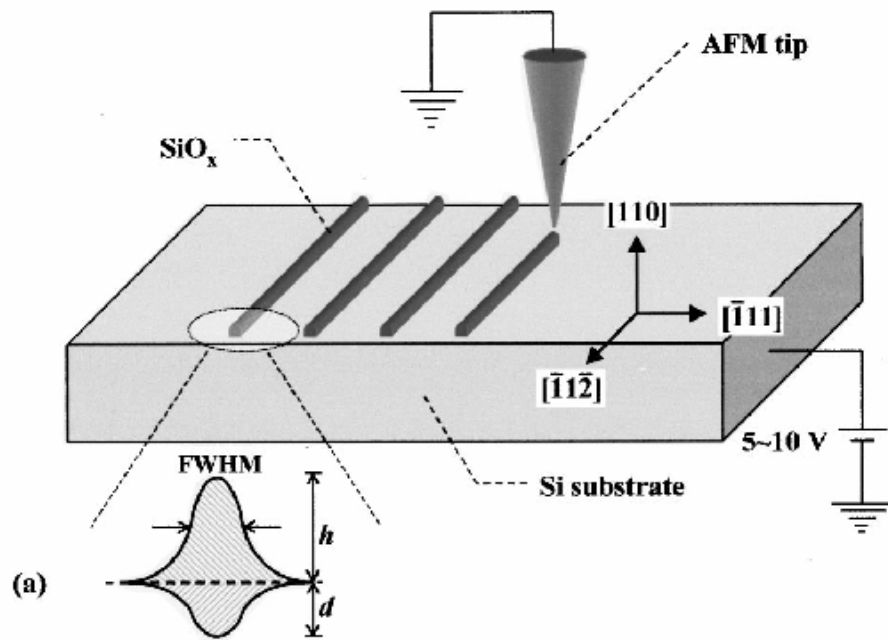
(2.5 μm \times 2.5 μm)

Image of polycarbonate film on silicon surface

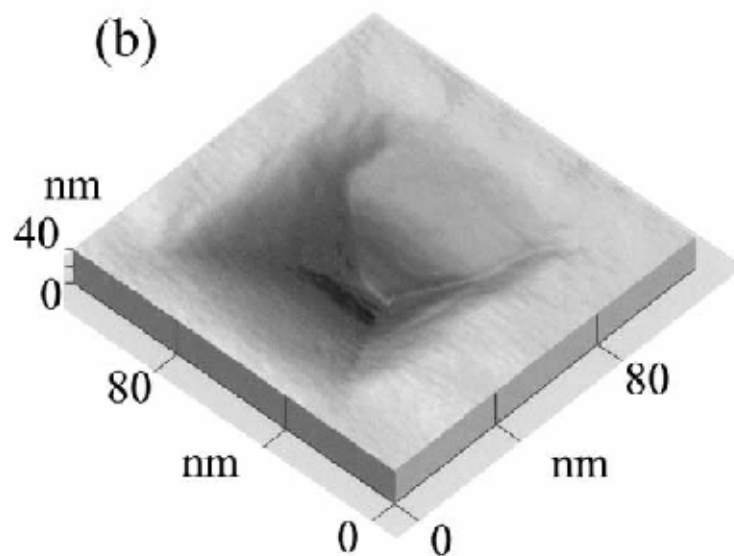
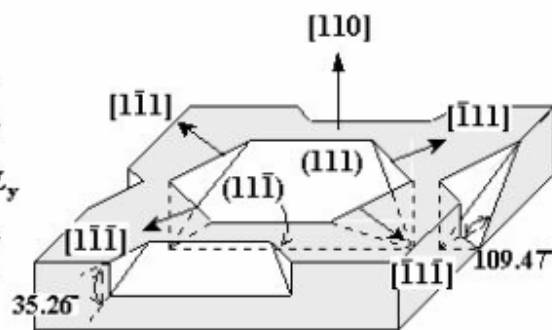
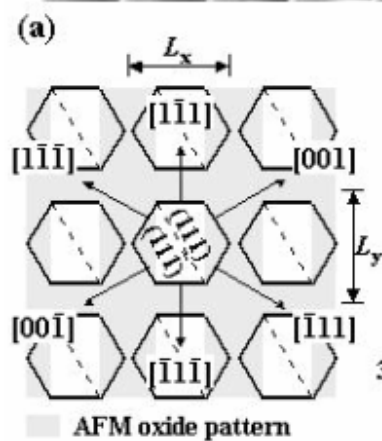
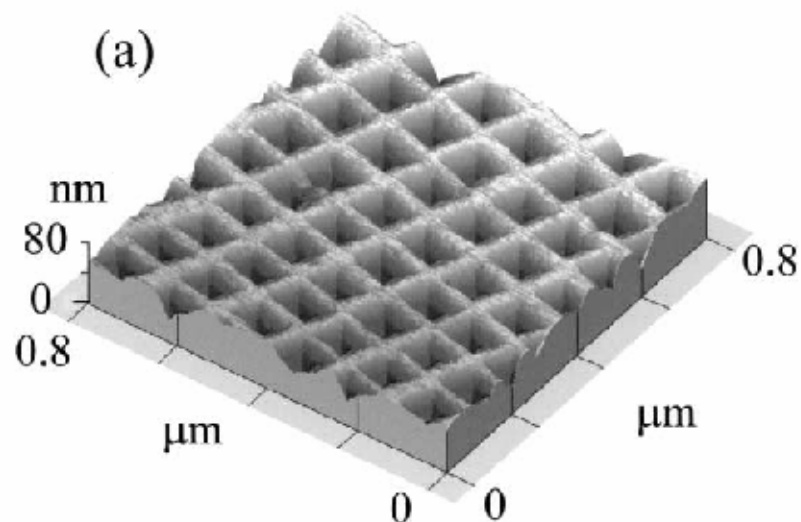
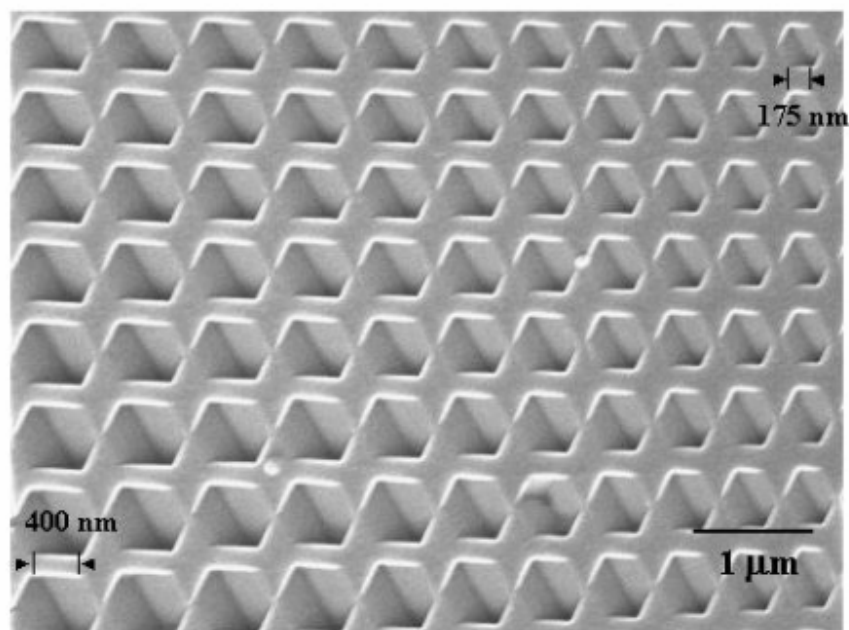
Nano-Lithography with an AFM tip



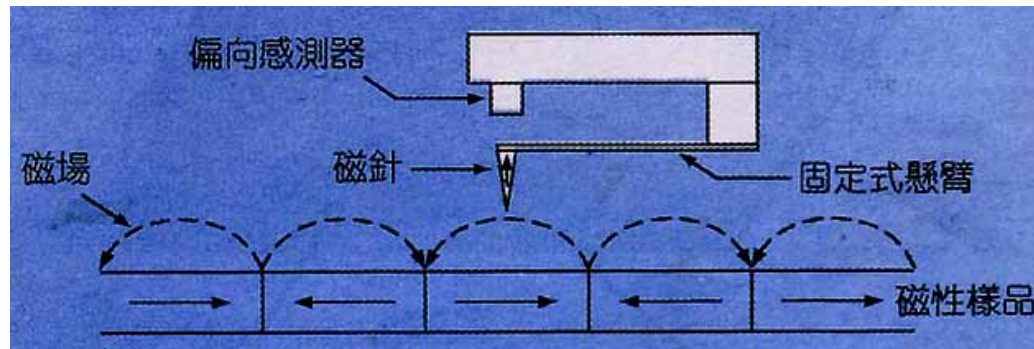
Physics Department
National Tsing Hua University



F.S.-S. Chien et al., APL 75, 2429 (1999)



Magnetic Force Microscopy (MFM)



$$F = (\mathbf{m} \cdot \nabla) H$$

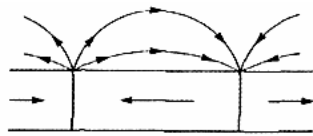
The tip is scanned several tens or hundreds of nanometers above the sample, avoiding contact. Magnetic field gradients exert a force on the tip's magnetic moment, and monitoring the tip/cantilever response gives a magnetic force image. To enhance sensitivity, most MFM instruments oscillate the cantilever near its resonant frequency with a piezoelectric element. Gradients in the magnetic forces on the tip shift the resonant frequency of the cantilever. Monitoring this shift, or related changes in oscillation amplitude or phase, produces a magnetic force image.

Tips: silicon probes are magnetically sensitized by sputter coating with a ferromagnetic material.

Resolution 10~25 nm.

Applications: hard disks, magnetic thin film materials, micromagnetism.

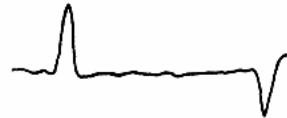
MFM Images



Parallel
Component

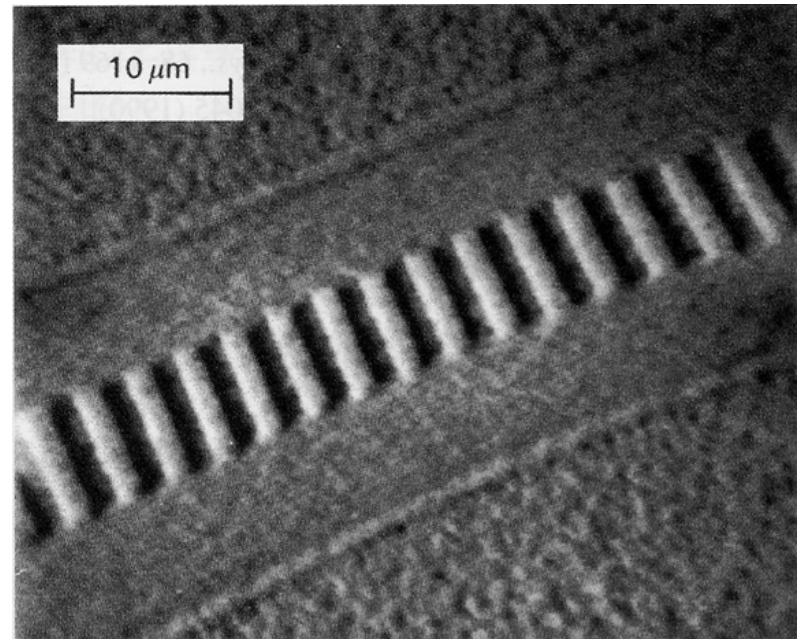
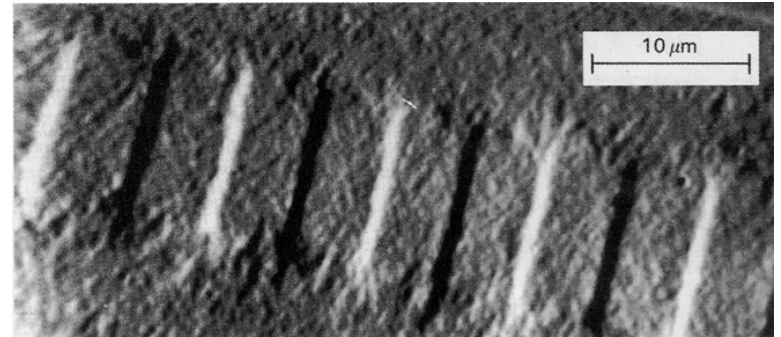


Perpendicular
Component

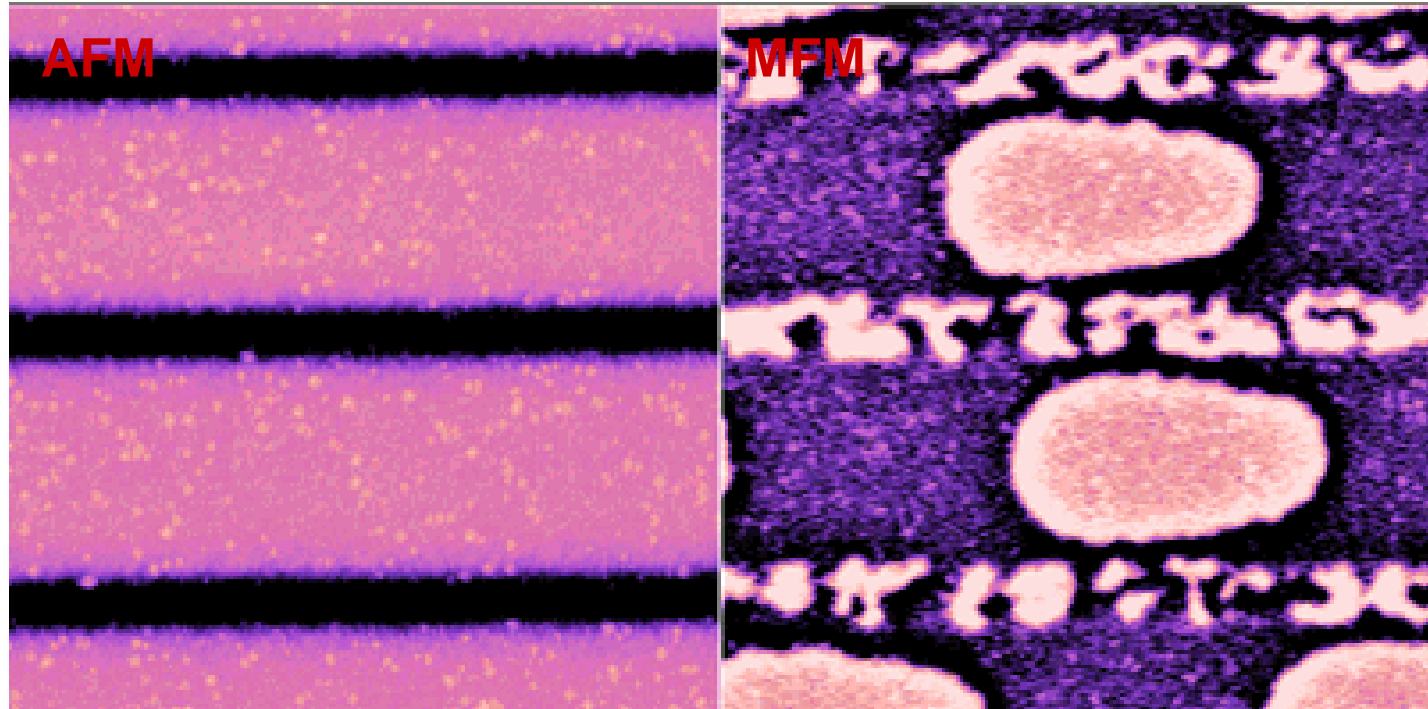


Magnetic Field from
Transitions

Experimental
MFM Traces



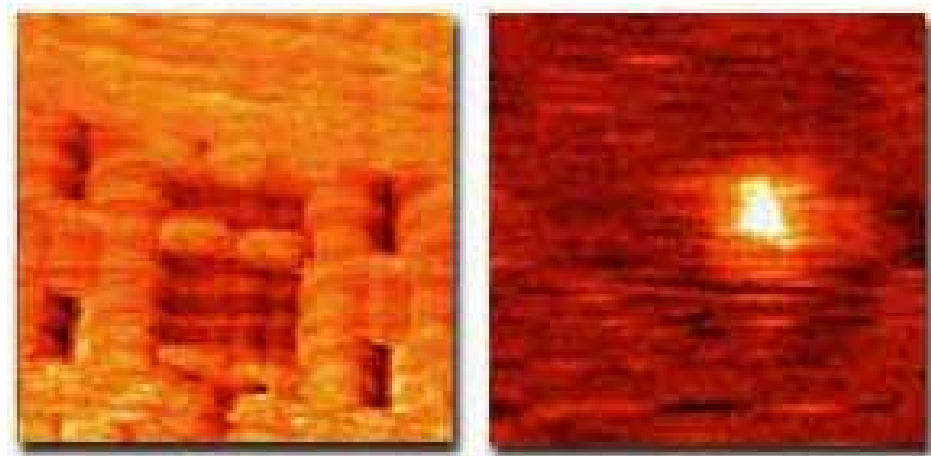
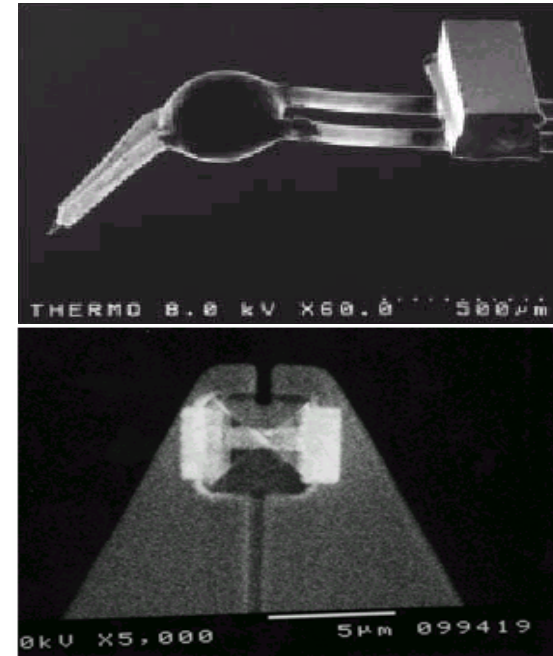
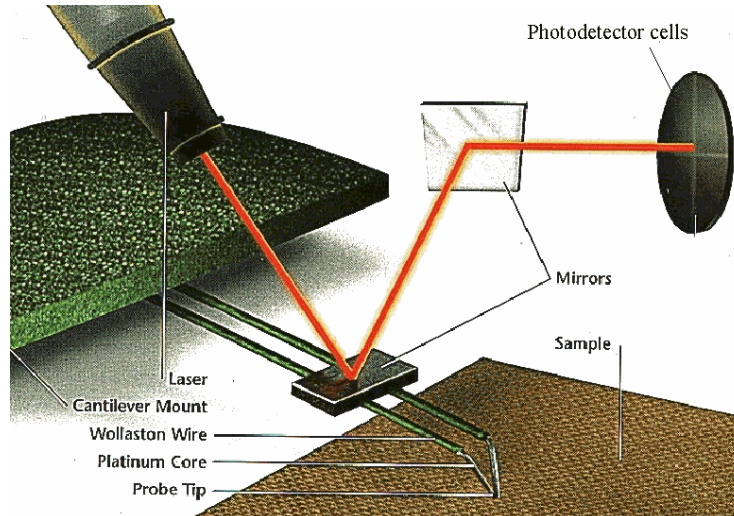
Magnetic Force Microscopy



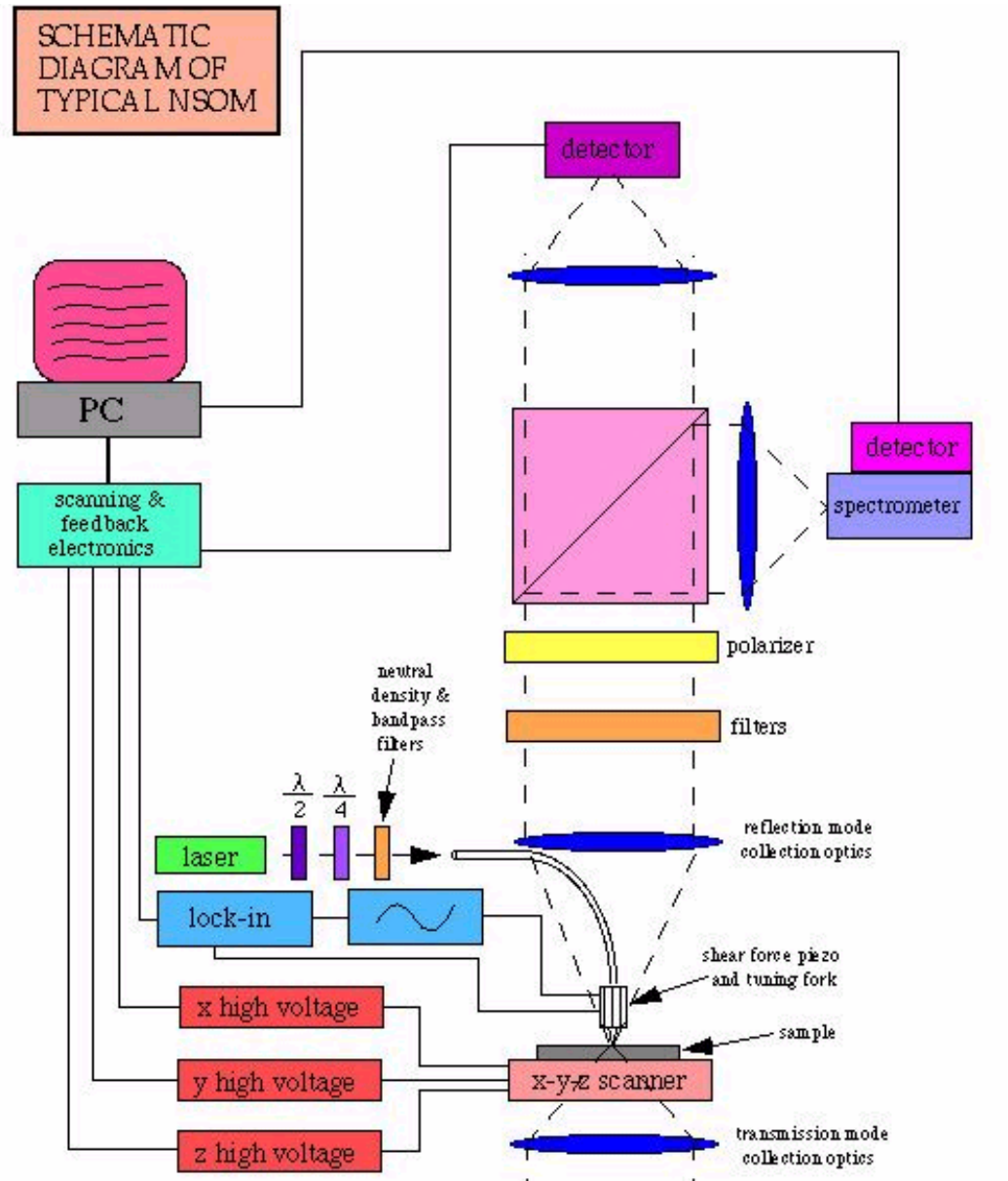
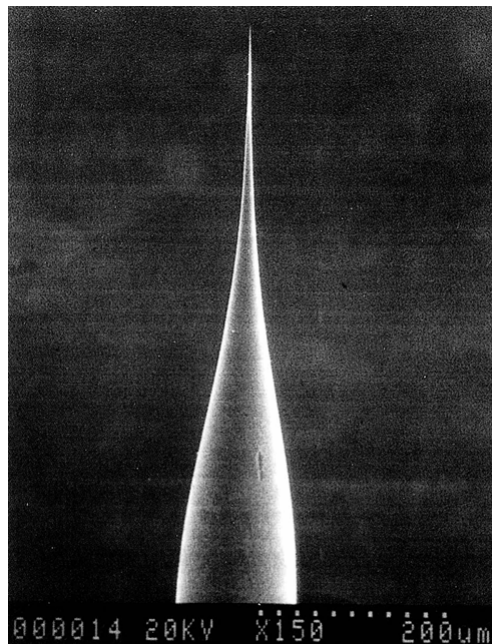
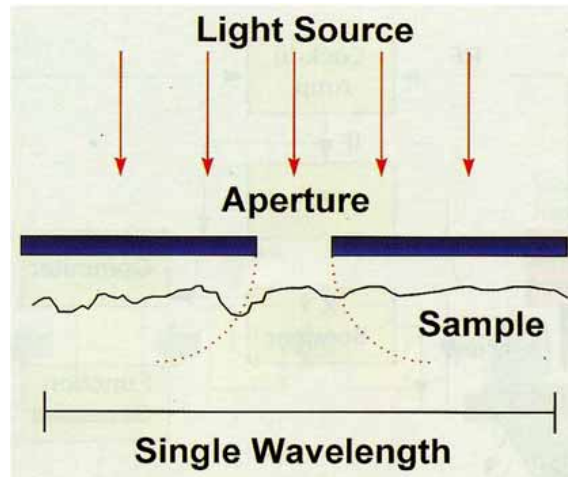
Bits (50 nm) on a magneto-optical disk.

Scan area (5 μ m x 5 μ m)

Scanning Thermal Microscopy (SThM)

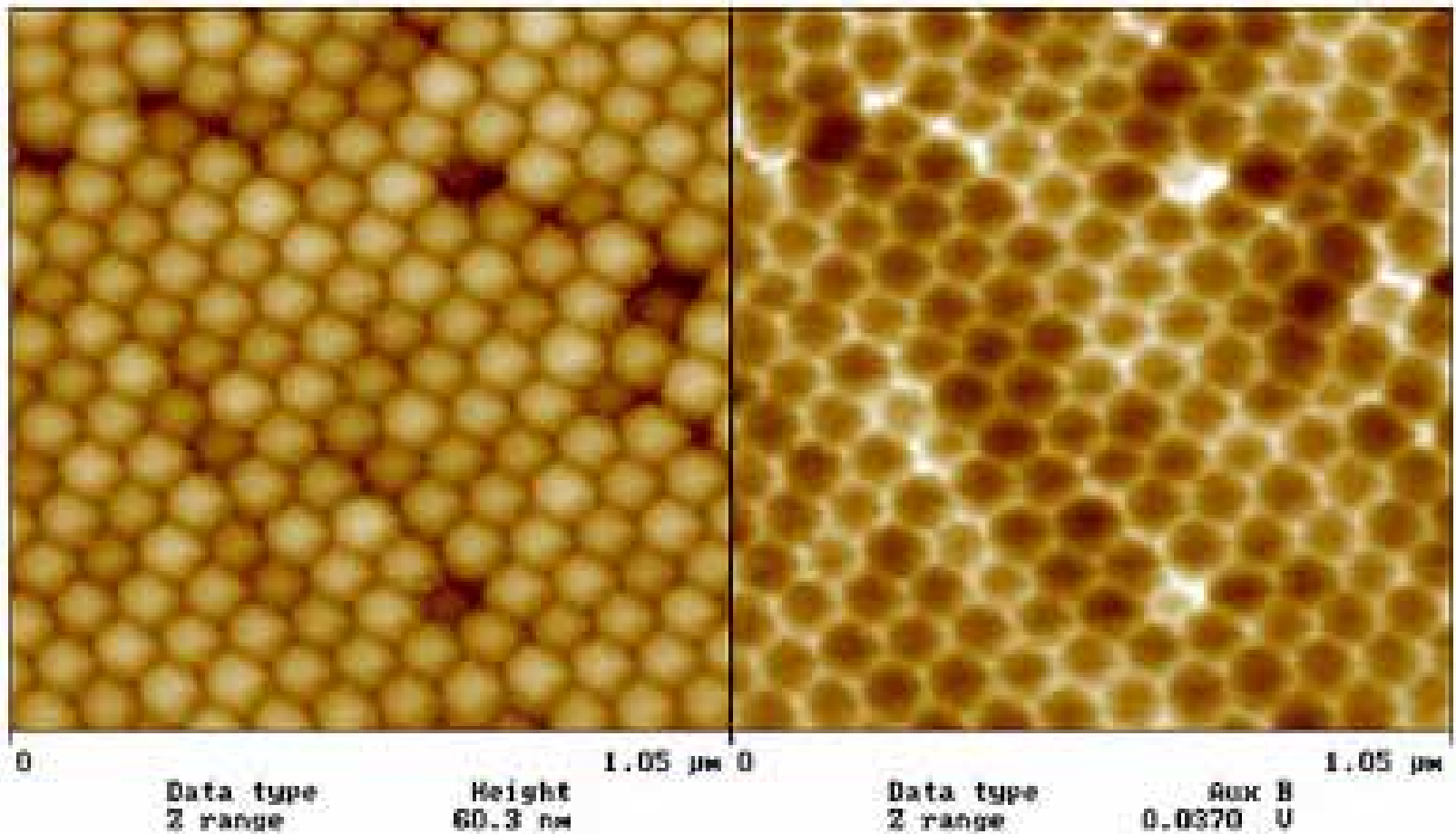


Near-field Scanning Optical Microscopy (NSOM)



Topography

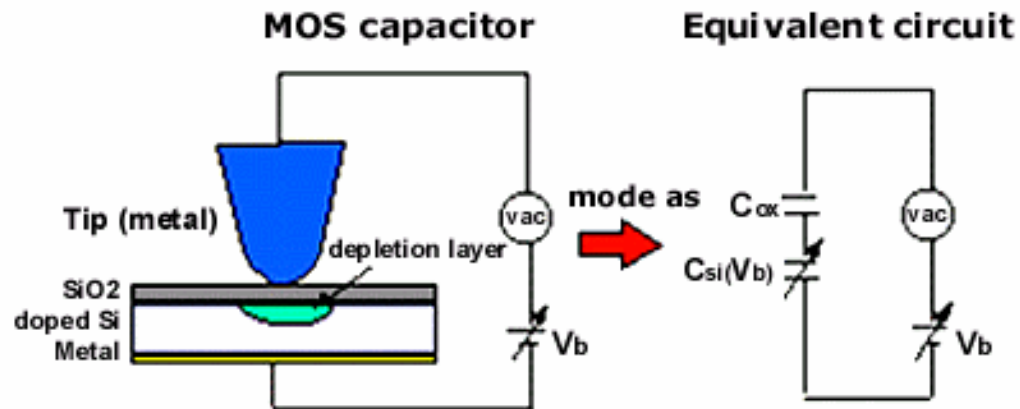
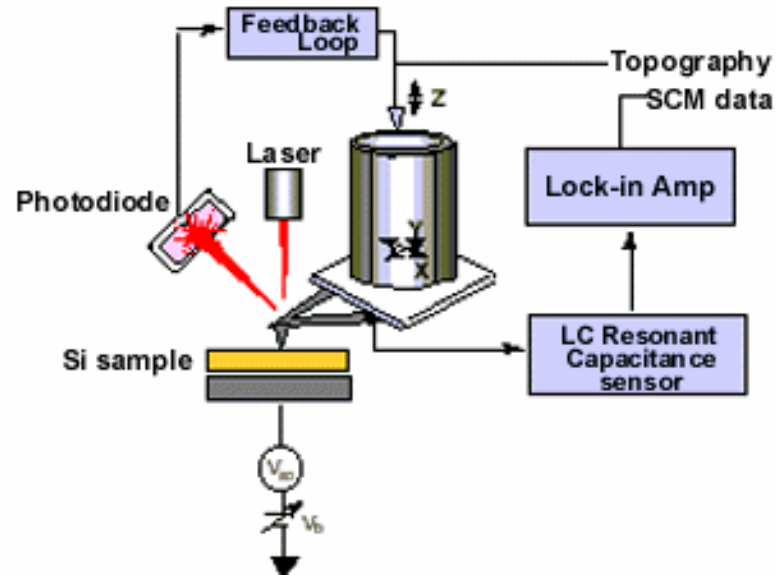
NSOM Image



100 奈米直徑之聚苯乙烯顆粒球的原子力顯微 (AFM) 影像 (左) 及穿透式近場光學顯微影像 (右)

Scanning Capacitance Microscopy (SCM)

Operational principle of the SCM

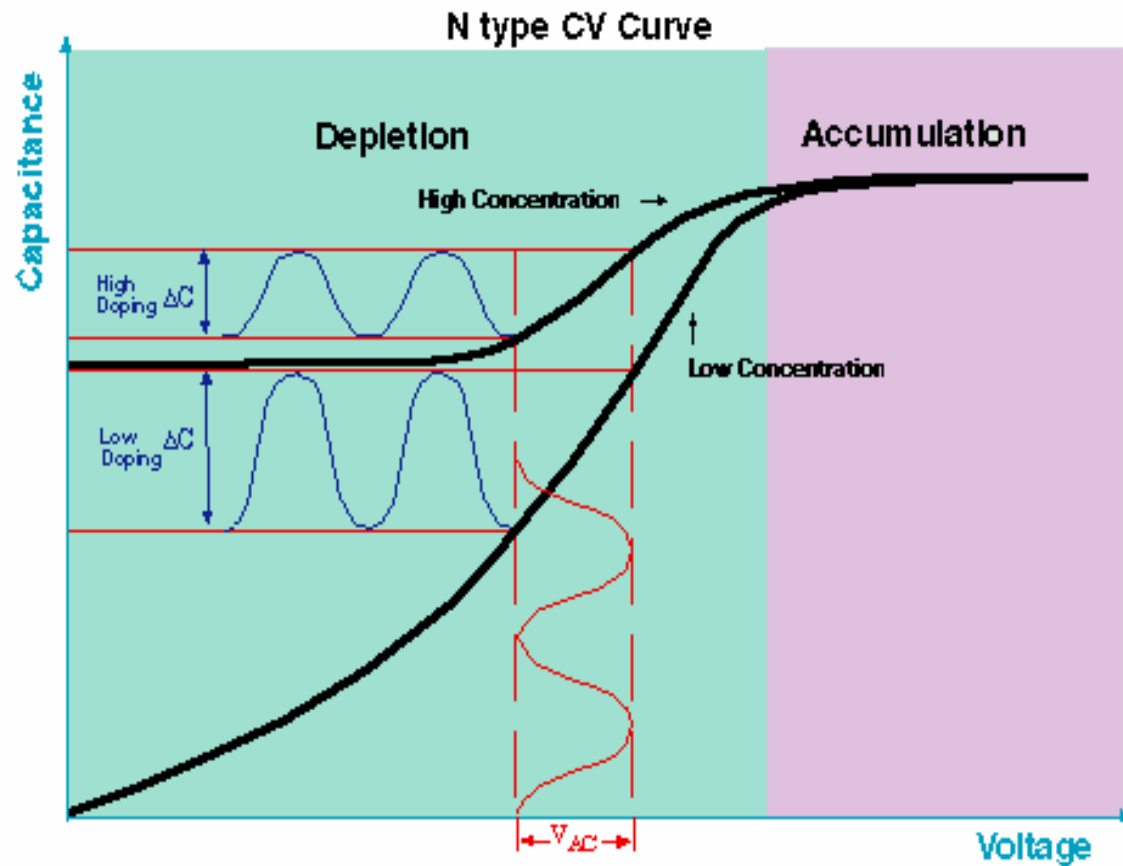


- 1. Most SCMs are based on contact-mode AFM with a conducting tip.**
- 2. In SCM, the sample (or the metallic tip) is covered with a thin dielectric layer, such that the tip-sample contact forms a MIS capacitor, whose C-V behavior is determined by the local carrier concentration of the semiconductor sample.**
- 3. By monitoring the capacitance variations as the probe scans across the sample surface, one can measure a 2D carrier concentration profile.**
- 4. One usually measures the capacitance variations (dC/dV), not the absolute capacitance values.**
- 5. No signal is measured if the probe is positioned over a dielectric or metallic region since these regions cannot be depleted.**

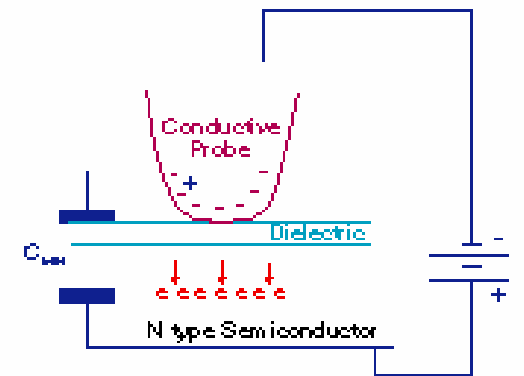
References:

- 1. C.C. Williams, Annu. Rev. Mater. Sci. **29**, 471 (1999).**
- 2. P.D. Wolf et al., J. Vac. Sci. Technol. B **18**, 361 (2000).**
- 3. R.N. Kleiman et al., J. Vac. Sci. Technol. B **18**, 2034 (2000).**
- 4. H. Edwards, et al., J. Appl. Phys. **87**, 1485 (2000).**
- 5. J. Isenbart et al., Appl. Phys. A **72**, S243 (2001).**

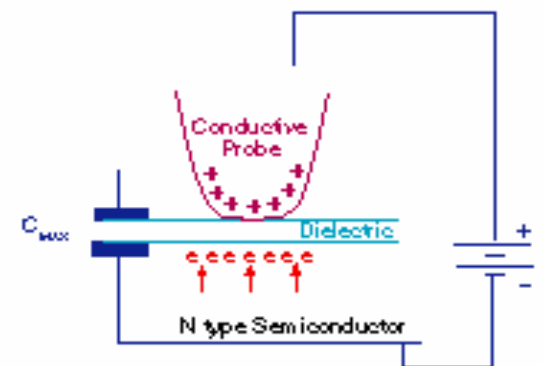
SCM CV Curve



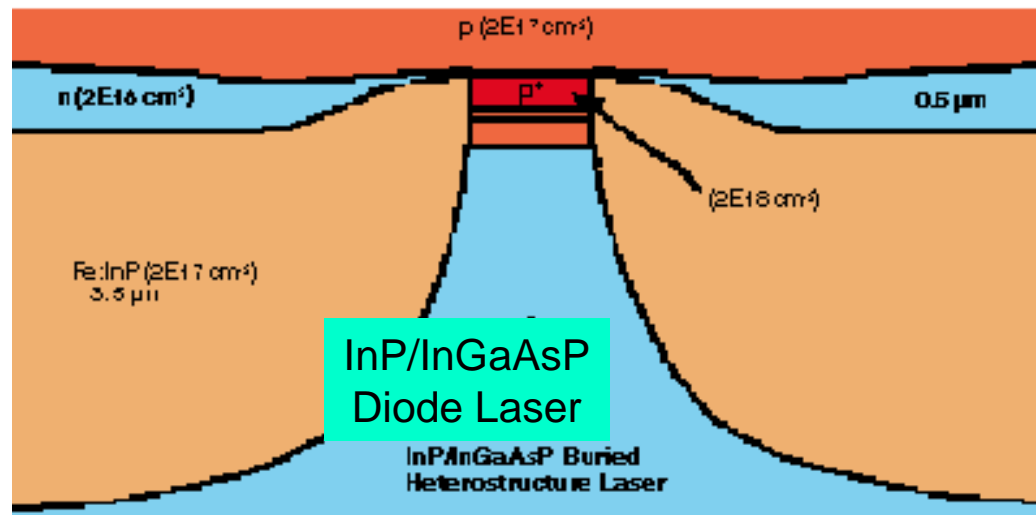
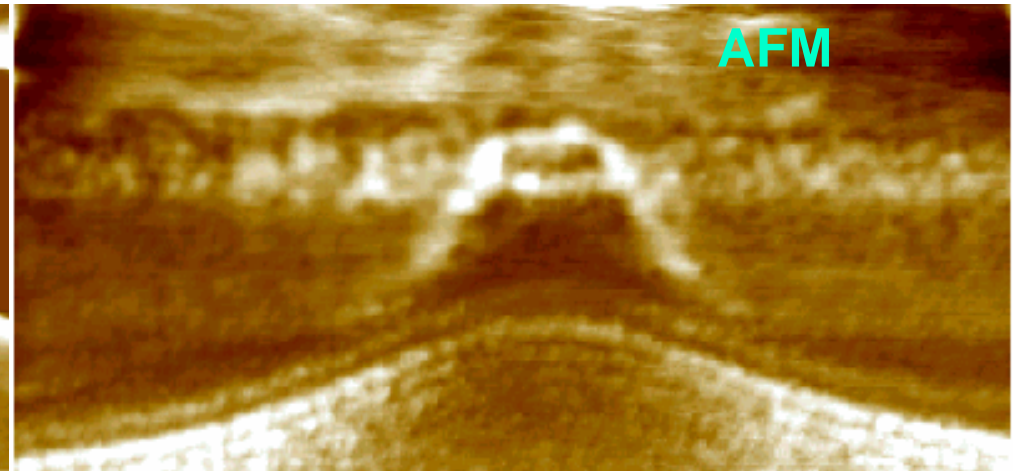
Depletion



Accumulation



Scanning Capacitance Microscopy



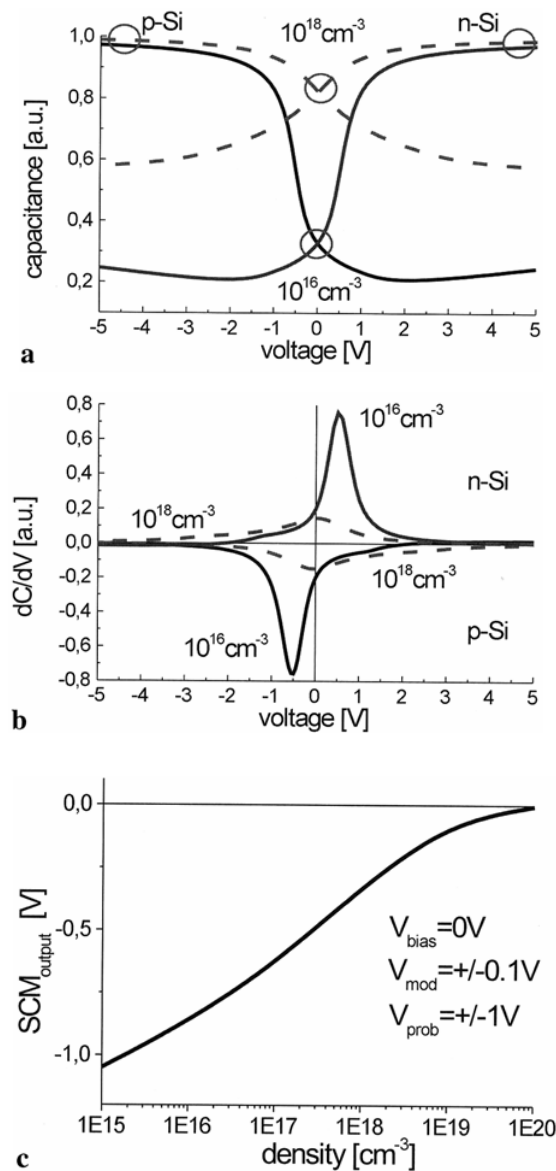


Fig. 2a–c. 3D simulations of SCM on homogeneously doped samples. The tip ($r_a = 25 \text{ nm}$, $r_i = 25 \text{ nm}$, $\alpha = 20^\circ$) is modelled in cylindrical coordinates; $d_{\text{ox}} = 10 \text{ nm}$. **a** $C(V)$ curves on p - and n -doped silicon with dopant concentrations of 10^{16} cm^{-3} and 10^{18} cm^{-3} , respectively. **b** The corresponding $dC/dV(V)$ curves are calculated analytically. **c** The calibration curve is calculated from $C(V)$ -curve simulations. The SCM output is calculated as $\Delta C/\Delta V(V)$ at $V_{\text{bias}} = 0 \text{ V}$ taking $V_{\text{mod}} = \pm 0.1 \text{ V}$ and $V_{\text{prob}} = \pm 1 \text{ V}$ into account

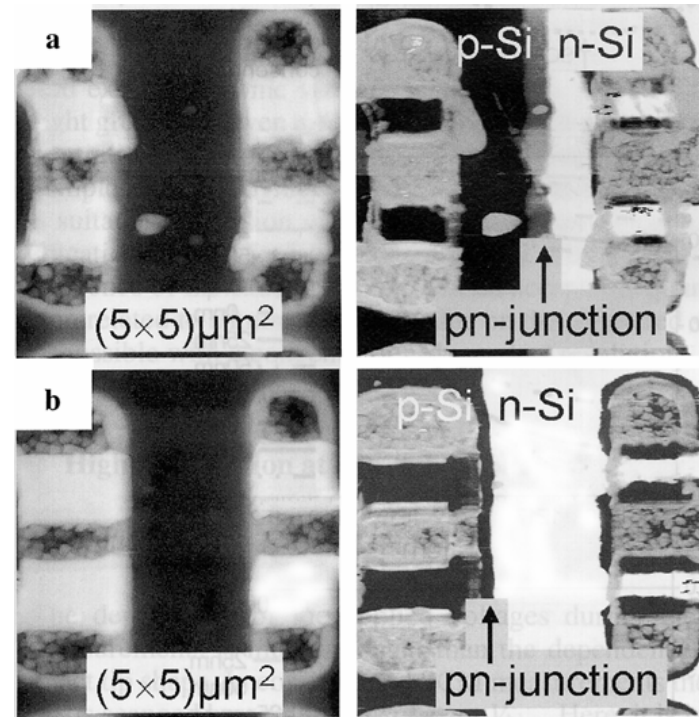


Fig. 3a,b. Failure analysis of an industrial device by means of SCM. Topography (left-hand side) and SCM image (right-hand side) are taken simultaneously. **a** Well-operating device with the pn junction implanted in the middle between the poly-silicon contacts. **b** Defective device with the pn junction shifted to the left-hand contacts. Both devices were measured at the same V_{bias} corresponding to the “zero voltage” (see text)

J. Isenbart et al., Appl. Phys. A **72**,
S243 (2001).

- 1. The SCM has proven its potential for the analysis of 2D dopant profiles on a scale down to less than 50 nm.**
- 2. The quantification of a measured dopant profile is still difficult due to the influence of parameters of the sample, the tip shape, and the capacitance sensor including the applied voltages.**
- 3. The properties of the sample, e.g. the roughness of the surface (fluctuation of the oxide thickness), the density of charged impurities and traps in the oxide layer and mobile surface charges, are mainly determined by the sample-preparation procedure.**
- 4. The most important influence on the measurements is due to the probing voltage of the capacitance sensor and the applied bias voltage.**
- 5. In SCM, not the dopant concentration, but rather the local charge-carrier concentration is measured because only the mobile carriers can contribute to $C(V)$ and thus only the local charge-carrier distribution can be detected.**